

UCGE Reports  
Number 20073

**Department of Geomatics Engineering**

**Development of a GPS Multi-Antenna  
System for Attitude Determination**

*PhD Thesis*

**Gang Lu**

**January 1995**



UNIVERSITY OF  
CALGARY

([www.ensu.ucalgary.ca/GradTheses.html](http://www.ensu.ucalgary.ca/GradTheses.html))

THE UNIVERSITY OF CALGARY

**Development of a GPS Multi-Antenna System  
for Attitude Determination**

by

Gang Lu

A DISSERTATION

SUBMITTED TO THE FACULTY OF GRADUATE STUDIES

IN PARTIAL FULFILLMENT OF THE REQUIREMENTS FOR THE

DEGREE OF DOCTOR OF PHILOSOPHY

DEPARTMENT OF GEOMATICS ENGINEERING

CALGARY, ALBERTA

DECEMBER, 1994

Gang Lu 1994

## ABSTRACT

A GPS multi-antenna system consisting of multiple off-the-shelf GPS sensors has been successfully developed and extensively tested in operational marine environments. The advantages to use such a system are the flexibility in the selection of GPS sensors, the cost-effectiveness of the system with the emerging low-cost high performance GPS products and the increased productivity of equipment which can be assembled into a multi-antenna system or dissembled for other positioning purposes. The underlying methodologies to integrate multiple GPS sensors into an attitude determination system are presented. Specifically, the observation model and its error sources are analyzed. A direct computation method and a least squares procedure for attitude estimation are given. On-the-fly carrier phase ambiguity resolution methods are investigated with emphasis on the use of baseline constraints, *a priori* attitude information from other low-cost attitude sensors, and special antenna configurations. A specialized post-processing software package for attitude estimation using raw GPS multi-antenna measurements has been developed. A marine test has shown that the proposed multi-antenna system and processing software give consistent results with those from a commercial dedicated attitude system. When a wide antenna spacing was used on a 52-metre long surveying vessel with a four GPS sensor attitude system, an accuracy better than 0.06 degrees at an output rate of 10 Hz for the estimated ship attitude parameters has been achieved, when the ship attitude reference was provided by a high accuracy INS. Such a performance of multiple GPS sensor attitude systems demonstrates an alternative means to provide accurate, cost-effective and reliable attitude information for hydrographic surveys and other applications.

## ACKNOWLEDGMENTS

I wish to express my deep gratitude to my supervisor, Dr. M. Elizabeth Cannon, for her continuous support and encouragement throughout my Ph. D. program. Her advice and guidance were essential for the completion of this thesis.

I am also grateful to Dr. Gérard Lachapelle who was my supervisor for the first year of my Ph. D. program. He has taught me to be a good student and a hard worker, which I shall benefit from throughout my life.

Special thanks go to Dr. Edward J. Krakiwsky for the discussions related to least squares adjustment methods and statistical testing. Thanks also go to Dr. Bosko Loncarevic at the Geological Survey of Canada, Bedford Institute of Oceanography for providing me the ship Matthew GPS multi-antenna data and to Mr. Jan Zywiel at Applied Analytics Corp., Markham, Ontario for providing me the shipborne INS data used for comparisons.

Graduate students in the navigation group, especially Huangqi Sun and Congyu Liu, are thanked for their help in the field experiments and data collection.

Financial support for this research was provided by the NSERC Postgraduate Scholarship and the Graduate Research Assistantships from the University of Calgary. This support is gratefully acknowledged.

## TABLE OF CONTENTS

|  | Page |
|--|------|
| APPROVAL PAGE .....  | ii   |
| ABSTRACT .....   | iii  |
| ACKNOWLEDGEMENTS .....   | iv   |
| TABLE OF CONTENTS .....  | v    |
| LIST OF TABLES .....   | viii |
| LIST OF FIGURES .....  | ix   |
| NOTATION .....   | xii  |
| <br><b>CHAPTER</b>   |      |
| 1 INTRODUCTION .....   | 1    |
| 1.1 Background and Objective .....   | 1    |
| 1.2 Outline .....  | 5    |
| 2 GPS OBSERVABLES AND ERROR SOURCES .....  | 8    |
| 2.1 Overview of GPS .....  | 8    |
| 2.2 GPS Receivers for Attitude Determination .....                               | 10   |
| 2.3 Observation Equations and Error Sources .....                                | 15   |
| 2.3.1 Observation Equations for Raw Measurements .....                           | 15   |
| 2.3.2 Double Difference Observations .....                                       | 20   |
| 2.4 Carrier Phase Multipath and Its Influence on Attitude<br>Determination ..... | 22   |
| 2.4.1 Description of Carrier Phase Multipath .....                               | 23   |
| 2.4.2 Carrier Phase Multipath Effects on Attitude<br>Estimation .....            | 26   |

|       |   |     |
|-------|---|-----|
| 3     | ATTITUDE ESTIMATION USING GPS .....   | 35  |
| 3.1   | Coordinate Systems and Rotation Matrix .....  | 35  |
| 3.1.1 | Coordinate Systems .....  | 36  |
| 3.1.2 | Rotation Matrix .....   | 41  |
| 3.2   | Attitude Determination Using GPS .....  | 44  |
| 3.2.1 | Review of Some Methods for Attitude Estimation<br>from Vector Observations .....    | 46  |
| 3.2.2 | Direct Computation Formulas for Attitude<br>Parameters .....                        | 51  |
| 3.2.3 | Attitude Estimation by an Implicit Least Squares<br>Model .....                     | 56  |
| 3.3   | Antenna Configuration Impact on the Accuracy of<br>Attitude Determination .....     | 59  |
| 4     | ON-THE-FLY CARRIER PHASE AMBIGUITY RESOLUTION<br>FOR MULTI-ANTENNA SYSTEMS .....    | 63  |
| 4.1   | On-the-fly Ambiguity Resolution by Least Squares Methods ....                       | 64  |
| 4.1.1 | General Concept .....   | 64  |
| 4.1.2 | The Least Squares Ambiguity Search Method .....                                     | 68  |
| 4.1.3 | Recent Developments for On-the-fly Ambiguity<br>Resolution .....                    | 77  |
| 4.2   | Ambiguity Resolution over a Fixed Baseline Length .....                             | 84  |
| 4.3   | Ambiguity Resolution with the Aiding of External Low<br>Cost Attitude Sensors ..... | 95  |
| 4.4   | Ambiguity Resolution with Special Antenna Configurations ..                         | 101 |

|       |  |     |
|-------|--|-----|
| 5     | SOFTWARE DEVELOPMENT AND SOME RELATED TOPICS .....   | 107 |
| 5.1   | Software Development .....   | 107 |
| 5.2   | Antenna Installation .....   | 111 |
| 5.3   | Initialization .....   | 112 |
| 5.3.1 | Misalignment Angle Determination .....   | 112 |
| 5.3.2 | Precise Baseline Determination .....   | 113 |
| 5.3.3 | Antenna Coordinate Determination .....   | 114 |
| 5.4   | Quality Control for Estimated Attitude Parameters .....  | 115 |
| 6     | TESTS AND RESULTS .....  | 122 |
| 6.1   | Shipborne Test with Dedicated and Non-dedicated GPS<br>Attitude Systems .....                      | 123 |
| 6.1.1 | Test Description .....   | 123 |
| 6.1.2 | Data Processing .....  | 126 |
| 6.1.3 | Misalignment Angle Determination .....   | 131 |
| 6.1.4 | Comparison of the Attitude Results from Dedicated<br>and Non-Dedicated Multi-Antenna Systems ..... | 133 |
| 6.2   | Shipborne Test of a Non-dedicated Multi-antenna GPS<br>System with an INS .....                    | 141 |
| 6.2.1 | Test Description and Antenna Setup .....   | 142 |
| 6.2.2 | INS Installation and Data Collection .....   | 145 |
| 6.2.3 | Data Processing and Analysis .....   | 146 |
| 7     | CONCLUSIONS AND RECOMMENDATIONS .....  | 157 |
|       | REFERENCES .....   | 165 |
|       | APPENDIX .....   | 177 |

## LIST OF TABLE S

|   | <b>Page</b> |
|---|-------------|
| 2.1 Requirements of GPS Sensors for Attitude Determination .....  | 13          |
| 4.1 Results of Least Squares Ambiguity Search with Cholesky<br>Decomposition Algorithm .....                                  | 90          |
| 4.2 Ambiguity Resolution Within the <i>a priori</i> Search Cube<br>(Static Baseline Test, 3 m Bar, 458 Sample Epochs) .....   | 98          |
| 4.3 Ambiguity Resolution with External Ship Attitude Information<br>(Ship-borne Data, May 31, 1993, 4067 Sample Epochs) ..... | 100         |
| 4.4 Ambiguity Resolution with a Special Antenna Configuration<br>(1 m and 4.5 m baselines, 598 epochs) .....                  | 104         |
| 6.1 Antenna Body Frame Coordinates ( Origin: Ant 1 [0, 0, 0] ) .....  | 127         |
| 6.2 Baseline Lengths between GPS Antennas .....   | 127         |
| 6.3 Input Parameters for Multi-Antenna GPS Data Processing .....  | 128         |
| 6.4 Attitude Differences Between the 3DF and<br>the CPSCard™ Systems .....  | 134         |
| 6.5 RMS of Double Difference Carrier Phase Residuals for the<br>Ashtech and GPSCard™ systems .....                            | 139         |
| 6.6 GPS Computed Antenna Coordinates in Antenna<br>Platform Coordinate System .....   | 144         |
| 6.7 Distances between GPS Antennas .....  | 144         |
| 6.8 Statistics of Comparisons between INS and GPS Estimated<br>Attitudes .....  | 148         |

## LIST OF FIGURES

|   | <b>Page</b> |
|---|-------------|
| 2.1 Functional Block Diagram for Dedicated Attitude Receivers .....   | 11          |
| 2.2 GPS Double Differencing .....   | 21          |
| 2.3 Static Roof Test of A Multi-Antenna System .....  | 27          |
| 2.4 Platform Yaw for March 4 and March 5 Static Tests .....   | 28          |
| 2.5 Platform Pitch for March 4 and March 5 Static Tests .....   | 28          |
| 2.6 Platform Roll for March 4 and March 5 Static Tests .....  | 28          |
| 2.7 Double Difference Carrier Phase Residuals for March 4<br>and 5 Static Tests .....                           | 30          |
| 3.1 Conventional Terrestrial System and Local Level System .....  | 37          |
| 3.2 Definition of Attitude Parameters in a Vehicle Platform<br>Coordinate System .....                          | 38          |
| 3.3 Antenna Body Frame Coordinate System .....  | 39          |
| 3.4 Pitch Accuracy as a Function of Baseline Length .....   | 60          |
| 4.1 General Concept of Ambiguity Search .....   | 66          |
| 4.2 Histogram for Carrier Phase Residuals Shown in Figure 6.25 .....  | 72          |
| 4.3 Histograms for Carrier Phase Residuals from the Static Roof<br>Test (Baseline 1-2 Observations) .....       | 73          |
| 4.4 Histogram for Carrier Phase Residuals with Incorrect<br>Ambiguities ( $N_{15-2}$ in Error by 1 Cycle) ..... | 74          |
| 4.5 Ambiguity Search Ranges from FASF .....   | 82          |
| 4.6 Test with Different Baseline Lengths .....  | 90          |
| 4.7 Adroit's Antenna Configuration .....  | 102         |

|      |   |     |
|------|---|-----|
| 4.8  | Modified Adroit Configuration For Long Baseline .....   | 105 |
| 5.1  | Flowchart of MULTINAV Program System .....  | 109 |
| 5.2  | Differences between the Known and the Computed Lengths<br>with Wrong Ambiguities for Baseline 1-2 ..... | 118 |
| 5.3  | Yaw and Pitch Differences for Test 1 with Correct and<br>Incorrect Ambiguities .....                    | 120 |
| 6.1  | Survey Launch GPS Antenna Configuration .....   | 124 |
| 6.2  | Survey Launch Trajectory .....  | 125 |
| 6.3  | Yaw of the Launch Estimated by LS method .....  | 130 |
| 6.4  | Pitch of the Launch Estimated by LS method .....  | 130 |
| 6.5  | Roll of the Launch Estimated by LS method .....   | 130 |
| 6.6  | Yaw Differences of the Launch from the Two Systems .....  | 135 |
| 6.7  | Pitch Differences of the Launch from the Two Systems .....  | 135 |
| 6.8  | Roll Differences of the Launch from the Two Systems .....   | 135 |
| 6.9  | Differences between GPS Computed and Fixed Baseline<br>Lengths for GPSCard™ System .....                | 137 |
| 6.10 | Differences between GPS Computed and Fixed Baseline<br>Lengths for Ashtech 3DF System .....             | 138 |
| 6.11 | Double Difference Carrier Phase Residuals for 3DF System<br>(SVs 21-23) .....                           | 140 |
| 6.12 | Double Difference Carrier Phase Residuals for GPSCard™<br>System (SVs 21-23) .....                      | 140 |
| 6.13 | Antenna Layout on Ship Matthew .....  | 143 |
| 6.14 | Yaw Differences (GPS-INS) for Day 180, 1993 .....   | 150 |
| 6.15 | Pitch Differences (GPS-INS) for Day 180, 1993 .....   | 151 |

|  |     |
|--|-----|
| 6.16 Roll Differences (GPS-INS) for Day 180, 1993 .....                                    | 151 |
| 6.17 Ship Trajectory for June 29 (Day 180) Test .....                                      | 152 |
| 6.18 Ship Yaw Derived from GPS Attitude System (Day 180) .....                             | 152 |
| 6.19 Ship Pitch Derived from GPS Attitude System (Day 180) .....                           | 152 |
| 6.20 Ship Roll Derived from GPS Attitude System (Day 180) .....                            | 152 |
| 6.21 Yaw Change Rate for Day 180 .....   | 153 |
| 6.22 Roll Change Rate for Day 180 .....  | 153 |
| 6.23 Differences between GPS computed and Known Baseline<br>Lengths for Day 180 Test ..... | 154 |
| 6.24 Double Difference Carrier Phase Residuals for Day 180 Test<br>(SVs 28-22) .....       | 155 |
| 6.25 Double Difference Carrier Phase Residuals for Day 180 Test<br>(SVs 3 -22) .....       | 156 |

## NOTATION

### i) Conventions

- a) Matrices are uppercase.
- b) Vectors are lowercase and bold.
- c) Master antenna and slave antennas:  
*master antenna* - the GPS antenna by which the platform position is computed and the origin of the antenna platform is defined.  
*slave antennas* - all the other GPS antennas that form the antenna platform.
- d) The following operators are defined as:
  - $\dot{a}$  derivative with respect to time
  - $H^T$  matrix transpose
  - $Q^{-1}$  matrix inverse
  - $\Delta r$  single difference between receivers
  - $\Delta s$  single difference between satellites
  - $\Delta r_s$  double difference between receivers and satellites
  - $\| \cdot \|$  norm operator
  - $\sim$  distributed as
  - $\hat{\phantom{a}}$  estimated value
  - $\sum w_i$  summation of  $w_i$
  - $\text{Tr}(A)$  trace of matrix  $A$
  - $\Leftrightarrow$  equivalent
  - $\text{nint}()$  nearest integer operator

$\frac{\mathbf{R}}{\mathbf{x}}$  partial derivatives of each elements in  $\mathbf{R}$  with respect to  $\mathbf{x}$

## ii) Symbols

|                                 |   |
|---------------------------------|---|
| $\mathbf{A}$                    | design matrix   |
| AZDOP                           | azimuth dilution of precision   |
| $\mathbf{B}$                    | matrix consisting of body frame coordinates as columns;<br>design matrix related to local level coordinates |
| $\mathbf{b}_i$                  | baseline vector in body frame   |
| $c$                             | speed of light  |
| $\mathbf{C}_{\hat{\mathbf{x}}}$ | covariance matrix of $\hat{\mathbf{x}}$   |
| $\mathbf{C}_{\sim}$             | covariance matrix of yaw, pitch and roll  |
| $\mathbf{C}_{\text{obs}}$       | covariance matrix of observations   |
| $dt$                            | satellite clock error   |
| $dT$                            | receiver clock error  |
| $d_{\text{ion}}$                | ionospheric correction (m)  |
| $d_{\text{trop}}$               | tropospheric correction (m)   |
| $\mathbf{d}$                    | baseline vector $\mathbf{d} = (x, y, z)^T$  |
| $d$                             | baseline length   |
| $\hat{d}$                       | computed baseline length by GPS observations  |
| $(p_{\text{rx}})$               | observation noise   |
| $f$                             | degree of freedom in Chi-square distribution  |
| L1                              | GPS L1 carrier frequency (1575.42 MHz)  |
| L2                              | GPS L2 carrier frequency (1227.60 MHz)  |
| $N$                             | carrier phase ambiguity; normal matrix  |

|                      |   |
|----------------------|---|
| $N(\mu_i, \sigma^2)$ | normal probability distribution with expectation $\mu_i$ and variance $\sigma^2$  |
| $p$                  | pseudorange measurement (m)<br>slant distance from antenna phase centre to satellite (m)<br>carrier phase observation<br>carrier wavelength (m) |
| $R$                  | earth radius; rotation matrix   |
| $R_1(\alpha)$        | rotation matrix about x-axis  |
| $R_2(\beta)$         | rotation matrix about y-axis  |
| $R_3(\gamma)$        | rotation matrix about z-axis  |
| $R_{H}^I$            | rotation matrix from frame H to frame I   |
| $R(y, p, r)$         | rotation matrix from local level to body frame  |
| $S$                  | received carrier signal voltage   |
| $S_d$                | direct carrier signal voltage   |
| $S_r$                | reflected carrier signal voltage  |
| $\mathbf{u}_i$       | baseline vector in local level frame  |
| $V_d$                | amplitude of direct carrier signal voltage  |
| $V_r$                | amplitude of reflected carrier signal voltage   |
| $\hat{\mathbf{v}}$   | adjusted carrier phase residuals  |
| $w_i$                | weighting factor for baseline $i$ ; misclosure  |
| $\hat{\mathbf{x}}$   | estimated unknowns vector   |
| $x, y, z$            | Cartesian coordinates in local level  |
| $x^b, y^b, z^b$      | Cartesian coordinates in body frame   |
| $y, p, r$            | yaw, pitch and roll, respectively<br>phase shift of the reflected carrier phase signal  |

|                             |  |             |
|-----------------------------|--|-------------|
|                             | significance level; ratio of voltage amplitudes                  | $= V_r/V_d$ |
|                             | carrier phase multipath error                                    |             |
| $\bar{y}, \bar{p}, \bar{r}$ | mean misalignment angle for yaw, pitch and roll,<br>respectively |             |
| y                           | standard deviation of yaw  |             |
| p                           | standard deviation of pitch                                      |             |
| r                           | standard deviation of roll                                       |             |
|                             | standard deviation of double difference phase observation        |             |
| RDOP                        | relative dilution of precision for latitude                      |             |
| RDOP                        | relative dilution of precision for longitude                     |             |
| VRDOP                       | relative dilution of precision for height                        |             |
|                             | quadratic form of carrier phase residuals                        |             |
| $\chi^2_{f,1-}$             | Chi-square distribution  |             |
|                             | non-centrality parameter in chi-square distribution              |             |
|                             | geodetic latitude  |             |
|                             | geodetic longitude   |             |
| h                           | geodetic height  |             |
| N                           | double difference carrier phase ambiguity                        |             |

### iii) Acronyms

|          |                               |
|----------|-------------------------------|
| C/A code | Clear / Acquisition code      |
| CHS      | Canadian Hydrographic Service |
| CT       | Conventional Terrestrial      |
| DD       | Double Difference             |
| DGPS     | Differential GPS              |
| FASF     | Fast Ambiguity Search Filter  |

|               |   |
|---------------|---|
| <b>GDOP</b>   | <b>Geometry Dilution of Precision</b>       |
| <b>GPS</b>    | <b>Global Positioning System</b>            |
| <b>INS</b>    | <b>Inertial Navigation System</b>           |
| <b>MEDLL</b>  | <b>Multipath Estimating Delay Look Loop</b> |
| <b>MRU</b>    | <b>Motion Reference Unit</b>                |
| <b>OEM</b>    | <b>Original Equipment Manufacturer</b>      |
| <b>P code</b> | <b>Precise code</b>                         |
| <b>PDOP</b>   | <b>Position Dilution of Precision</b>       |
| <b>PPS</b>    | <b>Pulse Per Second</b>                     |
| <b>RF</b>     | <b>Radio Frequency</b>                      |
| <b>RLG</b>    | <b>Ring Laser Gyro</b>                      |
| <b>RMS</b>    | <b>Root Mean Square</b>                     |
| <b>SD</b>     | <b>Single Difference</b>                    |
| <b>SV</b>     | <b>Space Vehicle</b>                        |
| <b>SVD</b>    | <b>Singular Value Decomposition</b>         |
| <b>TD</b>     | <b>Triple Difference</b>                    |
| <b>TSS</b>    | <b>TSS (UK) Ltd.</b>                        |
| <b>UTC</b>    | <b>Coordinated Universal Time</b>           |

## CHAPTER 1

### INTRODUCTION

#### 1.1 BACKGROUND AND OBJECTIVE

The satellite-based Global Positioning System (GPS) creates a new era for navigation, surveying and geodesy. Precise airborne and shipborne navigation, precise static geodetic positioning over baselines from a few metres up to thousands of kilometres, and kinematic positioning are just a few among numerous applications of GPS. The development of GPS multi-antenna systems, which integrate three or more GPS antennas into one system with a proper antenna configuration in a plane or in space, has resulted in another leap in GPS applications. In addition to providing position and velocity information, the multi-antenna GPS system can also determine the attitude parameters of the platform within an accuracy of several arc minutes. It has the potential of replacing, to some extent, some sophisticated and expensive attitude sensors such as Inertial Navigation Systems (INS) for air and marine applications.

Although GPS was primarily designed for precise positioning and time transfer, its potential for platform attitude determination was recognized at the early stages of the system development (Spinney, 1976; Ellis and Greswell, 1979). Using differential carrier phase measurements from three non-collinear GPS antennas which are properly mounted on a platform, the baseline vectors between all the antennas can be precisely determined and thus the attitude parameters of the platform defined by the three corresponding antennas can be derived from these baseline vectors.

In the early eighties, most of the investigations on GPS multi-antenna systems were restricted to simulation studies due to the relatively slow development of GPS hardware and its high cost, e.g. Brown et al. (1982) and Hermann (1985). The first attitude determination results using real GPS carrier phase measurements were reported by Evans (Evans, 1986) who proposed a method to measure platform attitude angles with a single antenna that periodically rotated in a plane. The first prototype GPS multi-antenna receiver was manufactured in 1988 and tested in a dynamic marine environment (Kruczynski et al., 1988, 1989). It was an 18 channel receiver consisting of three antennas with a reported accuracy for roll, pitch and heading determination of a few degrees for antenna separations ranging from 40 cm to 60 cm. Recently, there are a few GPS multi-antenna receivers commercially available, such as the Ashtech 3DF system (Ashtech, 1991) and the Trimble TANS VECTOR system (Wilson and Tonnemacher, 1992). These receivers integrate 4 antennas into one self-contained unit and operate all its tracking channels from a single receiver oscillator. Field tests have shown that the attitude accuracy of these receivers is at the level of 0.03 to 0.5 degrees (1<sup>σ</sup>) depending on the antenna

configuration, the separation between antennas as well as multipath influences on the measurements (Cohen et al., 1993; Schwarz et al., 1992). However, the proliferation of these dedicated GPS multi-antenna receivers may be limited by their overall lack of flexibility and cost. Furthermore, in some receivers, residual receiver clock biases among the different antenna banks may exist, which limits the advantage of using a common oscillator to integrate all tracking channels.

With the continuous advancement of GPS receiver technology in recent years, a wide range of high performance original equipment manufacturer (OEM) GPS sensors are available to users at a relatively low cost, e.g. Fenton et al. (1991), Cannon et al. (1993a). The term GPS sensor is understood as a generic GPS receiver, single or dual frequency, which may not have data memory, keyboard and other accessories that do not affect GPS signal tracking. By integrating three or more these GPS sensors through proper data processing algorithms and antenna configurations, a GPS multi-antenna system can then be developed. For example, Cannon et al. (1992) have successfully developed a heading determination system with two OEM GPS sensors, while Lu et al. (1993) have tested a prototype attitude determination system consisting of three OEM GPS sensors against a dedicated GPS attitude receiver Ashtech 3DF. Preliminary results have demonstrated that the attitude agreement between the proposed multiple GPS sensor attitude system and the dedicated 3DF receiver was about 5 to 15 arc minutes in yaw, pitch and roll components over an antenna separation from 4 to 5 metres.

The main objective of this research is to develop a GPS multi-antenna system by integrating multiple high performance OEM GPS sensors, to investigate the related data processing algorithms and to assess the system performance in real operational environments. The integration technique for the GPS multi-antenna system is mainly software-oriented so that little or no hardware change is required on each individual GPS sensor. Data processing algorithms are designed to optimally use all the positional information among the antennas and provide as much flexibility as possible for the GPS antenna configuration in order to accommodate a wide range of applications where platform attitude information is required.

Sub-centimetre level relative positioning between multiple antennas is the key to precise attitude determination using GPS. To achieve this level of accuracy, carrier phase observations with correctly resolved integer cycle ambiguities have to be used (Lachapelle et al., 1992). In integrated multiple GPS sensor attitude systems, double difference carrier phase observables are used in order to cancel the clock biases between different GPS sensors and thus exploit the integer characteristic of carrier phase ambiguities. Since the GPS multi-antenna system is used primarily in kinematic environments, various methods for 'on the fly' carrier phase ambiguity resolution are reviewed and discussed. The efficiency and reliability of carrier phase ambiguity resolution methods using constraints such as the known baseline lengths, antenna configurations and external attitude information will be investigated and evaluated.

Another aspect of GPS multi-antenna system development is the attitude estimation method from a multiple antenna array and the related accuracy analysis of the estimated attitude parameters. A fast direct computation method and a least squares estimation procedure for attitude estimation will be given (Lu et al., 1993). Formulas to estimate the attitude accuracy based on these methods will be derived.

Successful application is the final purpose of any GPS technology. Recently, GPS multi-antenna receivers have been applied to aircraft attitude determination (Cohen et al., 1993; Cohen and Parkinson, 1992; Van Grass and Braasch, 1991). The use of such receivers on low earth orbit satellites has been demonstrated by Cohen et al. (1993) and Axelrad et al. (1994). This research will therefore mainly focus on another important area which is the marine application. In hydrographic surveying, for example, ship attitude information is needed for seafloor mapping and precise water level profiling. Attitude information is also important for ship navigation. The use and performance of non-dedicated GPS multi-antenna systems with a wide antenna spacing, e.g. >20 m, in an operational marine environment have not been investigated in the past.

## **1.2 OUTLINE**

This dissertation is divided into seven chapters. Previous studies and the research objective are introduced in Chapter 1. In Chapter 2, GPS observables and their error sources are reviewed. In particular, the carrier

phase multipath effect, which is one of the major errors affecting the platform attitude estimation, is discussed.

In Chapter 3, existing methods for attitude estimation are examined, and a least squares platform attitude estimation algorithm is developed based on the implicit least squares adjustment model which is able to incorporate the full covariance information of the baseline vector observables. The formulas for accuracy analysis of the estimated attitude parameters are also derived.

Chapter 4 deals with on-the-fly carrier phase ambiguity resolution methods which are of essential importance to multi-antenna GPS systems. In addition to the effects of satellite geometry, random and systematic errors on carrier phase ambiguity resolution, the effects of special constraints available within a multi-antenna system, such as the known baseline lengths and special antenna configurations, are investigated. The feasibility and performance of integrating a GPS multi-antenna system with other low cost, lower accuracy attitude sensors, such as the gyrocompass, are also discussed.

In Chapter 5, the software design for GPS multi-antenna data processing is outlined. Some quality control methods are studied in order to detect the effects from small cycle slips on the platform attitude results.

In Chapter 6, two marine experiments with GPS multi-antenna systems and their data analyses are described. One of the experiments was carried out on a small Canadian Hydrographic Service (CHS) survey launch, while the other was performed on the 52 metre long CHS ship Matthew where an INS was used as an external attitude reference. The performance and the

achievable attitude accuracy from the GPS multi-antenna system and the developed processing algorithms are investigated.

Chapter 7 contains conclusions and recommendations formed throughout this thesis as well as the topics that need further development and research.

## CHAPTER 2

### GPS OBSERVABLES AND ERROR SOURCES

Three types of measurements are provided by GPS, namely pseudorange, carrier phase and instantaneous Doppler. The mathematical models and the error sources related to these measurements are discussed in this chapter, with the emphasis of their effects on the platform attitude determination. In particular, the non-differentiable, site-dependent multipath effects are analyzed and demonstrated through numerical examples.

#### 2.1 OVERVIEW OF GPS

GPS is an all-weather, radio-based satellite navigation system established by the U.S. Department of Defense (DoD) to meet the military requirements of world-wide positioning, velocity determination and time keeping. The overall system is composed of three major segments: space segment, control segment and user segment. The space segment consists of 24 radio navigation satellites (21 plus 3 active spares) which are deployed in six orbital planes (four satellites per plane) inclined at a 55 degree angle with respect to the equator. The satellite orbits are designed in such a way that at least four satellites are visible

at any time in any location on the earth's surface. The altitude of the satellites is about 20,000 km (Wells et al., 1986). The control segment consists of five ground control stations around the world, with the master control station being at Colorado Springs. The main tasks of the control segment are to track and monitor the satellite performance, precisely compute satellite orbits and clock corrections, and periodically upload satellite ephemeris and other system data to all satellites for retransmission to the user segment. The user segment is the collection of all GPS users on land, sea and in the air or in space. Despite the fact that GPS is a military system, its civilian applications have grown exponentially in the last decade due to the great potential of the positioning and navigation capability of the system. In fact, the civilian community now outnumbers the military community.

Two frequencies are continuously transmitted from each GPS satellite for positioning. The first frequency is at 1575.42 MHz for a wavelength of 19 cm and the second is at 1227.60 MHz for a wavelength of 24 cm. They are called carrier frequencies L1 and L2 since pseudo-random noise (PRN) codes and navigation messages are modulated on each frequency. Coarse Acquisition (C/A) code is modulated on L1, while Precise (P) code is modulated on both L1 and L2.

With 24 satellites in the orbits and the system in its full operational capability (FOC), the Selective Availability (SA) and Anti-Spoofing (AS) are now implemented on GPS by the US military. SA is introduced by a combination of degraded satellite orbital information and satellite clock dithering. Only the military or authorized users can remove SA effects by using a special

cryptographic key. AS is accomplished by translating the P-code to the Y-code which denies its use by civilian community. Only the C/A code is unrestricted to all civilian users. Under SA, the single point positioning accuracy provided by C/A code is about 100 m in horizontal components and 156 m in the vertical component (Lachapelle, 1993). For GPS attitude determination, the most important measurements are L1 C/A code carrier phase measurements which are provided by most GPS receivers or sensors. Even though the P code is not available to civilian users, some modern GPS receivers can still measure the full L2 (24 cm wavelength) carrier phases using the so-called cross-correlation and P-W tracking technologies (Meehan et al., 1992; Ashjaee and Lorenz, 1992). The benefits of having dual frequency full carrier phase measurements for high precision static and kinematic GPS positioning are that the relative ionospheric corrections can be computed and the wide-lane and extrawidelane ambiguity resolution techniques can be used (e.g. Wubanna, 1989; Abdin, 1993).

## **2.2 GPS RECEIVERS FOR ATTITUDE DETERMINATION**

GPS receiver technology has experienced rapid developments in recent years in terms of hardware and signal processing techniques. From the very low cost GPS sensors or boards which only possess basic navigation functions to expensive dual frequency geodetic receivers, a wide selection is available to meet the needs of different application fields. For platform attitude determination with GPS, two types of specially designed receivers are commercially available through manufacturers. One is the Ashtech 3DF<sup>TM</sup> receiver and the other is the Trimble TANS Vector<sup>TM</sup> attitude receiver. Both

receivers are single frequency C/A code receivers, namely the receiver tracks C/A code and provides C/A code pseudorange and L1 carrier phase measurements. In order to obtain accurate attitude parameters from relatively short baselines on a moving platform, the most accurate measurements from a receiver, i.e. C/A code carrier phase, have to be used. Usually, both receivers have 24 dedicated tracking channels which divided into four banks, with each bank being assigned to an antenna. The functional block diagram for both receivers may be depicted in Figure 2.1.

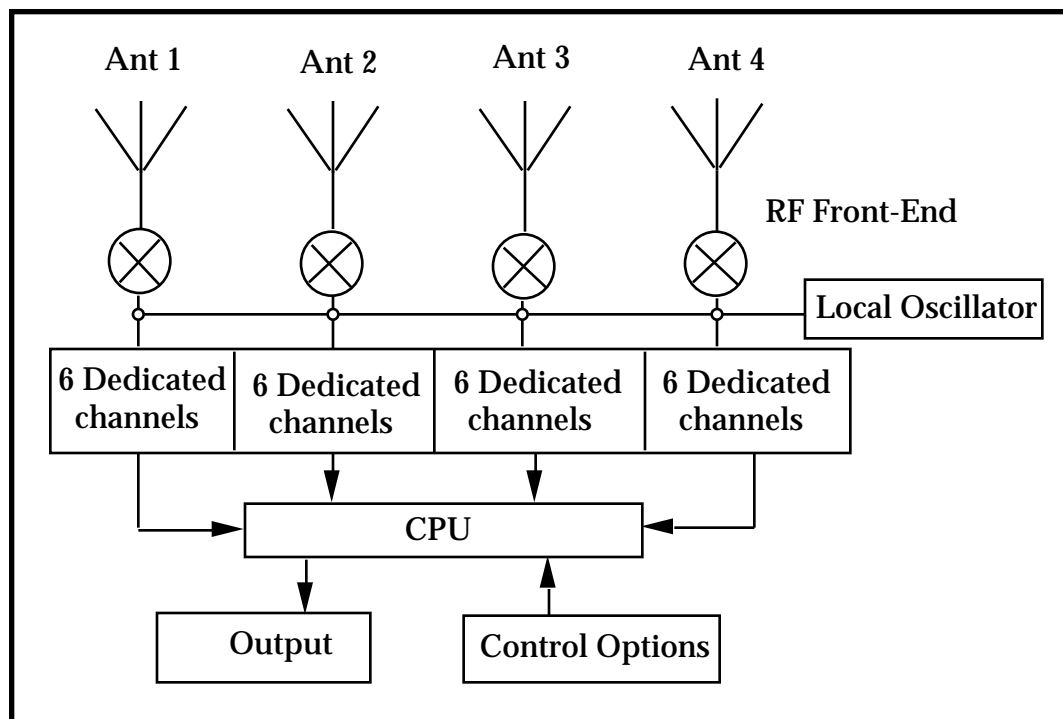


**Figure 2.1 Functional Block Diagram for Dedicated Attitude Receivers**

A unique feature of these receivers is that a single oscillator is used to control all the tracking channels of the multiple antennas. Theoretically, the biases associated with the oscillator, i. e. the receiver clock, will cancel out when single difference observations between two antennas are formed. The

advantages to be able to use single difference carrier phase observations directly are the lower carrier phase noise with single differencing as opposed to double differencing, and also the additional redundant measurement for attitude estimation and ambiguity resolution. Unfortunately, previous experiments have shown that residual receiver clock biases or the so-called line biases still existed between different antenna banks and the special treatment or calibration has to be carried out (Cohen and Parkinson, 1991; Axelrad and Ward, 1994; Lu et al., 1993). For the Trimble TANS Vector™ receiver, the inter-bank biases are constant and can be calibrated through a long static 'self-survey' proposed by Cohen et al. (1992) or through a 'bootstrapping algorithm' developed by Axelrad and Ward (1994). For the Ashtech 3DF™ receiver, double difference observations are usually used to cancel the residual receiver clock bias between the different antenna banks (Ashtech, 1991; Lu et al., 1993). This means that the advantage to use single difference observations can not be realized in this receiver. Even though exceptionally low noise carrier phase measurements can be made by these dedicated attitude receivers with a common oscillator, the limiting factor for high accuracy attitude determination is carrier phase multipath rather than receiver noise (Cohen and Parkinson, 1991). From this aspect, it is reasonable to postulate that instead of using dedicated attitude receivers, the same accuracy level of attitude estimation may be obtained by using three or four non-dedicated, off-the-shelf C/A code GPS sensors with high quality carrier phase output. This is another motivation of this research.

The advantages to use multiple off-the-shelf GPS sensors for attitude determination are the flexibility and cost-effectiveness of the system as well as

the increased productivity of equipment which can be assembled into a multi-antenna system or dissembled for other positioning purposes. Depending on the function and quality, the current price range for GPS sensors is between \$200 to some \$10,000 (Phillips Business Information, Inc., 1993). However, for a GPS sensor to be used for attitude determination, there are certain requirements that have to be met. The desired characteristics are listed in Table 2.1.

**Table 2.1 Requirements of GPS Sensors for Attitude Determination**

| <b>Characteristic</b>  | <b>Specification</b>                                       |
|------------------------|--|
| Raw measurement output | C/A code pseudorange and carrier phase (Doppler desirable) |
| Data rate              | 1 Hz   |
| Carrier phase noise    | < 1 mm   |
| Pseudorange noise      | < 3 m (< 15 cm desirable)                                  |
| Tracking channels      | 8  |
| Dynamics               | 300 m/s (velocity), 4g (acceleration)                      |
| Weight / Power         | < 500 grams / < 4 watts                                    |

The development trend for GPS sensor technologies are continuously driven to the low cost and high performance direction under the strong competition and the user's demand. It is expected that 12 channel GPS sensors will eventually become standard, which provide all-in-view capability (Bingham and Fryer, 1993; Van Diredock, 1994). The high precision C/A code pseudorange measurements, i. e. noise level less than 15 to 20 cm, will also be available from some high performance GPS sensors, such as the NovAtel GPSCard™. Depending on the algorithms, accurate pseudorange

measurements may improve the reliability and convergence time of carrier phase ambiguity resolution. Data rate is also an important issue for some applications. For instance, ocean mapping and bottom imagery with multi-beam echo sounders in shallow waters require at least 10 Hz (normally 25 Hz) attitude information to correct the echoed signals (Loncarevic, 1993). Currently, only a few receivers, such as the NovAtel GPSCard™ sensor and the TANS Vector™ dedicated attitude receiver, are capable of outputting 10 Hz data. One solution to this problem is to integrate low cost, high data rate gyro- and accelerometer-based shipborne attitude sensors with an GPS multi-antenna system, as discussed later in Chapter 4. Generally speaking, single frequency C/A code GPS sensors are used to form a multi-antenna system due to the short baselines between antennas. Dual frequency GPS sensors, however, can significantly increase the reliability and speed of carrier phase ambiguity resolution, leading to instantaneous ambiguity resolution (Quinn, 1993). Therefore, there is a trade-off between cost and performance when selecting appropriate GPS sensors.

Depending on the cost, the availability of equipment and the application environment, a user may select dedicated attitude receivers or non-dedicated multiple GPS sensor attitude systems that fit the requirement. For example, extremely compact dedicated attitude receivers may have to be used for attitude determination of low earth orbit satellites due to the limited installation space on satellites, while low-cost non-dedicated sensor attitude systems may well suit for hydrographic surveying vessels. It is no doubt that the cost for both dedicated attitude receivers and high performance GPS sensors will

continue to decrease in the future due to the competition and the advancement of receiver technologies.

## **2.3 OBSERVATION EQUATIONS AND ERROR SOURCES**

Most GPS receivers or sensors offer three basic types of measurements, namely the pseudorange (code), carrier phase and the instantaneous Doppler frequency. In a GPS multi-antenna system, all these measurements are used to provide the related information of the platform. Pseudoranges are used to solve the platform location in the WGS84 system at each instantaneous epoch, while Doppler frequency measurements are utilized to compute the platform velocities. The platform attitude parameters, e.g. yaw, pitch and roll are determined using at least two non-collinear antenna baseline vectors derived from the differential carrier phase measurements.

### **2.3.1 Observation Equations for Raw Measurements**

The fundamental observation equations and their error sources for pseudorange, carrier phase and Doppler frequency are well described in the literature, e.g. Wells et al. (1986) and Lachapelle (1993). In the following, only a brief discussion of the errors is given with the emphasis being on their effects on attitude estimation.

The basic observation equation for pseudorange measurements can be expressed as (Lachapelle, 1992):

$$p = + c(dt - dT) + d + d_{\text{ion}} + d_{\text{trop}} + (p_{\text{mult}}) + (p_{\text{rx}}) \quad (2.1)$$

where  $p$  ... is the pseudorange measurement (m),

$c$  ... is the speed of light (m/s),

$dt$  ... is the satellite clock correction (s),

$dT$  ... is the receiver clock error (s),

$d$  ... is the orbital error (m),

$d_{\text{ion}}$  ... is the ionospheric correction (m),

$d_{\text{trop}}$  ... is the tropospheric corrections (m),

$(p_{\text{mult}})$  ... is the code multipath error (m),

and  $(p_{\text{rx}})$  ... is the receiver code measurement noise (m).

Pseudorange measurements are instantaneous and generally unambiguous. The geometric information of the receiver coordinates  $\mathbf{r} = (x_r, y_r, z_r)^T$  and satellites coordinates  $\mathbf{R} = (x^s, y^s, z^s)^T$  is contained in the term  $= || \mathbf{R} - \mathbf{r} ||$ . Since the satellite coordinates and clock correction can be computed from the satellite ephemeris, the receiver antenna position  $\mathbf{r}$  and the receiver clock parameter,  $dT$ , can be estimated using measurements from at least four GPS satellites. Clearly, such a solution is affected by tropospheric error, ionospheric error, orbital error, multipath and receiver noise. The single point positioning accuracy is about 100 m (2DRMS) horizontally and 156 m vertically under SA (Wells, et al., 1986).

In a multi-antenna GPS system, pseudorange measurements play two roles. Firstly, they are used for the computation of the absolute platform location which is needed at each observation epoch to define the local level coordinate system on the WGS84 ellipsoid. Secondly, depending on the

antenna baseline lengths or the carrier ambiguity resolution methods adopted, the differential pseudorange solution between two antennas may also be used for the determination of carrier phase ambiguity search volume. To define a local level coordinate system to which the platform attitude is referred, the horizontal position, e.g. latitude and longitude, of the moving platform is needed (Torge, 1980). For such a purpose, the single point pseudorange solution obtained from the master antenna on the platform can be used. With a horizontal accuracy of about 100 m (2DRMS) from pseudorange solutions, the errors induced from the origin uncertainty of the local level coordinate system for the baseline vector between the antennas are less than 0.5 mm for a 50 metre long baseline (See Appendix). These magnitudes are much less than those of carrier phase multipath influences on baseline vectors, which can easily reach 1~2 cm in a strong multipath environment. Therefore, the errors resulting from the position uncertainty of the local level coordinate system can be neglected, especially for short baseline multi-antenna systems.

In the case that pseudorange measurements are used to define the carrier phase ambiguity search volume of a remote (slave) antenna, the double difference (receiver-satellite) pseudorange observables are usually formed for this purpose. Due to the short baseline lengths (e.g. < 50 m) between the multiple GPS antennas, most of the errors such as tropospheric and ionospheric effects, orbital errors, satellite and receiver clock errors are cancelled through the differencing process. The receiver code measurement noise ( $p_{rx}$ ) and the multipath error ( $p_{mult}$ ), however, are amplified. In a standard one-chip spacing delay-lock-loop (DLL) C/A code receiver, the pseudorange receiver measurement noise is at the level of 1~3 m, while the multipath influences on

the C/A code can typically reach about 10 to 20 m in the marine environment (Lachapelle et al., 1989). Recently, a new C/A code tracking technology, e.g. Narrow Correlator Spacing, has been implemented in some receivers such as NovAtel GPSCard™ sensors. The correlator spacing in this new generation of receivers can be adjusted to a 0.05 C/A code chip length resulting in a 10-15 cm C/A code measurement noise and improved multipath rejection (Fenton et al., 1991; Van Dierendonck et al., 1992). Multipath effects on double difference pseudorange observables range from 20 to 70 cm in a land kinematic environment. One metre (1 ) differential positioning accuracy using these precise C/A code measurements has been achieved in both land and marine applications (Cannon and Lachapelle, 1992; Lachapelle et al., 1993).

The most accurate measurement provided by GPS receivers for positioning is the carrier phase. The observation equation for the raw carrier phase measurement is given as (Wells et al., 1986)

$$= + c(dt - dT) + N + d - d_{\text{ion}} + d_{\text{trop}} + (\text{mult}) + (\text{rx}) \quad (2.2)$$

where  $\text{mult}$  = measured cycles ( in metres),

$N$  ... is the integer carrier phase cycle ambiguity,

$d$  ... is the carrier wavelength (m),

$(\text{mult})$  ... is the carrier phase multipath error (m),

$(\text{rx})$  ... is the receiver carrier phase measurement noise (m),

while the remaining terms in Eqn. (2.2) are the same as those defined in Eqn. (2.1).

Compared with pseudorange measurements, the main advantages of carrier phase measurements are the low measurement noise level which is usually less than 1 mm, and the low multipath effects which are less than 0.25 (Georgiadou and Kleusberg, 1988). For accurate platform attitude determination, differential carrier phase observations have to be used in order to derive very precise baseline vectors between antennas in a multi-antenna system. One challenging requirement using the carrier phase observation is that the integer ambiguity  $N$  has to be correctly resolved and any cycle slips in the carrier phase data need to be detected and corrected. Otherwise, the estimated attitude parameters will be severely distorted due to the incorrect baseline vectors computed from the wrong ambiguities. Carrier phase ambiguity resolution and cycle slip detection will be further investigated in Chapters 4 and 5.

The carrier phase rate or Doppler frequency is another measurement output by most GPS receivers. As the name implies, the carrier phase rate is the time derivative of the phase, and reflects the relative motion between the satellite and the vehicle. The observation equation for raw phase rate measurements can be expressed as

$$\dot{\phi} = \dot{\phi} + c(\dot{d}_I - \dot{d}_T) + \dot{d} - \dot{d}_{ion} + \dot{d}_{trop} + (\dot{\phi}_{mult}) + (\dot{\phi}_{rx}) \quad (2.3)$$

where  $\dot{\phi}$  ... is the phase rate measurement (m/s),  
 $\dot{d} = \|\dot{\mathbf{r}} - \dot{\mathbf{R}}\|$  is the range rate between satellite and receiver,  
 and  $(\dot{\phantom{x}})$  ... denotes a derivative with respect to time.

Since the satellite velocity and clock drift is known from the ephemeris, the vehicle velocity and receiver clock drift can then be determined using Doppler

frequency measurements from at least four satellites. Doppler frequency measurements have no cycle ambiguity problems and are not affected by cycle slips. Low frequency errors such as ionospheric and tropospheric errors and multipath effects are attenuated by the time derivative. The Doppler frequency measurement noise can be as low as 0.001 Hz (0.2 mm/s) for some receivers (Ashjaee et al., 1989). Single point velocity estimation accuracy is about 30 cm/s with SA on and 2 cm/s with SA off (Zhang, 1993).

### **2.3.2 Double Difference Observations**

Raw pseudorange and carrier phase measurements given by Eqns. (2.1) and (2.2) are affected by a number of errors. One effective way to remove or reduce these errors is to difference the measurements between satellites and receivers. Differencing measurements simultaneously collected by two receivers with respect to the same satellite will cancel the satellite clock errors and greatly reduce satellite orbit and atmospheric errors. This process is called single differencing ( ) between receivers. If the simultaneous 'between-receiver' single differences related to two different satellites are further differenced, the receiver clock error is eliminated and the resultant observation is called the double difference ( ). This process is depicted in Figure 2.2.

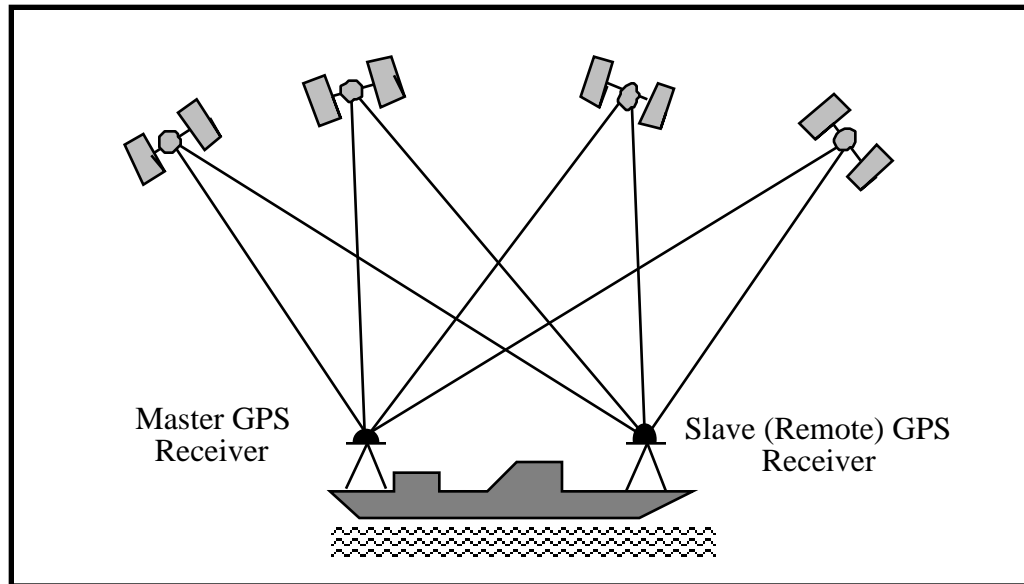


Figure 2.2

### GPS Double Differencing

The double difference observation equations are usually expressed as

$$p = + d + d_{ion} + d_{trop} + (p_{mult}) + (p_{rx}) \quad (2.4)$$

$$= + N + d - d_{ion} + d_{trop} + (mult) + (rx) \quad (2.5)$$

$$= + d - d_{ion} + d_{trop} + (mult) + (rx) \quad (2.6)$$

where represents the between receiver difference and is the between satellite difference.

Because of the short baseline separations between the multiple antennas in a multi-antenna system, e.g. generally < 50 m, the spatially correlated ionospheric and tropospheric errors as well as the orbital errors as indicated in Eqns. (2.4), (2.5) and (2.6) are virtually eliminated by differencing and their effects on relative positioning can be neglected. The remaining errors are

receiver noise and multipath effects, which are amplified through the differencing process.

For a GPS multi-antenna system which integrates three or four off-the-shelf independent GPS sensors, double difference observations have to be used to eliminate the receiver clock errors. As discussed in Section 2.2, double difference observations are also used in some dedicated attitude receivers which use a common oscillator for all the multiple antenna banks. This is because the residual receiver clock errors or the so-called line biases still exist between different antenna banks. In order to use single difference observations with dedicated attitude receivers, the line biases should be carefully calibrated for each receiver and taken into account in the data processing (Cohen et al., 1992; Axelrad and Ward, 1994). Obviously, the calibrated line biases will be valid only if they keep constant during the following surveying mission. In order to adapt to a wide range of hardware configurations and applications, the double difference model will be used for algorithm and software development throughout this research.

#### **2.4 CARRIER PHASE MULTIPATH AND ITS INFLUENCE ON ATTITUDE DETERMINATION**

As pointed out in the last sub-section, atmospheric errors, orbit errors, satellite and receiver clock errors in raw carrier phase measurements are almost eliminated by double differencing due to the short antenna separations within a GPS multi-antenna system. The remaining errors are receiver noise

and multipath effects. The combined receiver noise on double difference carrier phase observations is less than 2 mm since the undifferenced carrier phase receiver noise is usually less than 1 mm in modern GPS receivers (Cannon, 1992; Nolan et al., 1992). Multipath effects, however, can easily reach 1 to 2 cm in marine and land environments. Therefore, multipath is the dominant error source for baseline vector determination and attitude estimation in GPS multi-antenna systems.

#### 2.4.1 Description of Carrier Phase Multipath

Multipath is the phenomenon whereby a signal arrives at a GPS antenna via two or more different paths. In the vicinity of reflective objects like walls, buildings, trees and water surfaces, multipath errors are likely to occur. In this case, the received signal is a composition of the direct signal and one or more constituents which are reflected from nearby objects. A mathematical description of carrier phase multipath can be found in the papers by Bishop et al. (1985), Georgiadou and Kleusberg (1988) and Van Nee (1993). In the following, only a brief illustration is given with regard to some properties of carrier phase multipath effects.

In the presence of a single reflector near an antenna, the received signal voltage,  $S$ , at the antenna phase centre can be expressed as (Georgiadou and Kleusberg, 1988; Van Nee, 1993):

$$S = S_d + S_r , \quad (2.7)$$

with  $S_d = V_d \cos( \quad )$ , (2.8)

$$S_r = V_r \cos(\phi_r + \theta), \quad (2.9)$$

where  $S$  ... is the received signal,  
 $S_d$  ... is the direct line-of-sight signal,  
 $S_r$  ... is the reflected signal,  
 $V_d$  ... is the amplitude of the direct signal  $S_d$   
 $\phi_d$  ... is the phase of  $S_d$   
 $V_r$  ... is the amplitude of the reflected signal  $S_r$ ,  
and  $\theta$  ... is the phase shift of the reflected signal.

Usually, the reflected signal has a much smaller signal strength,  $V_r$ , and a phase shift,  $\theta$ , when compared with the direct signal. After some trigonometric manipulations with Eqns. (2.7), (2.8) and (2.9), the received signal can be written as

$$S = V_d \cos(\phi_d + \theta), \quad (2.10)$$

$$\text{with } \theta = (1 + \cos \phi) (1 + 2 \cos \phi + 2 \cos^2 \phi)^{1/2} / (\sin \phi), \quad (2.11)$$

$$= \arctan(\sin \phi / (-1 + \cos \phi)), \quad (2.12)$$

$$\text{and } \phi = V_r / V_d. \quad (2.13)$$

The phase change  $\theta$  in the received composite signal  $S$  is the carrier phase multipath error due to the interference. For a fixed  $\phi$ , the maximum multipath error can be derived from Eqn. (2.12) by setting its first derivative with respect to  $\phi$  to zero,

$$\theta_{\max} = \pm \arcsin(\phi). \quad (2.14)$$

Eqn. (2.14) indicates that the maximum phase multipath error depends on the ratio of signal strength between the reflected signal and the line-of-sight signal. The maximum absolute value is  $90^\circ$  for  $\rho = 1$ , which is 4.8 cm for the L1 GPS carrier phase and 6.0 cm for the L2 carrier phase.

If we assume  $\rho \ll 1$  and neglect the high order terms, the multipath effect in eqn. (2.12) can be approximated as

$$\sin(\theta). \quad (2.15)$$

Due to the changing geometry between the satellite and reflector, the phase shift angle  $\theta$  between the reflected signal and the direct signal will slowly change in time, resulting in a sinusoidal change in carrier phase multipath errors (Bishop et al., 1985; Georgiadou and Kleusberg, 1988). In the case of multiple reflectors, the above simple sinusoidal error pattern of multipath will be further complicated due the different strengths and initial phase angles of the reflected signals from different objects. However, periodical changes or time-dependent variations will always prevail in carrier phase errors over short baselines in a multipath environment, which gives a means to detect multipath effects in most situations. Using the double difference carrier phase observations with known integer ambiguities, carrier phase residuals from a least squares adjustment will absorb most of the multipath effects on double difference observables except for the long period (low frequency) variations which will be absorbed in the parameter estimation. For kinematic positioning with low and medium dynamic platforms, such as hydrographic surveying ships, the periodic pattern of multipath errors can still be observed, e.g. Lachapelle et al., (1993), Lu et al. (1993). This is due to the relatively fixed

surroundings in the vicinity of a GPS antenna and its rigid mounting on a ship. In an airborne environment, previous investigations by Braasch and Van Graas (1991) had indicated that code multipath errors were randomized when the aircraft was in motion and flexing. Even though the code and carrier are intimately related, the extension of this conclusion to carrier phase multipath effects needs more support from real carrier phase data analyses in airborne environments.

In addition to multipath and receiver noise, another kind of error which may affect attitude estimation is antenna phase centre variations. For micro-strip GPS antennas, which are used with most GPS receivers, the differential phase centre variation will be reduced significantly if the same kind of antennas in the same orientation are used in a GPS multi-antenna system (Geiger, 1988). Usually, the phase centre variation is within 1.5 mm (Jurgens et al., 1991). This error is not going to be discussed further in this research.

#### **2.4.2 Carrier Phase Multipath Effects on Attitude Estimation**

In order to show carrier phase multipath effects on platform attitude estimation, static tests with a four-receiver GPS multi-antenna system were performed on March 4 and 5, 1994 on the lower roof of the Engineering Building at The University of Calgary. The antenna baseline lengths are within the range of 3 to 5 m in this test. The antenna configuration is shown in Figure 2.3.

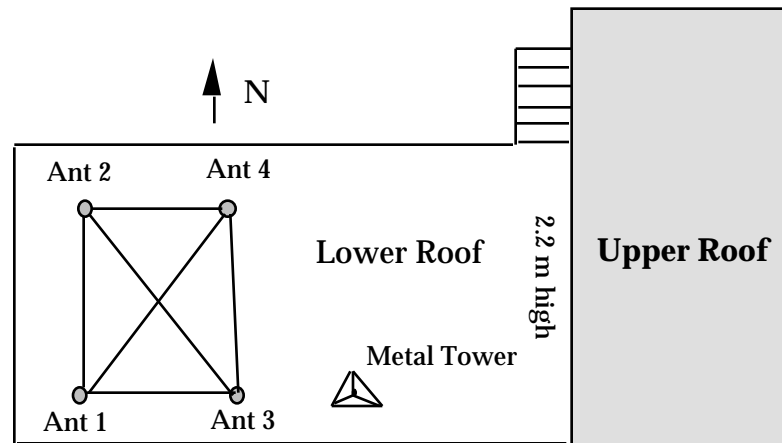


**Figure 2.3 Static Roof Test of a Multi-Antenna System**

Due to the reflections from the wall and metal tower above the antennas, the roof is considered to be a high multipath location. Since the antenna platform is stationary, the estimated platform attitude parameters should be constant from epoch to epoch. This provides a way to show multipath effects on the estimated attitude parameters if periodic or time-related variations occur and are correlated from day to day. It should be noted that receiver noise only causes small random changes of attitude parameters.

Shown in Figures 2.4, 2.5 and 2.6 are the estimated antenna platform yaw, pitch and roll from epoch to epoch for two consecutive days. In order to compare the results, the components from the second day were offset by 0.3 degrees and moved back 4 minutes in time. In a fixed static environment, multipath errors will repeat themselves about four minutes early from day to day due to the approximate 11 hours and 58 minutes orbital period of the GPS satellites around the earth.

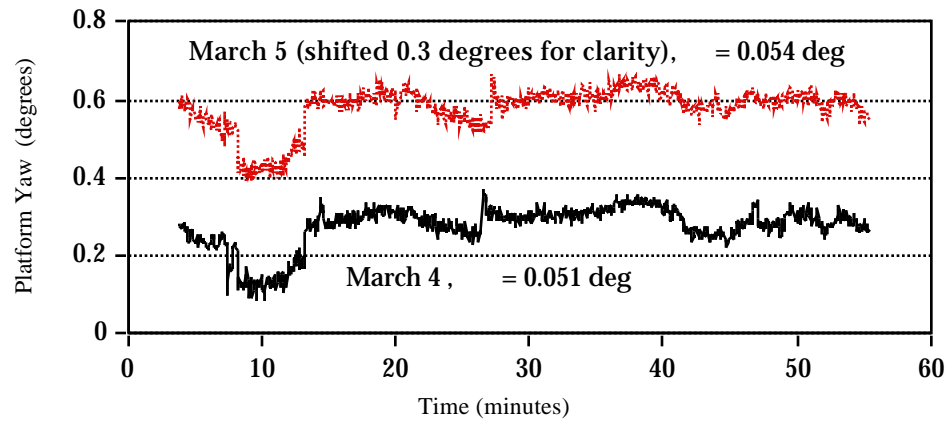


**Figure 2.4 Platform Yaw for March 4 and March 5 Static Tests**

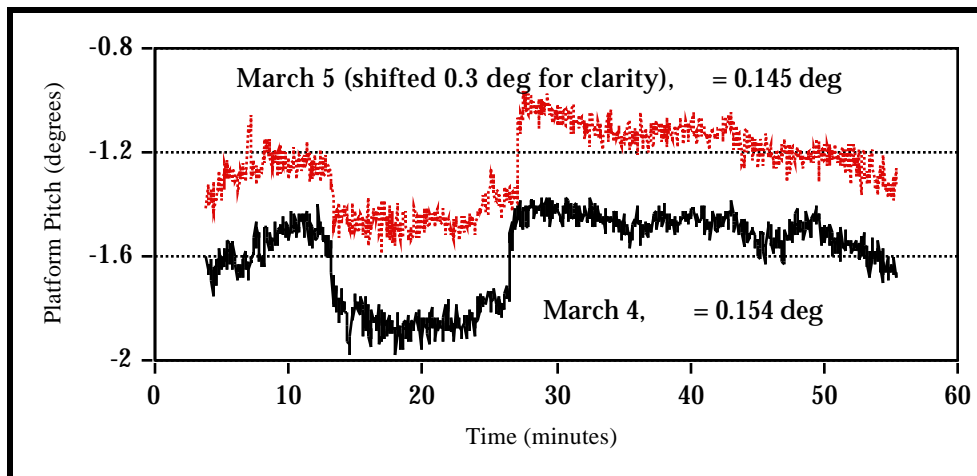


**Figure 2.5 Platform Pitch for March 4 and March 5 Static Tests**

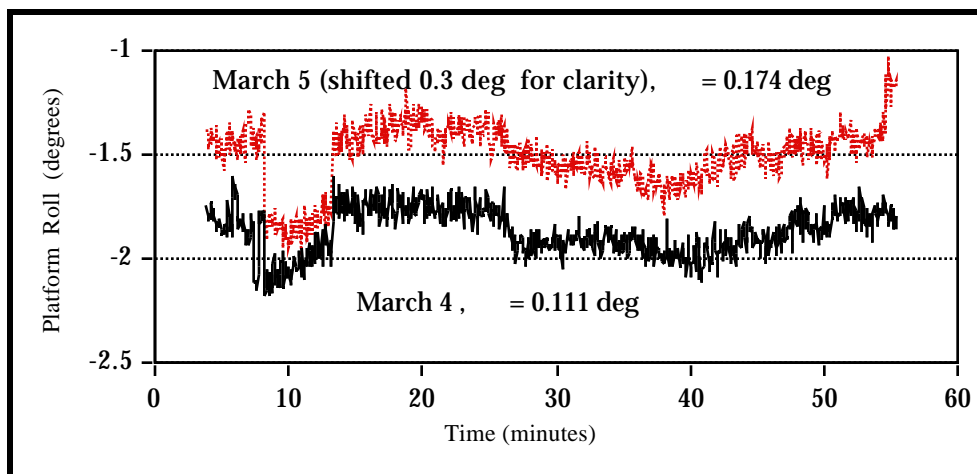


**Figure 2.6 Platform Roll for March 4 and March 5 Static Tests**

It can be seen clearly from the results in Figures 2.4, 2.5 and 2.6 that the variation pattern of the estimated attitude parameters for the second day is very similar to that of the first day. The maximum correlation reaches 0.89, which indicates that the errors are indeed caused by multipath that is repeatable in a fixed location. The jumps in yaw, pitch and roll components were caused by changes in satellite geometry. The loss of a low elevation satellite SV 27 at time  $t = 7$  minutes induced a drop in yaw and roll values, while the acquiring of a new satellite SV 4 at time  $t = 12$  minutes corresponded to a jump in yaw and roll components as well as a drop in the pitch component. Depending on the relative geometry between the satellite and baseline vector, the effect of losing or acquiring a satellite on yaw, pitch and roll may be different. For example, the loss of SV 7 at time  $t = 25.9$  minutes caused a noticeable jump in the pitch values but very small changes in yaw and roll components. Usually, the low elevation satellite significantly strengthens the satellite geometry but is much more affected by multipath.

The computed standard deviation in this example is 0.05 degrees for yaw, 0.15 degrees for pitch and about 0.17 degrees for roll. The relative baseline positioning accuracy, translated from the above computed standard deviation for attitude parameters, is about 0.34 cm to 1 cm level by using an average baseline length of 4 metres in this test. This level of accuracy is within the expected accuracy range of carrier phase positioning in a multipath environment. The relationship between the estimated attitude accuracy and the positioning accuracy will be investigated in Chapter 3.

Shown in Figure 2.7 are the double difference carrier phase residuals for the satellite pair SV 15 - SV 2 over baseline 1-2. The plotted residuals for the second day (March 5, 1994) were offset by 1 cm for clarity.

The results again clearly indicate the existence of multipath influence on carrier phase measurements. The residual series from the two consecutive days have very similar variation patterns and the maximum correlation coefficient is 0.69. The computed RMS of the double difference carrier phase residuals are 0.44 cm for March 4 test and 0.39 cm for March 5 test. The maximum residuals reach about -1.2 cm. No chokering ground planes were used in this test.

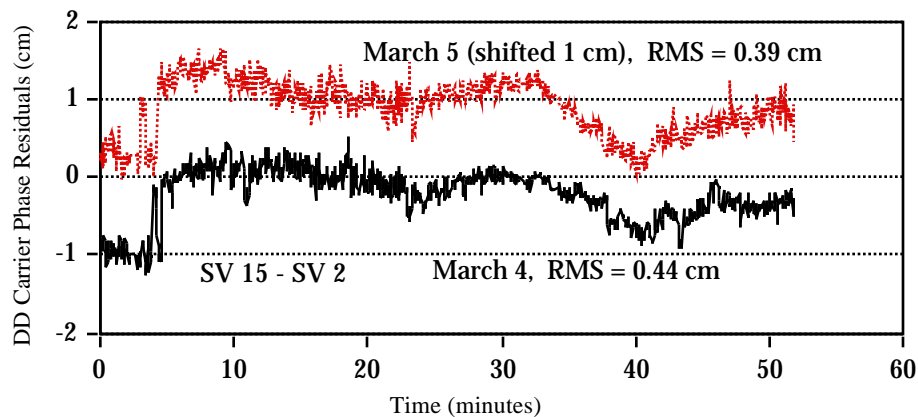


**Figure 2.7 Double Difference Carrier Phase Residuals for March 4 and 5 Static Tests**

The above example has shown that carrier phase multipath is the main error source for attitude determination using multi-antenna GPS systems. In order to achieve the highest accuracy in attitude determination, multipath

should be avoided or reduced as much as possible. Generally, there are four ways to reduce multipath effects:

- (1) Selection of a clear antenna site where no reflective objects are within the vicinity of the antenna,
- (2) Use of the effective ground planes such as RF absorbent ground planes and chokering ground planes,
- (3) Mathematical modeling of multipath signatures, and
- (4) On-line receiver multipath reduction techniques.

Selection of a clear antenna location is the common technique in GPS surveying and navigation. It can reduce multipath effects and chances of signal obstruction. Unfortunately, it is not always possible to do this in some situations, especially on a ship or on an airplane with limited space for mounting GPS antennas.

Use of an RF absorbent ground plane or chokering ground plane with GPS antennas can reduce the multipath effects on both pseudorange and carrier phase measurements. These ground planes can effectively prevent the interference of signals reflected from low elevation objects such as pavement and water surface. Depending on the multipath environment, the accuracy improvement can reach 20% ~ 50% for pseudorange and about 30% for carrier phase measurements (Cannon and Lachapelle, 1992; Lachapelle et al., 1993; Lu et al., 1993).

Mathematical modeling of multipath errors has been studied by a number of researchers. For example, Cohen and Parkinson (1991) used an 8th order spherical harmonic function to model the multipath errors generated by 24 hours differential carrier phase data collected in a fixed antenna environment. Based on the repeatability of multipath errors in a fixed antenna environment, the expected multipath error for a satellite appeared in a certain azimuth and elevation seen from the antenna body frame can then be computed using the model and applied to the corresponding differential carrier phase observation. Apparently, the derived multipath model will only work well if the relative antenna environment remains constant. A different multipath correction method proposed recently by Axelrad et al. (1994) overcomes the above problem. The theoretical background behind this method is that like phase angles, the amplitude of the received carrier signal is also affected by multipath. Therefore, the recovered carrier signal to noise ratio (SNR) output from a GPS receiver and the known antenna gain can be used to model the multipath signals, namely to determine the frequency, amplitude and phase offset of each multipath constituent presented in the data set. By directly working with SNR values output from GPS receivers, multipath corrections can be generated for each data set without worrying about the change of the antenna environment. A static test conducted over a short baseline showed that significant multipath reduction can be achieved by this method. However, the application of this method to real-time or near real-time multipath correction remains a challenge. The key requirement is the development of fast and reliable adaptive frequency estimation techniques based on the available real-time data segment. In a complex multipath

environment where no dominant frequencies prevail, the efficiency of this method may also decrease due to the difficulty of frequency identification by spectral methods.

On-line receiver multipath reduction techniques are the most promising methods to reduce the multipath effects on GPS pseudoranges and carrier phase observations. For example, the so-called Narrow Correlator Spacing technology can reduce the C/A code measurement noise to 10 cm level and significantly alleviate multipath influences on code measurements. This is because the degree of multipath effects on code tracking is proportional to the correlator spacing between the "early" and "late" correlators (Van Dierendonck et al., 1992; Meehan and Young, 1992; Van Nee, 1993). However, the carrier phase multipath, which is the dominant error for attitude determination, is not reduced at all by narrow correlator spacing.

Multipath estimating delay lock loop (MEDLL™) and an antenna design with multipath rejection capability are two emerging receiver technologies which are capable of reducing multipath effects significantly on pseudoranges and carrier phase measurements (Van Nee, 1992; Van Nee et al., 1994). A detailed discussion of these techniques is out of the scope of this research, however. The basic concept of MEDLL is to find an optimal set of spread-spectrum signals, say  $M+1$  signals including the line-of-sight signal plus  $M$  multipath signals, which give the best possible fit to the received signal from a GPS satellite. The amplitudes, phases, time delays and even the number of signals are estimated simultaneously within the delay lock loop using the samples of the incoming signal over a short period. The multipath signal

effects can then be removed by subtracting the estimated multipath correlation functions from the total down-converted correlation function. Tests with a prototype MEDLL receiver have shown that 60% to 90% of code multipath can be removed and a similar performance on carrier phase multipath reduction is expected (Van Nee et al., 1994). With further improvements of MEDLL technology as well as the GPS antenna design with better multipath rejection capability, multipath effects on GPS measurements will be alleviated dramatically in the future.

## CHAPTER 3

### ATTITUDE ESTIMATION USING GPS

GPS is basically a ranging system which provides position, velocity and time information to users. By determining the precise relative positions of at least three points in space, attitude parameters of the platform associated with these three points can be derived. In this chapter, the coordinate systems, the rotation matrix and several existing attitude estimation methods are reviewed. A least squares attitude estimation procedure is developed. Error analysis of the estimated attitude parameters is performed and the impact of the antenna configuration is discussed.

#### 3.1 COORDINATE SYSTEMS AND ROTATION MATRIX

The attitude of a platform is the orientation of its body frame coordinate system with respect to a reference coordinate system in space. It is well known that the orientation of one coordinate system can be made identical to the other through some rotations which can be expressed in the form of a rotation matrix. Therefore, the coordinate system and rotation matrix are two basic elements in defining and estimating the platform attitude.

### 3.1.1 Coordinate Systems

In order to define the platform attitude precisely and adapt to various applications, three coordinate systems are usually used in GPS attitude determination. They are the local level, vehicle platform and GPS antenna body frame coordinate systems.

#### ***Local level coordinate system***

The local level coordinate system is used as the reference to measure the attitude of a platform. This coordinate system is a topocentric system defined on the best-fitting ellipsoid (e. g. WGS84) and rotates with the earth. In case that a platform is perfectly aligned with this reference system, the roll, pitch and yaw of the platform will be zero. The definition of the local level frame is as follows:

- origin - at the master antenna of the multi-antenna GPS system,
- $X^l$ -axis - towards ellipsoidal east
- $Y^l$ -axis - towards ellipsoidal north,
- $Z^l$ -axis - pointing upwards along the ellipsoidal normal and forming a right hand system with  $X^l$  and  $Y^l$  axes.

A graphical representation of the local level frame on an ellipsoid is given in Figure 3.1.

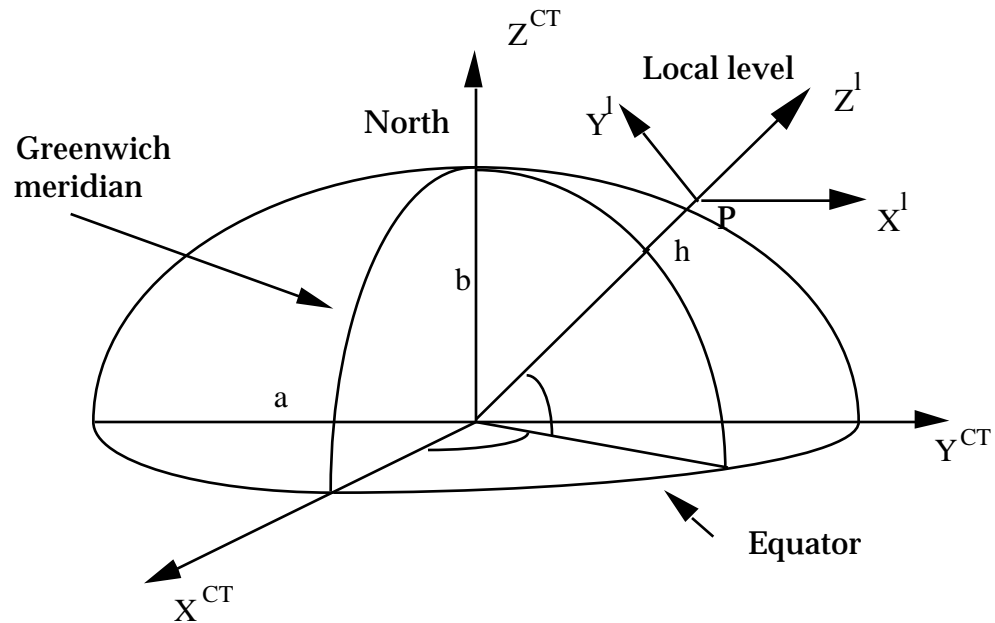


**Figure 3.1 Conventional Terrestrial System and Local Level System**

The Conventional Terrestrial (CT) system used in GPS positioning is WGS84 (Wells et al., 1986). Suppose that a baseline vector from Antenna 1 (master antenna) to Antenna 2 (slave antenna) and its associated covariance matrix are determined by GPS in the WGS84 system. In order to use this baseline vector for attitude determination, it needs to be transformed into the current local level system with the origin at Antenna 1 whose location  $(\lambda, \phi, h)$  is determined, for instance, by single point positioning using pseudorange measurements from Antenna 1. The transformation formulas from the CT-system to a local level system for a baseline vector, as well as its associated covariance matrix, are well documented in, e.g. Torge (1980), Schwarz and Krynski (1993) and also given in the Appendix. From geometric intuition, the variances for local level coordinates  $(x, y, z)$  should be equal to the variances of longitude, latitude and height of Antenna 2, since  $x$  is in the longitude direction,

y is in the latitude direction and z is in the height direction. This is shown clearly in the Appendix.

### ***Vehicle platform coordinate system***

The vehicle platform coordinate system is defined by the user. This is the platform whose attitude is of interest. For instance, a ship's platform coordinate system may be defined by the plane of the main deck. The yaw direction is the ship's centre line (y-axis) laying on the plane of the main deck. The x-axis is perpendicular to the centre line pointing to the starboard and also laying on the plane of the main deck. The z-axis then forms a right-handed coordinate system with the x and y axes. The ship's attitude components are then the rotation angles of this ship's platform system with respect to the local level coordinate system. Yaw is the rotation angle about the z-axis, count-clockwise positive. Pitch is the rotation angle about the rotated x-axis, upward positive. Roll is the rotation angle about the rotated y-axis, left-side up positive. These definitions are depicted in Figure 3.2.

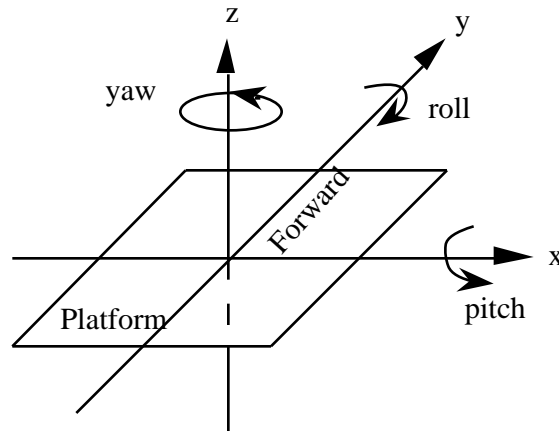


**Figure 3.2 Definition of Attitude Parameters in a Vehicle Platform Coordinate System**

### **Antenna body frame coordinate system**

The antenna body frame coordinate system is usually formed by choosing three GPS antennas, as three points in space defining a plane. Once the antenna plane or platform is defined, a coordinate system can then be set up. Without loss of generality, it can be assumed that Antenna 1, Antenna 2 and Antenna 3 form the desired antenna plane. The origin is chosen at Antenna 1. The y-axis (yaw direction) is along the baseline from Antenna 1 to Antenna 2. The x-axis lies in the plane formed by Antenna 1, Antenna 2 and Antenna 3, points to the right and is perpendicular to the y-axis. The z-axis then forms a right-handed system with x and y axes. For simplicity, this coordinate system is sometimes is called the *body frame system*. A graphical representation of the antenna body frame coordinate system is shown in Figure 3.3.

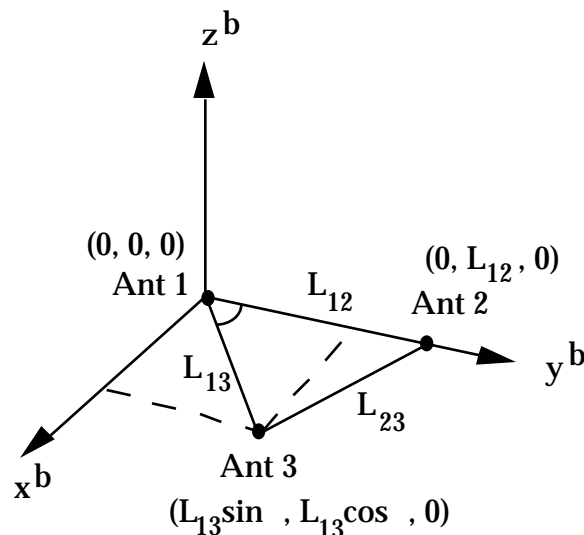


**Figure 3.3 Antenna Body Frame Coordinate System**

The antenna body frame coordinate system is considered as a rigid body frame and the relative positions between the antennas remain unchanged during all kinematic movements. Depending on the situation, the GPS antenna coordinates in this antenna body frame coordinate system can be precisely determined by using GPS static or "on-the-fly" kinematic methods, or even conventional surveying methods. These antenna coordinates are only needed to be determined once for a rigid body antenna configuration and can be held fixed in later applications.

On some occasions, the antenna body frame coordinate system may be identical or parallel to the vehicle platform coordinate system. If this is the case, the attitude of the antenna body frame system is equal to the attitude of the vehicle platform that is considered. In most cases, however, it is very difficult to set up the GPS antennas exactly parallel to the vehicle's platform coordinate system. Therefore, misalignment angles between the two coordinate systems need to be determined and taken into account in the computations to give the correct attitude information for the vehicle platform. If the GPS antennas are mounted rigidly on a vehicle or ship, the misalignment angles between the vehicle platform and the antenna body frame will be constant.

By using a GPS multi-antenna system, the attitude of the GPS antenna body frame with respect to the local level frame can be precisely computed at each observation epoch. These attitude values can then be rotated into the defined vehicle platform coordinate system if the misalignment angles between

the two platforms are known. Therefore, the main problem is to determine antenna body frame attitude parameters using GPS observations.

### 3.1.2 Rotation Matrix

To bring two Cartesian coordinate systems together identically involves two operations, namely translation and rotation. In attitude determination, only the rotation is of interest, since the translation does not change the orientation of a coordinate system. Assuming that two coordinate systems have the same origin but different orientation, it is well known that one system can be rotated into the other system by three consecutive rotations along the coordinate axes. Each rotation can be expressed by a matrix. In a right-handed system, the rotation matrices correspond to rotations about the x, y and z axes are given by (Wertz et al., 1978; Schwarz and Krynski, 1992)

$$R_1(\alpha) = \begin{bmatrix} 1 & 0 & 0 \\ 0 & \cos \alpha & \sin \alpha \\ 0 & -\sin \alpha & \cos \alpha \end{bmatrix}, \quad \text{rotation about x-axis,} \quad (3.1a)$$

$$R_2(\beta) = \begin{bmatrix} \cos \beta & 0 & -\sin \beta \\ 0 & 1 & 0 \\ \sin \beta & 0 & \cos \beta \end{bmatrix}, \quad \text{rotation about y-axis,} \quad (3.1b)$$

$$R_3(\gamma) = \begin{bmatrix} \cos \gamma & \sin \gamma & 0 \\ -\sin \gamma & \cos \gamma & 0 \\ 0 & 0 & 1 \end{bmatrix}, \quad \text{rotation about z-axis.} \quad (3.1c)$$

There are many types of rotation sequences to align one coordinate system with another. For example, the rotations can be made first about the x-

axis, secondly about the rotated  $y'$ -axis and then about the rotated  $z''$ -axis. This sequence is denoted by 1-2-3 sequence and the overall rotation matrix which aligns the two coordinate systems is the matrix product of  $R_1(\alpha)R_2(\beta)R_3(\gamma)$ . The three rotation angles are called Euler angles. In a similar fashion, the rotations can also be made in the 3-1-2 sequence with the first rotation about the  $z$ -axis, the second about the rotated  $x'$ -axis, and the third about the rotated  $y''$ -axis. The overall rotation matrix in this sequence is  $R_2(r)R_1(p)R_3(y)$ . This means that the three Euler rotation angles which align two coordinate systems are not unique and they depend on the specified rotation sequence. Any overall rotation matrix which aligns two Cartesian coordinate systems will fix the orientation of one coordinate system with respect to the other completely in a specific sequence. For this reason, the overall rotation matrix is also called an attitude *matrix*.

There are different ways to express an attitude matrix. A detailed discussion on the attitude matrix and its different expressions can be found in Wertz (1978). The quaternion form and the Euler axis/angle expression for the attitude matrix are often used in spacecraft attitude determination algorithms (Shuster and Oh, 1981; Markley, 1988). In this research, the rotation matrix parameterized by three Euler angles with the rotation sequence 3-1-2 is adopted because it is widely used in marine and inertial surveying applications (Loncarevic, 1993; Wong, 1988). The three Euler rotation angles are called yaw (heading), pitch and roll. The overall rotation matrix can be easily obtained as

$$R_{312}(y, p, r) = R_2(r)R_1(p)R_3(y) =$$

$$\begin{pmatrix} \cos(r)\cos(y) - \sin(r)\sin(p)\sin(y) & \cos(r)\sin(y) + \sin(r)\sin(p)\cos(y) & -\sin(r)\cos(p) \\ -\cos(p)\sin(y) & \cos(p)\cos(y) & \sin(p) \\ \sin(r)\cos(y) + \cos(r)\sin(p)\sin(y) & \sin(r)\sin(y) - \cos(r)\sin(p)\cos(y) & \cos(r)\cos(p) \end{pmatrix}, \quad (3.2)$$

where  $y$  denotes yaw,  $p$  denotes pitch and  $r$  denotes roll. The relationship between the rotation angles and the elements of the attitude matrix,  $R(i,j)$ , is

$$y = -\arctan\left(\frac{R(2,1)}{R(2,2)}\right), \quad (3.3a)$$

$$p = \arcsin(R(2,3)), \quad (3.3b)$$

$$r = -\arctan\left(\frac{R(1,3)}{R(3,3)}\right). \quad (3.3c)$$

By using Eqn. (3.3), the rotation angles can be easily computed if the attitude matrix (3.2) is known, or vice versa. It should be noted that all the rotations are defined in right-handed rotations in the above formulas.

The attitude matrix (3.2) rotates vectors in the reference frame to the body frame. This means that a vector  $(x, y, z)^T$  in the local level system (the current reference frame) will be mapped into  $(x^b, y^b, z^b)^T$  in the antenna body frame coordinate system through the attitude matrix, e.g.

$$\begin{pmatrix} x^b \\ y^b \\ z^b \end{pmatrix} = R_2(r)R_1(p)R_3(y) \begin{pmatrix} x \\ y \\ z \end{pmatrix}. \quad (3.4)$$

The yaw, pitch and roll angles are the orientations of the antenna platform with respect to the local level frame.

Even though the attitude matrix can have very different mathematical expressions, it possesses some common properties as a whole. The following

properties are applied to all the rotation matrices and are used throughout this research.

*Orthogonality:* Rotation matrix is an orthogonal matrix, i. e.

$$\mathbf{R}(y,p,r) \mathbf{R}^T(y,p,r) = \mathbf{I}; \quad \mathbf{R}^{-1}(y,p,r) = \mathbf{R}^T(y,p,r) . \quad (3.5)$$

From orthogonality, it is known that only three parameters in a rotation matrix are independent. The inverse of a rotation matrix equals its transpose and is also a rotation matrix. If  $\mathbf{R}(y, p, r)$  is a rotation matrix from the reference frame to the body frame,  $\mathbf{R}^T(y, p, r)$  is then the rotation matrix from the body frame to the reference frame.

*Product of rotation matrices:* The product of rotation matrices is again an orthogonal rotation matrix which is equivalent to applying the rotations sequentially.

*Cascade:* 
$$\mathbf{R}_H^I = \mathbf{R}_G^I \mathbf{R}_H^G , \quad (3.6)$$

where  $\mathbf{R}_G^I$  is the rotation matrix from the G-frame to the I-frame,  $\mathbf{R}_H^G$  is the rotation matrix from the H-frame to the G-frame and  $\mathbf{R}_H^I$  is the rotation matrix from the H-frame to the I-frame.

### 3.2 ATTITUDE DETERMINATION USING GPS

GPS is a ranging system which mainly provides position and time information to the users. If three GPS antennas are properly mounted on a platform and the differential GPS measurements are simultaneously collected,

the baseline vectors from Antenna 1 (master antenna) to Antenna 2 and Antenna 3 can be determined. The orientation of the antenna platform defined by the three antennas can then be computed from the derived baseline vectors. Usually, the baseline vectors obtained by GPS are in the WGS84 system and are transformed into the local level coordinate system with the origin at the master antenna. The problem of attitude parameter estimation using GPS is formulated as follow:

***Problem of attitude estimation using GPS:*** Given  $n$  ( $n \geq 2$ ) non-collinear baseline vectors whose coordinates or directions are determined in a local level coordinate system as well as in a specified antenna body frame coordinate system, find the rotation matrix or the orientation parameters which rotate the baseline vectors in the local level system into the corresponding antenna body frame system.

A similar problem has existed in spacecraft attitude determination before the appearance of GPS, where the platform attitude parameters are sought from a set of vector measurements made by celestial sensors (Wertz, 1978). In GPS multi-antenna systems, the vector measurements, e. g. the baseline vectors, or, equivalently the differential carrier phase measurements with ambiguities resolved, are provided by GPS. In this section, some existing methods are reviewed and a least squares attitude estimation procedure is given which can take the full covariance matrix of vector observations into account and is easy for accuracy analysis of the estimated attitude parameters.

### 3.2.1 Review of Some Methods for Attitude Estimation from Vector Observations

Attitude estimation using vector observations was originated from early works on spacecraft attitude determination with celestial sensors. Wahba (1965) defined this problem as finding the optimal attitude matrix,  $R(3 \times 3)$ , that minimizes the least squares loss function

$$J(R) = \sum_{i=1}^n w_i \| \mathbf{b}_i - R\mathbf{u}_i \|^2, \quad (3.7)$$

where  $\mathbf{b}_i$  ... is the unit vector in the platform body frame,  
 $\mathbf{u}_i$  ... is the unit vector in the reference frame and,  
 $w_i$  ... is a scale weighting factor related to  $\mathbf{u}_i$ .

After some algebraic operations, it is easy to show that Eqn. (3.7) can be modified as

$$J(R) = \text{tr}(\mathbf{B}^T \mathbf{B}) + \text{tr}(\mathbf{U}^T \mathbf{U}) - 2\text{tr}(\mathbf{R} \mathbf{A}^T), \quad (3.8)$$

where  $\mathbf{A} = \mathbf{B} \mathbf{U}^T$ ,

$$\mathbf{B} = (\sqrt{w_1} \mathbf{b}_1, \sqrt{w_2} \mathbf{b}_2, \dots, \sqrt{w_n} \mathbf{b}_n),$$

$$\mathbf{U} = (\sqrt{w_1} \mathbf{u}_1, \sqrt{w_2} \mathbf{u}_2, \dots, \sqrt{w_n} \mathbf{u}_n),$$

and  $\text{tr}()$  is the trace of a matrix.

Clearly, minimizing Eqn. (3.7) is equivalent to maximizing the last term in Eqn. (3.8), i. e.

$$J'(R) = 2\text{tr}(\mathbf{R} \mathbf{A}^T) \Rightarrow \max. \quad (3.9)$$

There have been several methods developed to directly solve for the attitude matrix  $R(3 \times 3)$  in the above equations. The well-known ones are the singular value decomposition (SVD) method by Markley (1988) and q-method by Davenport (Wertz, 1978; Shuster and Oh, 1981). All of them are based on some type of singular value decomposition or eigenvalue decomposition of the matrix  $A$  or its variants.

In the SVD method, the matrix  $A$  is replaced by its singular value decomposition and the attitude matrix  $R$  is expressed by the Euler axis/angle form. The minimization of the loss function, Eqn. (3.8), is then obtained by properly choosing the rotation angle of the rotation matrix. In the q-method, the rotation matrix  $R$  in (3.9) is expressed by its quaternion form. The four quaternions representing the optimal rotation matrix are obtained as the eigenvector corresponding to the maximum eigenvalue of a symmetric  $4 \times 4$  matrix, the elements of which are simple linear combinations of the elements of matrix  $A$ . Detailed derivations of these two methods can be found in Markley (1988) and Shuster and Oh (1981).

One drawback related to SVD and eigenvector decomposition methods is the complexity of accuracy analysis of the estimated attitude parameters. For each method, one has to independently derive the covariance analysis formulas for attitude parameters through the error propagation into the steps of eigenvalue decomposition and estimation. This results in lengthy formulas and extra computation for error analysis which is needed for system integration and surveying applications.

Another drawback of the direct solution of the rotation matrix  $R$  by a SVD or eigenvector method is that the variance and covariance information related to the vector  $\mathbf{b}_i$  and  $\mathbf{u}_i$  are not properly taken into account in the estimation process. In case both  $\mathbf{b}_i$  and  $\mathbf{u}_i$  have errors which are propagated into the estimation through different ways, it is not a straightforward task to represent both kinds of errors by using a single scale  $w_i$ . Furthermore, in multi-antenna GPS systems, the vector  $\mathbf{b}_i$  and  $\mathbf{u}_i$  are vector observations which have three components with a covariance matrix obtained from GPS differential positioning. Representing a covariance matrix using a scale factor will result in the loss of some information. To overcome this problem, Cohen et al. (1992) modified the loss function (3.7) into a special form suitable for GPS multi-antenna attitude determination. In this case, the loss function is defined as:

$$J(\mathbf{R}) = \left| \mathbf{W}_B^{1/2} (\mathbf{R} - \mathbf{B}^T \mathbf{R}_S) \mathbf{W}_S^{1/2} \right|^2, \quad (3.10)$$

where

$$= \begin{matrix} & \begin{matrix} 11 & 12 & \cdots & 1m \end{matrix} \\ \begin{matrix} 21 \\ 22 \\ \cdots \\ n1 \end{matrix} & \begin{matrix} 22 & \cdots & 2m \\ \cdots & \cdots & \cdots \\ n2 & \cdots & nm \end{matrix} \end{matrix}$$

with  $\varphi_{ij}$  representing the single difference carrier phase measurement over baseline  $i$  to satellite  $j$ ,

$\mathbf{B} = (\mathbf{b}_1, \mathbf{b}_2, \dots, \mathbf{b}_n)$  is the matrix with body frame baseline vectors,

$\mathbf{S} = (\mathbf{s}_1, \mathbf{s}_2, \dots, \mathbf{s}_m)$  is the matrix consisting of line-of-sight unit

vectors, i.e. partial derivatives, to all the satellites,

- $R$  ... is the rotation matrix,
- $W_S$  ... is the weighting matrix for differential phase measurements,
- $W_B$  ... is the weighting factor for body frame baselines.

The solution of the attitude matrix  $R$  in (3.10) is obtained by a similar SVD method as used for Eqn. (3.8) when the baseline weighting matrix is chosen as  $W_B = V_B^{-2} V_B^T$ , where  $V_B$  and  $U_B$  are the SVD of  $B$  such that  $B = U_B V_B^T$  (Cohen et al., 1992). In this solution, the measurement errors are fully taken into account in the estimation process by  $W_S$ , but the body frame coordinate errors are not, because  $W_B$  has to be taken as a special form and the baseline vectors should not be coplanar. The difficulties in accuracy analysis of the estimated attitude parameters remain the same as the previous SVD method.

In view of the above problems with SVD or eigenvector methods, a least squares estimation procedure is presented in the research. This procedure is based on the implicit least squares model where both the body frame vectors and the corresponding reference frame vectors are treated as vector observations whose covariance matrices can be properly taken into account. The accuracy analysis of the estimated attitude parameters is naturally included in the least squares process.

As a final remark on the existing methods for attitude estimation, an algebraic method or direct computation method is described, which computes platform attitude using only the two non-collinear baseline vectors that define the antenna platform (Wertz, 1978). Suppose that two non-collinear unit

vectors  $\mathbf{u}_1$  and  $\mathbf{u}_2$  in the reference frame and the corresponding unit vectors  $\mathbf{b}_1$  and  $\mathbf{b}_2$  in the body frame are given. The task is to find an attitude matrix  $\mathbf{R}$  which satisfies

$$\mathbf{R} \mathbf{u}_1 = \mathbf{b}_1, \quad \mathbf{R} \mathbf{u}_2 = \mathbf{b}_2. \quad (3.11)$$

Using vectors  $\mathbf{u}_1$  and  $\mathbf{u}_2$ , an orthogonal triad  $(\mathbf{g}_1, \mathbf{g}_2, \mathbf{g}_3)$  in the reference system can be set up as

$$\mathbf{g}_1 = \mathbf{u}_1, \quad \mathbf{g}_2 = \mathbf{u}_1 \times \mathbf{u}_2 / |\mathbf{u}_1 \times \mathbf{u}_2|, \quad \mathbf{g}_3 = \mathbf{g}_1 \times \mathbf{g}_2. \quad (3.12)$$

Similarly, an orthogonal triad  $(\mathbf{s}_1, \mathbf{s}_2, \mathbf{s}_3)$  in the body frame system can also be constructed by  $\mathbf{b}_1$  and  $\mathbf{b}_2$  as

$$\mathbf{s}_1 = \mathbf{b}_1, \quad \mathbf{s}_2 = \mathbf{b}_1 \times \mathbf{b}_2 / |\mathbf{b}_1 \times \mathbf{b}_2|, \quad \mathbf{s}_3 = \mathbf{s}_1 \times \mathbf{s}_2. \quad (3.13)$$

By definition, the rotation or attitude matrix  $\mathbf{R}$  will map the triad in the reference frame into the corresponding triad in the body frame, i.e.

$$\mathbf{R}(\mathbf{g}_1, \mathbf{g}_2, \mathbf{g}_3) = (\mathbf{s}_1, \mathbf{s}_2, \mathbf{s}_3) \Leftrightarrow \mathbf{R} \mathbf{M}_g = \mathbf{M}_s, \quad (3.14)$$

where  $\mathbf{M}_g$  and  $\mathbf{M}_s$  are 3x3 orthogonal matrices. From Eqn. (3.14), the attitude matrix can be solved as

$$\mathbf{R} = \mathbf{M}_s \mathbf{M}_g^T. \quad (3.15)$$

Once the attitude matrix is obtained, the rotation angles can be computed by Eqn. (3.3). This method is simple in derivation and fast in computation. No inverse and trigonometric functions are involved to compute  $\mathbf{R}$ . The only requirement is that the two vectors should be non-collinear

(independent). From a statistical point of view, however, this method is sub-optimal because only partial information of the two vectors is used and only two vectors can be used at a time. In practice, it is often used as an onboard processing scheme or an approximation method to provide good initial attitude values for least squares estimation algorithms.

### **3.2.2 Direct Computation Formulas for Attitude Parameters**

It has been shown that to compute attitude parameters, two sets of coordinates are needed for each baseline. One set is the reference frame coordinates, the other set is the body frame coordinates. In GPS multi-antenna systems, the reference frame coordinates are derived by GPS differential positioning for each epoch in a local level frame with the origin at the master antenna. The body frame coordinates, on the other hand, are assumed to have been determined through an initialization process and remain unchanged in all kinematic movements. In this section, it will be shown that the attitude of a GPS antenna platform can be directly computed using only the antenna local level frame coordinates derived by GPS. The body frame coordinates of the GPS antennas are not needed explicitly because some of the body frame coordinate components take zero values.

Assuming that a GPS antenna platform coordinate system or body frame is defined as in Figure 3.3 based on three antennas. Antenna 1 is the origin of the coordinate system and the baseline from Antenna 1 to Antenna 2 defines the yaw, i.e. y-axis. As indicated in Figure 3.3, the body frame

coordinates for Antenna 2 and Antenna 3 are  $\mathbf{b}_2 = (0, L_{12}, 0)^T$  and  $\mathbf{b}_3 = (L_{13}\sin(\theta), L_{13}\cos(\theta), 0)^T$ , respectively. The corresponding GPS-derived local level coordinates for these two antennas are  $\mathbf{u}_2 = (x_2, y_2, z_2)^T$  and  $\mathbf{u}_3 = (x_3, y_3, z_3)^T$ . Mathematically, the local level frame coordinates for each slave GPS antenna should be rotated into the corresponding body frame coordinates by the attitude matrix, i.e.

$$\mathbf{b}_i = \mathbf{R}_{213}(y, p, r)\mathbf{u}_i \quad . \quad (3.16)$$

Substituting Antenna 2 coordinates  $\mathbf{b}_2$  and  $\mathbf{u}_2$  into Eqn. (3.16) and using the orthogonality of attitude matrix  $\mathbf{R}_{213}(y, p, r)$ , the formulas for computing yaw and pitch are immediately obtained as

$$y = -\tan^{-1}(x_2 / y_2) \quad , \quad (3.17)$$

$$p = -\tan^{-1}(z_2 / \sqrt{x_2^2 + y_2^2}) \quad . \quad (3.18)$$

It can be seen from the formulas that the baseline between Antennas 1 and 2 actually determines the yaw and pitch of the antenna platform. Once the yaw and pitch are obtained, the local-level coordinates  $\mathbf{u}_3 = (x_3, y_3, z_3)^T$  of antenna 3 can be first rotated about the local level z-axis by an amount  $y$ , and then rotated again about the rotated local level x'-axis by an amount  $p$ . The resultant coordinates of Antenna 3 after these two rotations are denoted by  $(x_3'', y_3'', z_3'')$ . A third rotation,  $\mathbf{R}_2(r)$ , rotates  $(x_3'', y_3'', z_3'')$  to its body frame coordinates  $\mathbf{b}_3 = (L_{13}\sin(\theta), L_{13}\cos(\theta), 0)^T$ , namely

$$\begin{pmatrix} L_{13}\sin(\theta) \\ L_{13}\cos(\theta) \\ 0 \end{pmatrix} = \begin{pmatrix} \cos(r) & 0 & -\sin(r) \\ 0 & 1 & 0 \\ \sin(r) & 0 & \cos(r) \end{pmatrix} \begin{pmatrix} x_3'' \\ y_3'' \\ z_3'' \end{pmatrix} \quad . \quad (3.19)$$

From the third row in Eqn. (3.19), roll can be computed as

$$r = -\tan^{-1}(z_3'' / x_3'') \quad . \quad (3.20)$$

Eqns. (3.17), (3.18) and (3.20) are the direct computation formulas for yaw, pitch and roll. They only use GPS-derived local-level coordinates from three GPS antennas which define the platform and thus are not dependent on *a priori* body frame coordinates. This property is very useful in some situations where the antenna body frame coordinates are not known or in the initialization stage where the antenna body frame coordinates actually need to be determined precisely from GPS measurements.

As can be seen from the derivations, the direct computation method for attitude determination can only use two baseline vectors at a time. If more than two vectors are available, these can be utilized only by cumbersome combining the attitude solutions for various vector-pairs. The direct computation method is also sub-optimal in a sense that only three out of four independent direction angles provided by two vectors are used. This is reflected in the formulas as not using the  $y_3''$  component which is parallel to vector  $\mathbf{u}_2$ .

The accuracy of the computed yaw, pitch and roll by direct computation formulas can be easily derived based on error propagation laws. For instance, by differentiating Eqn. (3.17), the yaw error is

$$dy = - \frac{y_2 dx_2 - x_2 dy_2}{x_2^2 + y_2^2} \quad . \quad (3.21)$$

Applying the error propagation law to the above equation and neglecting the correlation among the coordinate components, the standard deviation of yaw is obtained as

$$\sigma_y = \sqrt{\cos^2(\gamma) \sigma_{x_2}^2 + \sin^2(\gamma) \sigma_{y_2}^2} / L_{12} \cos(p) \quad (3.22)$$

From the Appendix, the variances of local level coordinates ( $x_2$ ,  $y_2$ ,  $z_2$ ) are known to equal the variances of longitude, latitude and height of antenna 2, i.e.

$$\sigma_{x_2}^2 = \sigma_{\lambda}^2 = \text{RDOP}^2$$

$$\sigma_{y_2}^2 = \sigma_{\phi}^2 = \text{RDOP}^2$$

$$\sigma_{z_2}^2 = \sigma_h^2 = \text{RDOP}^2$$

$$\sigma_{z_2}^2 = \sigma_h^2 = \text{RVDOP}^2$$

where RDOP, RDOP and RVDOP are relative dilution of precision for longitude, latitude and height, respectively (Lachapelle, 1993). Thus Eqn.(3.22) becomes

$$\sigma_y = \text{AZDOP} / L_{12} \cos(p) \quad (3.23)$$

with  $\text{AZDOP} = \sqrt{\cos^2(\gamma) \text{RDOP}^2 + \sin^2(\gamma) \text{RDOP}^2}$ . AZDOP is often called azimuth DOP which is a figure of merit to measure the impact of satellite geometry and baseline orientation on the heading determination.

In the design or planning stage, it is often convenient to use an approximate formula to estimate the anticipated accuracy of the attitude determination system. Substituting  $\sigma_{x_2}$  and  $\sigma_{y_2}$  in Eqn. (3.22) with  $\max(\sigma_{x_2}, \sigma_{y_2})$  results in

$$\sigma_y = \max(\sigma_{x2}, \sigma_{y2}) / L_{12} \cos(p) = \max(\sigma_{x2}, \sigma_{y2}) / L_{12} \cos(p) . \quad (3.24)$$

It is apparent that the heading estimation accuracy is inversely proportional to the heading direction baseline length  $L_{12}$  when the positioning accuracy  $\max(\sigma_{x2}, \sigma_{y2})$  is fixed.

Through similar derivations, the formulas for pitch and roll accuracies can be obtained as

$$\sigma_p = \sqrt{\cos^2(p) \sigma_{h2}^2 + \sin^2(p) \cos^2(y) \sigma_{z2}^2 + \sin^2(p) \sin^2(y) \sigma_{x2}^2} / L_{12} , \quad (3.25)$$

$$\sigma_r = \sqrt{\cos^2(r) \sigma_{z3}^2 + \sin^2(r) \sigma_{x3}^2} / L_{13} \cos(\alpha) , \quad (3.26)$$

where  $\sigma_{x3}^2 = \cos^2(y) \sigma_{z3}^2 + \sin^2(y) \sigma_{x2}^2$ ,

$$\sigma_{z3}^2 = \sin^2(p) \sin^2(y) \sigma_{z2}^2 + \sin^2(p) \cos^2(y) \sigma_{x2}^2 + \cos^2(p) \sigma_{h3}^2 ,$$

and  $\alpha$  is the angle between baseline  $L_{13}$  and antenna body frame  $x^b$ -axis.

For approximate accuracy estimation during planning stages, the following formulas for pitch and roll can be used

$$\sigma_p = \sigma_{h2} / L_{12} = \text{VRDOP} / L_{12} , \quad (3.27)$$

$$\sigma_r = \max(\sigma_{x3}, \sigma_{z3}) / L_{13} \cos(\alpha) . \quad (3.28)$$

To derive Eqn. (3.27),  $\sigma_{x2}$  and  $\sigma_{y2}$  in Eqn. (3.25) are replaced by  $\sigma_{h2}$  because in GPS positioning, the accuracy of the height component is usually poorer than those of the horizontal components. From Eqns. (3.26) or (3.28), it can be seen that the roll error is minimum when the baseline  $L_{13}$  is perpendicular to the heading baseline  $L_{12}$ .

### 3.2.3 Attitude Estimation by an Implicit Least Squares Model

From Eqn. (3.2) it can be seen that the rotation matrix is solely defined by three rotation angles, i.e. yaw, pitch and roll. If the precise body frame coordinates for each antenna are known *a priori* through a survey or initialization process, least squares estimation of the three rotation angles ( $y$ ,  $p$ ,  $r$ ) can be made based on Eqn. (3.4). Suppose  $\mathbf{b}_i = (x_i^b, y_i^b, z_i^b)^T$  and  $\mathbf{u}_i = (x_i, y_i, z_i)^T$  are the body frame coordinates and their corresponding local level coordinates for antenna  $i$ . Based on Eqn. (3.4), for all the slave GPS antenna positions the following relation is obtained, i. e.

$$\mathbf{b}_i = R(y, p, r) \mathbf{u}_i, \quad i = 1, 2, \dots, n, \quad (3.29)$$

where  $n$  is the number of slave GPS antennas in the multi-antenna system.

In Eqn. (3.29), both  $\mathbf{b}_i$  and  $\mathbf{u}_i$  are treated as observations with covariance matrices  $C_{b_i}$  and  $C_{u_i}$ , respectively. The unknown parameters to be resolved are ( $y$ ,  $p$ ,  $r$ ). Such a model is a standard *implicit* least squares adjustment model and the solution is described in Krakiwsky (1987). A unique feature of this method is that the covariance matrix of the *a priori* body frame coordinates,  $\mathbf{b}_i$ , can also be included in estimation process. The linearized form of Eqn. (3.29) with respect to ( $y$ ,  $p$ ,  $r$ ) is expressed as

$$\mathbf{A}_i \hat{\mathbf{u}}_i + (\mathbf{B}_i \mathbf{I}) \hat{\mathbf{b}}_i + \mathbf{w}_i = \mathbf{0} \quad \text{with } C_{1_i} = \begin{bmatrix} C_{u_i} & \mathbf{0} \\ \mathbf{0} & C_{b_i} \end{bmatrix}, \quad (3.30)$$

where  $\mathbf{A}_i = \begin{bmatrix} \frac{\partial R}{\partial y} \mathbf{u}_i & \frac{\partial R}{\partial p} \mathbf{u}_i & \frac{\partial R}{\partial r} \mathbf{u}_i \end{bmatrix}_{3 \times 3}$  at initial values ( $y^0, p^0, r^0$ ),

$$\hat{\mathbf{c}} = (\hat{y}, \hat{p}, \hat{r})^T,$$

$\mathbf{B}_i = \mathbf{R}(y^0, p^0, r^0)$ ,  $\mathbf{I}$  is a 3x3 identity matrix and

$$\mathbf{w}_i = \mathbf{R}(y^0, p^0, r^0)\mathbf{u}_i - \mathbf{b}_i.$$

Assuming no correlation between various antenna positions and concatenating Eqn. (3.30) for  $n$  slave GPS antennas, the least squares solution for the three rotation angle corrections  $(\hat{y}, \hat{p}, \hat{r})$  is

$$\begin{aligned} \hat{\mathbf{c}} &= -\mathbf{N}^{-1}\mathbf{U} \\ &= -\left[ \sum_{i=1}^n \mathbf{A}_i^T (\mathbf{B}_i^T \mathbf{C}_{u_i} \mathbf{B}_i + \mathbf{C}_{b_i})^{-1} \mathbf{A}_i \right]^{-1} \left[ \sum_{i=1}^n \mathbf{A}_i^T (\mathbf{B}_i^T \mathbf{C}_{u_i} \mathbf{B}_i + \mathbf{C}_{b_i})^{-1} \mathbf{w}_i \right]. \end{aligned} \quad (3.31)$$

The least squares solution for  $(y, p, r)$  and its covariance matrix are given by:

$$\begin{aligned} \hat{y} &= y^0 + \hat{y} \\ \hat{p} &= p^0 + \hat{p} \\ \hat{r} &= r^0 + \hat{r} \end{aligned}, \quad (3.32)$$

$$\mathbf{C}_{\hat{\mathbf{c}}} = \mathbf{C}(\hat{y}, \hat{p}, \hat{r}) = \left[ \sum_{i=1}^n \mathbf{A}_i^T (\mathbf{B}_i^T \mathbf{C}_{u_i} \mathbf{B}_i + \mathbf{C}_{b_i})^{-1} \mathbf{A}_i \right]^{-1}. \quad (3.33)$$

The initial approximate values  $(y^0, p^0, r^0)$  used for linearization in Eqn. (3.30) can be provided by the fast direct computation formulas (3.17), (3.18) and (3.20), which are so accurate that none to a few iterations are needed in the least squares process. The matrix inversion is only 3x3 and the accuracy of the estimated attitude parameters can be easily analyzed using Eqn. (3.33) which is already computed in the solution stage, i.e. Eqn. (3.31).

If the baseline lengths in a multi-antenna system are known precisely, only three satellites are needed to determine the baseline vectors between the master and slave antennas and thus to determine the platform attitude. It should be also noted that instead of using baseline vectors, the attitude parameters can be directly expressed as a function of double difference carrier phase measurements. For a baseline vector between the master and slave antennas, the double difference observation equation is

$$\begin{aligned}
 - \quad N &= D \mathbf{x} \\
 &= D T \mathbf{u} \\
 &= D T R^T(\mathbf{y}, \mathbf{p}, \mathbf{r}) \mathbf{b}
 \end{aligned} \tag{3.34}$$

where  $D$  ... is the design matrix (partial derivatives),  
 $\mathbf{x}$  ... is the vector in the CT-system,  
 $T$  ... is the transformation matrix from the CT-system to local level,  
 $\mathbf{u}$  ... is the vector in local level system  
 $R^T(\mathbf{y}, \mathbf{p}, \mathbf{r})$  is the attitude matrix and  
 $\mathbf{b}$  ... is the vector in the antenna body frame coordinate system.

Since the ambiguities are assumed to have been resolved and  $\mathbf{b}$  is known *a priori*, the unknowns to be solved for are yaw, pitch and roll in the attitude matrix  $R(\mathbf{y}, \mathbf{p}, \mathbf{r})$ . Concatenating all the observation equations from all the baselines between the master and slave antennas, a least squares estimation problem with an implicit model is again obtained. The standard procedure given in Krakivsky (1987) can be used for a solution.

Mathematically speaking, if all the variance and covariance information from the observations and body frame coordinates  $\mathbf{b}$  is properly propagated

through the estimation steps, the resulting attitude parameters should be equal for the baseline approach in Eqn. (3.29) and the carrier phase measurement approach in Eqn. (3.34).

Compared with the direct computation method, the least squares estimation of the attitude parameters is optimal since all the position information contained in the multiple GPS antenna system is used. The accuracy of the estimated attitude parameters is obtained through the diagonal elements of the inverse of the normal matrix. Another advantage of least squares estimation over the direct computation is that the least squares solution is less affected by multipath on a single antenna since the solution is made by the best fit over all antenna positions.

### **3.3 ANTENNA CONFIGURATION IMPACT ON THE ACCURACY OF ATTITUDE DETERMINATION**

Platform attitude parameters are computed using baseline vectors or differential carrier phase observations from at least three non-collinear antennas. Depending on the satellite geometry, the antenna configuration and antenna separation, the computed attitude values and their accuracy will vary. The user community does not have much control over the GPS satellite geometry. Fortunately, with 24 satellites operational, the GDOP is normally less than three with six to eight satellites visible. The work to be done during the planning stage of setting up a GPS multi-antenna system is to properly select the antenna configuration to minimize the impact of errors on attitude

estimation. It should be noted, however, that GPS multi-antenna systems are usually used on moving platforms such as ships and airplanes. On such platforms, the locations suitable to place GPS antennas are very limited due to the shape of the aircraft, or to obstructions from various equipment on a ship, such as radar, bridge and masts. This makes the optimization of the antenna configuration virtually impossible in some practical situations where there is little space to move the antennas around.

As a general rule, the accuracy of the estimated attitude parameters is inversely proportional to the baseline lengths that define the platform. This means that the antenna separation within a multi-antenna system should be as long as possible in order to get high accuracy attitude parameters. Taking the pitch as an example, the relationship between pitch accuracy and baseline length is  $\sigma_p \approx h/L_{12}$ , as derived in the case of Eqn. (3.27) for the direct computation method. Shown in Figure 3.4 is the pitch accuracy as a function of baseline length when  $h$  is fixed to 1 cm and 2 cm, respectively.

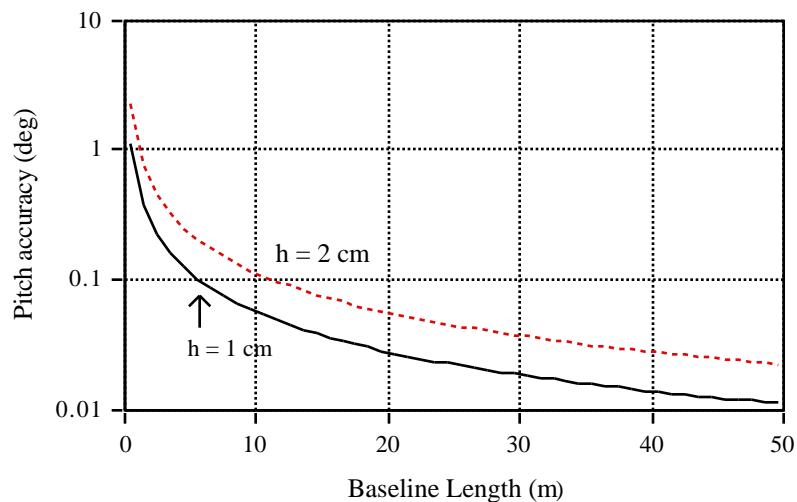


**Figure 3.4 Pitch Accuracy as a Function of Baseline Length**

Similar accuracy patterns are hold for yaw and roll components based on Eqns. (3.24) and (3.28). It can be seen from Figure 3.4 that a long baseline length is needed to get high accuracy attitude parameters. For instance, the baseline length required would be more than 50 metres long in order to reach an accuracy of  $0.01^\circ$  (36 arc-seconds) when  $h = 1$  cm. For most applications where small to medium size ships and airplanes are used, the baseline lengths are usually within 5 ~ 20 metres, which corresponds to an accuracy range from  $0.12^\circ \sim 0.03^\circ$ .

In the least squares estimation procedure, the accuracy of yaw, pitch and roll is given by the covariance matrix, Eqn. (3.33)

$$C^{\wedge} = C(\hat{y}, \hat{p}, \hat{r}) = [ \sum_{i=1}^n A_i^T (B_i^T C_{u_i} B_i + C_{b_i})^{-1} A_i ]^{-1},$$

where  $C_{u_i}$  is determined by the satellite geometry and measurement errors,  $C_{b_i}$  is obtained *a priori* through an initialization process and  $A_i$  reflects the antenna configuration impact on the accuracy of attitude parameters. The general optimization problem is then defined as seeking the minimum trace of matrix  $C^{\wedge}$ , i. e.

$$\text{tr}(C^{\wedge}) = \frac{1}{\text{tr}(\sum_{i=1}^n A_i^T (B_i^T C_{u_i} B_i + C_{b_i})^{-1} A_i)} \Rightarrow \text{minimum}. \quad (3.35)$$

The overall minimization of Eqn. (3.35) is too complicated and almost impossible in practice because it relates to satellite geometry, baseline lengths, antenna configuration and even the initial platform attitude values themselves. If all the baseline lengths are fixed to a constant value  $k$  and only the antenna

configuration effects are considered, Cohen et al. (1992) and Comp (1993) have pointed out that the optimal antenna configuration is the one for which

$$BB^T = k^2I, \quad \text{with } B = (\mathbf{b}_1, \mathbf{b}_2, \dots, \mathbf{b}_n) \text{ and identity matrix } I. \quad (3.36)$$

This means that the antenna vectors from the master antenna to slave antennas are equidistant and orthogonal. An actual small orthogonal triad using four GPS antennas is described and tested by Comp (1993). In practice, it would be very difficult, if it is not impossible, to set up such an orthogonal triad with wide antenna spacing on a ship or aircraft due to the limited space suitable for antenna locations. Therefore, the optimization of antenna configurations will not be discussed further in this research. The main purpose is to develop a multi-antenna system with flexibility and yet with optimal accuracy based on all the available information.

**CHAPTER 4**  
**ON-THE-FLY CARRIER PHASE AMBIGUITY RESOLUTION**  
**FOR MULTI-ANTENNA SYSTEMS**

Carrier phase measurements are inevitably required in order to estimate high accuracy attitude parameters using GPS. Since GPS receivers provide very accurate measurements of fractional carrier wave cycles plus the total number of integer cycle counts from the start of tracking, carrier phase measurements are ambiguous by an unknown number of integer cycles, the so-called phase ambiguity, before they give meaningful range information for positioning. Therefore, carrier phase ambiguity resolution plays a key role in high precision GPS positioning and thus attitude determination.

For multi-antenna GPS systems which are to be used on moving platforms for real-time applications, fast and reliable on-the-fly ambiguity resolution, i.e., ambiguity resolution while the receiver is in motion, is needed. Based on the integer nature of carrier phase ambiguities and least squares adjustment, several methods have been developed for this task. The typical ones are the Hatch's least squares ambiguity search method and the fast ambiguity search filter technique, both of which are successfully applied to on-

the-fly differential kinematic GPS positioning (Hatch, 1991; Lachapelle et al, 1993; Chen, 1994). In this chapter, modifications and improvements of these methods were carried out with the special conditions under a GPS multi-antenna system. In particular, the construction of potential ambiguity solutions, the impact of baseline and geometric constraints, the utilization of *a priori* attitude information from other onboard instruments and special antenna configurations are investigated and studied.

## **4.1 ON-THE-FLY AMBIGUITY RESOLUTION BY LEAST SQUARES METHODS**

### **4.1.1 General Concept**

In order to retain the integer characteristic of ambiguities, double difference observables between the satellite and receiver ( ) are used as the basic observation model in this research. For multi-antenna systems consisting of multiple GPS sensors, double differencing effectively cancels all the clock errors, orbital errors and atmospheric errors. The unknowns in observation equations consist of three position components and double difference integer ambiguities. If  $n$  satellites are tracked at an epoch,  $n-1$  carrier phase double difference observation equations are available to solve for  $3+(n-1)$  unknowns. Mathematically speaking, this is an underdetermined problem with many possible solutions. Fortunately, the ambiguities only take integer values and will be constant for the whole observation span if no cycle slips occur. This

allows employment of some mathematical strategies to solve for the cycle ambiguity problem while the receiver is either in motion or stationary.

A number of techniques have been proposed for on-the-fly carrier phase ambiguity resolution. Among them are the ambiguity function technique (Remondi, 1984; Mader, 1990), the narrow-lane and extrawide-lane technique (Wubben, 1989), the Hatch's least squares ambiguity search method (Hatch, 1989, 1991) and the fast ambiguity search filter technique (Chen and Lachapelle, 1994; Landau and Vollath, 1994). The ambiguity function technique is not sensitive to cycle slips, but requires extensive computation time (1 to 2 minutes), even for a 1-metre search cube. For this reason, the ambiguity function method is not suitable for use in GPS multi-antenna systems which aim at real-time applications. The extrawide-lane technique is primarily designed for working only with dual frequency P-code receivers which are rarely used for platform attitude determination tasks. The most appealing techniques capable of use in GPS multi-antenna systems are therefore the Hatch's least squares ambiguity search method and the fast ambiguity search filter method. Both of them are based upon the (sequential) least squares adjustment and upon the assumption that within a properly defined ambiguity search space and under normal error distributions, the correct ambiguity set will always be included in the search space and give the smallest sum of squares of carrier phase residuals among all the potential ambiguity sets. The conceptual steps for on-the-fly ambiguity resolution by least squares method are given in Figure 4.1.

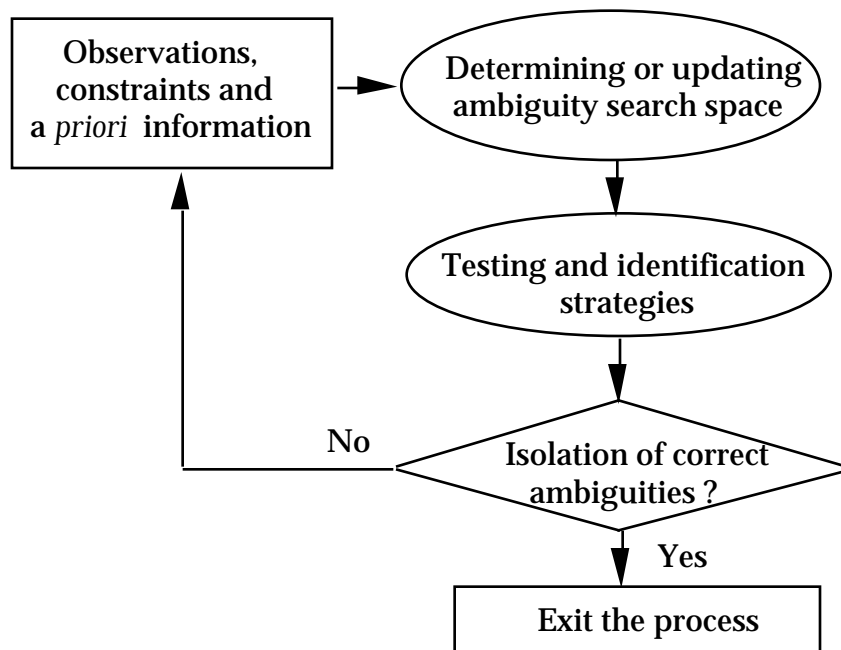


**Figure 4.1 General Concept of Ambiguity Search**

The process starts at a certain epoch with the GPS carrier phase and pseudorange observations plus the available *a priori* information. Usually, a least squares adjustment is performed based on all the provided data including carrier phases. The ambiguity search space, i.e., the change intervals of integer ambiguity, is derived from the related statistics. The potential ambiguity sets within the ambiguity search space are tested to determine the correct one. The testing criteria are usually based on statistics, such as the sum of squares of carrier phase residuals and floating ambiguity confidence intervals. To speed up the computation and improve efficiency, some special numerical algorithms can be employed or even the determination of search space and the testing of potential ambiguities can be interwoven so that an early exit or the inability of ambiguity resolution can be made before all the potential ambiguity sets are tried (Landau and Euler, 1992; Chen, 1994). The major difference between

Hatch's ambiguity search method and the fast ambiguity search filter technique lies in the way of construction of the ambiguity search space. In Hatch's method, only three ambiguity change intervals related to the four primary satellites are determined using the available information upon to that epoch. In the fast ambiguity search filter technique, however, the change interval for each ambiguity is determined sequentially as if the ambiguity parameters were eliminated or set to integers one by one. A more detailed discussion will be given in the next two sections.

Ambiguity resolution on-the-fly is not an easy task. It is affected by a number of factors which typically include errors and biases, satellite geometry and the search algorithms used. In least squares adjustment and statistical testing, the errors are normally assumed to be Gaussian and the derived statistics are tested under this assumption. In GPS positioning and attitude determination, however, this is not always true due to the corruption of multipath effects which tend to be cyclic in nature. Therefore, there exists a possibility that incorrect ambiguities may be chosen due the abnormal behaviour of the statistics in the presence of excessive non-Gaussian errors. The satellite geometry, including the number of satellites, also affects the reliability of on-the-fly ambiguity resolution. The bottom line is that enough geometric information has to be obtained or accumulated in the observations so that all the errors can be suppressed or smoothed out and the correct ambiguities become separable with the other alternatives. The general trend is that the more satellites in view and more geometry information accumulated, the greater the reliability for ambiguity resolution. The algorithm development for on-the-fly ambiguity resolution has been the focus on high

accuracy (cm-level) kinematic positioning for many years. In a general sense, an optimal on-the-fly technique for kinematic or real-time applications should possess the following properties:

- (1) Fast in computation and short in observation time span required for ambiguity resolution,
- (2) High reliability to ensure the correct ambiguity resolution and robust in the presence of non-Gaussian errors, and
- (3) Quality control against incorrect ambiguities and cycle slips.

Apparently, some of the above requirements are contradictory to each other and compromises may be necessary. For example, higher reliability of ambiguity resolution may require a longer time span of observations, while real-time applications may demand the observation span for ambiguity resolution as short as possible. Up to now, no ambiguity resolution method has met all the above requirements and improvements for the existing methods are needed.

#### **4.1.2 The Least Squares Ambiguity Search Method**

The least-squares ambiguity search method has been used in high precision static GPS positioning for a long time, e.g. Langley et al. (1984) and Wei (1986). In those early works, the ambiguities from all the satellites tracked are treated as independent parameters and the ambiguity search space was spanned over all the double difference ambiguity parameters which appeared

in the least squares adjustment. Such a treatment of ambiguities leads to a heavy computational burden. For instance, the possible ambiguity combinations to be tested will mount to  $21^5 = 3.9 \times 10^6$  if the ambiguity change interval is  $\pm 10$  cycles for six satellites in view.

A major improvement of the least squares ambiguity search method and its expansion for use in kinematic on-the-fly ambiguity resolution were made by Hatch in the late eighties (Hatch, 1989; 1991). In this improved method, two properties are used: (1) only three of the double difference carrier phase ambiguities are independent, and (2) the sum of squares of the adjusted carrier phase residuals (or equivalently the estimated variance factor) should be minimum at the correct ambiguity solution, provided the residuals have a Gaussian distribution. The first property means that once three double difference phase ambiguities are known correctly, the position of the moving receiver can be determined precisely, and therefore the ambiguities of the remaining satellites can be fixed. The four satellites chosen to be used to determine the ambiguities of the rest satellites are called *primary* satellites and the rest satellites are called *secondary* satellites. The change intervals of the three *primary* double difference ambiguities can be calculated either from a properly derived initial search cube around the remote GPS antenna or from the confidence intervals of the related floating ambiguity solutions from a sequential least squares adjustment. Since only three double difference ambiguities are searched, the ambiguity search space is three dimensional regardless of the number of satellites in view. If each ambiguity change interval is again assumed to be  $\pm 10$  cycles, the total ambiguity combinations to be tested would be  $21^3 = 9261$ . This is clearly less computationally intensive

when compared with the least squares ambiguity search method proposed in the early eighties. Each potential ambiguity set, i.e. three primary ambiguities given in the ambiguity search space, is checked using the observations from the remaining or secondary satellites. At the potentially correct solution, the computed observations for the secondary satellites should be very close to the corresponding measured observations, or in other words, the residuals should be minimized. From a statistical point of view, the agreement between the measured and the adjusted observations related to a chosen potential ambiguity set can be quantified by the quadratic form of residuals,  $\hat{v}^T C_{\text{obs}}^{-1} \hat{v}$ , where  $\hat{v}$  is the vector of least squares adjusted observation residuals and  $C_{\text{obs}}$  is the covariance matrix of observations. If the errors in observations are Gaussian and the tested ambiguity set is the correct one,  $\hat{v}^T C_{\text{obs}}^{-1} \hat{v}$  will have a Chi-square distribution (Koch, 1989). Therefore, testing the potential ambiguity set can be formulated as

$$\hat{v}^T C_{\text{obs}}^{-1} \hat{v} \leq \chi_{f,1-\alpha}^2, \quad (4.1)$$

where  $\chi_{f,1-\alpha}^2$  is the Chi-square percentile corresponding to the degrees of freedom  $f$  and confidence level  $1-\alpha$ . Usually,  $f = n-4$ , with  $n$  being the number of satellites. If the above test fails for a particular potential ambiguity set, this set is rejected from the potential solutions.

Due to the insufficient geometry information and error effects, more than one potential ambiguity set may pass the Chi-square test at a certain epoch. In this case, each passed ambiguity set is saved and further tested using the observations from the following epochs. The quadratic form of residuals related to an ambiguity set that passed the test is also saved and accumulated

with those from the following epochs. The test is then performed on the accumulated quadratic forms of residuals, which is called the 'global' test. As more epochs of observations are used, all the false ambiguity sets of the primary satellites will gradually be rejected except the correct one.

In order to accelerate the convergence time and reduce the effect of the *a priori* carrier phase variance ( $\sigma^2$ ), a ratio test is also used. When the number of potential ambiguity sets is reduced to a relatively low number after the global testing or the residual quadratic forms have been summed over a preset time period, the ratio of the two smallest quadratic forms of residuals is computed, namely

$$\text{Ratio} = \frac{(\hat{\mathbf{v}}^T \mathbf{C}_{\text{obs}}^{-1} \hat{\mathbf{v}})_{\text{secondmin}}}{(\hat{\mathbf{v}}^T \mathbf{C}_{\text{obs}}^{-1} \hat{\mathbf{v}})_{\text{min}}} > \text{threshold?} \quad (4.2)$$

If Ratio is greater than a preset threshold, the potential ambiguity set with the smaller quadratic form of residuals is selected as the correct ambiguity set. The idea behind the ratio test is that the residual quadratic form related to the correct integer ambiguity set should be relatively smaller than those related to the rest (wrong) ambiguity sets if enough geometric information is accumulated. The determination of the threshold value usually depends on the error magnitudes and multipath effects on carrier phase and 2 to 3 is often used in practice (Wei, 1986; Landau and Euler, 1992; Lachapelle et al., 1993). In some literature (Abidin, 1993), it is said that the ratio test is Fisher-distributed and the threshold is set at the F-percentile value. This is not generally true, however, because the two residual quadratic forms in Eqn. (4.2) are not statistically decorrelated.

As pointed out in Chapter 2, the errors in double difference carrier phase observations from a multi-antenna system mainly consist of multipath effects and the receiver noise. Under favourable conditions when multipath is low, the double difference carrier phase residuals will generally exhibit a normal distribution, which provides the foundation for statistical testing. Plotted in Figure 4.2 is the histogram for carrier phase residuals obtained from a ship-borne multi-antenna experiment which will be described in Chapter 6 (see Figure 6.25).

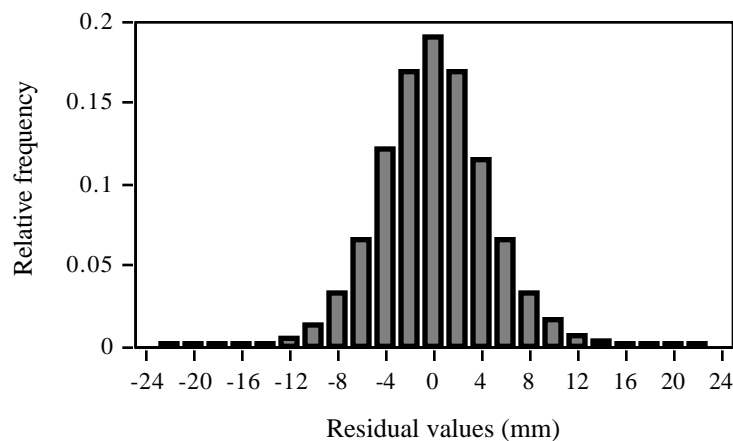


**Figure 4.2 Histogram for Carrier Phase Residuals Shown in Figure 6.25 (Baseline 1-3 Observations, SV 3 - SV 22)**

Due to good antenna locations and the use of chocking ground planes in this test, the multipath effects are relatively small and the histogram of the double difference carrier phase residuals have a Gaussian shape. Unfortunately, this is not always the case. In a strong multipath environment, the error distribution of carrier phase residuals may not be strictly Gaussian. For example, shown in Figure 4.3 are the histograms of adjusted carrier phase

residuals for the static roof test described in Chapter 2 (Figures 2.3 and 2.7), where strong multipath was experienced by the antennas. Histograms for a low elevation satellite SV 15 ( $26^\circ$  to  $10^\circ$ ) and a high elevation satellite SV 12 ( $23^\circ$  to  $50^\circ$ ) are plotted. The base satellite is SV 2.

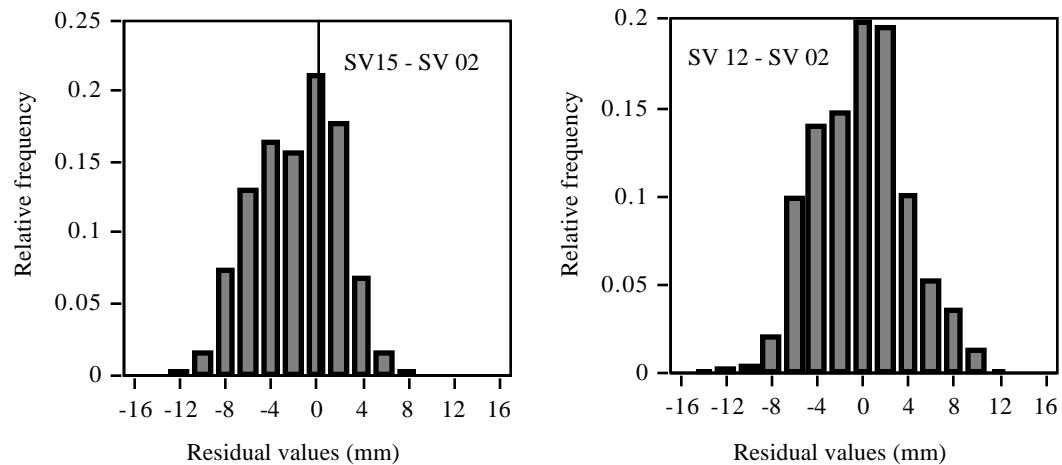


**Figure 4.3 Histograms for Carrier Phase Residuals from the Static Roof Test (Baseline 1-2 Observations)**

It can be seen that these histograms are not symmetric and are tailed on one side, especially for the low elevation satellite. If they are postulated with zero mean normal distributions, it is obvious that relatively large variances will be obtained (Vanicek and Krakiwsky, 1986). This is the main reason that a conservative carrier phase variance factor has to be used for statistical testing with Eqn. (4.1), in order to prevent the rejection of correct ambiguity set under a multipath environment.

As a comparison, the histograms of double difference carrier phase residuals corresponding to the incorrect ambiguities are also shown in Figure 4.4. The double difference ambiguity related to the satellite pair SV15 - SV 2 of baseline 1-2 for the static roof test was intentionally set to be in error by 1 cycle.

Again, the histograms for the low elevation satellite SV 15 and the high elevation satellite SV 12 are plotted.

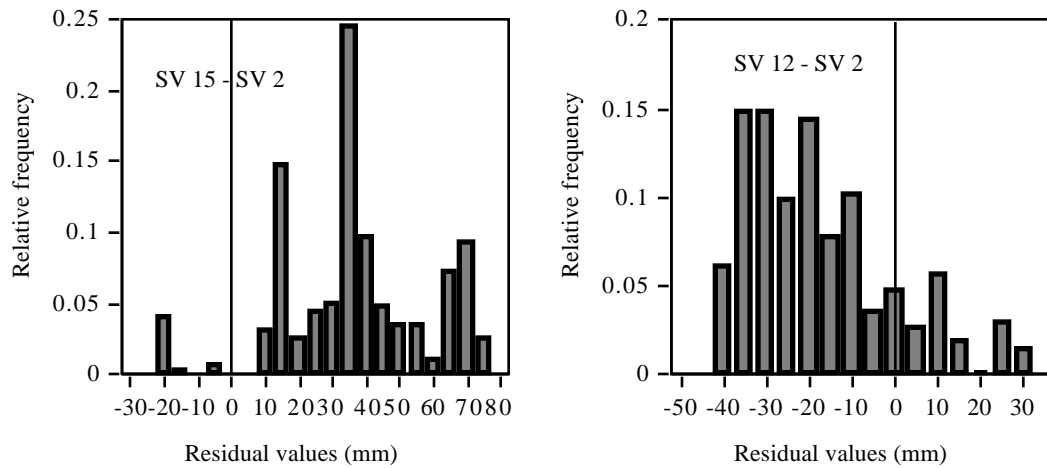


**Figure 4.4 Histogram for Carrier Phase Residuals with Incorrect Ambiguities ( $\nabla\Delta N_{15-2}$  in Error by 1 Cycle)**

It can be seen that the histograms of carrier phase residuals with the incorrect ambiguities are significantly different from Gaussian shape. Even though there are some residuals falling within  $\pm 10$  mm interval, the majority of them are larger than 20 mm level. With the relative geometry change resulting from the motion of satellites and the multi-antenna platform, the carrier phase residuals related to the wrong ambiguities will drift if five or more satellites are used in an adjustment. This means that if enough geometric information is obtained or accumulated, the wrong ambiguities will eventually be rejected.

For ambiguity resolution with a GPS multi-antenna system, residual testing is not the only testing criterion. The fixed baseline lengths among the antennas mounting on a rigid body platform provide another reliable and external criterion to select the correct ambiguities. The computed baseline lengths using the correct ambiguities should agree with the known baseline

lengths within the error limit caused by the measurement noise and multipath effects, which is usually less than 2 to 3 cm. All the ambiguity sets that do not meet the baseline constraints can be immediately rejected. For the incorrect ambiguity sets which pass the baseline test at a certain epoch, the computed baseline lengths with these ambiguity sets at subsequent epochs will eventually drift away from the known baseline length due to the relative geometry change between the baseline vector and satellites, as shown by Cannon (1991) and the example which will be given in Chapter 5. From this point of view, the baseline constraints can be used as the only means to select correct ambiguities for a GPS multi-antenna system mounted on a rigid body platform. However, combining the geometric information from the redundant satellites as well as the fixed antenna configuration will give a faster and reliable ambiguity solution.

For each potential ambiguity set related to the four primary satellites, a corresponding potential position of the remote antenna can be computed. The integer ambiguities for the secondary satellites can be determined by the formula

$$N_s(j) = \text{nint} \left( \frac{\text{obs}(j) - \text{calc}(j)}{\lambda} \right), \quad (4.3)$$

where  $N_s(j)$  is the calculated ambiguity related to the secondary satellite  $j$ ,  $\text{nint}(\cdot)$  is the nearest integer operator,  $\text{obs}(j)$  is the measured double difference carrier phase observation of the secondary satellite  $j$  in metres,  $\text{calc}(j)$  is the calculated double difference observation using the satellite coordinates and the potential position derived from the four primary satellites, and  $\lambda$  is the carrier wavelength. When all the ambiguities of the secondary

satellites are computed, a batch least-squares adjustment including all the primary and second satellites is carried out and the residual quadratic form related to the given potential ambiguity set can be calculated and tested.

In addition to the carrier phase noise and multipath effects discussed previously, other factors which affect the the speed and reliability of integer ambiguity resolution using the least squares search method include

- (1) the initial ambiguity search space,
- (2) the satellite geometry and the number of satellites in view, and
- (3) the selection of four primary satellites.

The prerequisite of determination of the initial ambiguity search space is to include the correct ambiguity set. This requires the search space is large enough to take into account all the effects of errors and biases on ambiguities. However, the search space can not be too large because the computational burden will increase rapidly and the test reliability will deteriorate. The best situation would be a search space as small as possible while including the correct ambiguity set inside. In later sections, a Cholesky decomposition method to construct the potential ambiguity sets on the sphere with a fixed baseline length will be developed. The use of *a priori* attitude information and special antenna configurations to reduce the ambiguity search space is investigated.

A minimum of five satellites is needed to carry out residual quadratic form testing, since residuals will be zero in the case of four satellites. The more satellites available at each epoch, the more redundant observations can be used

to check the potential ambiguity sets and the more reliable the test statistic. A more detailed investigation of satellite geometrical impact on the least squares ambiguity resolution can be found in Abidin (1993).

The selection of four primary satellites has two impacts on the ambiguity search. Firstly, it will affect the number of potential ambiguity sets within a given search cube. Secondly, it affects the computation of the ambiguities of secondary satellites. From previous studies (Hatch, 1989, 1991; Abidin, 1993), it is known that a poorer GDOP of the primary satellites will result in a smaller number of potential ambiguity sets to be tested within a given search cube. However, the GDOP of the primary satellites can not be too poor, otherwise incorrect ambiguities for the secondary satellites may be derived from the poor position determined by the primary satellites. In a multi-antenna system, the position determined by the primary satellites are also used for coarse check of the corresponding potential ambiguity set against the known baseline length. Usually, the GDOP of the selected primary satellites should not be larger than 10.

#### **4.1.3 Recent Developments for On-the-Fly Ambiguity Resolution**

On-the-fly ambiguity resolution has been the main focus for high precision kinematic GPS positioning and attitude determination. Recent advancements in this area include the ambiguity transformation method presented by Teunissen (Teunissen, 1994; Jonge and Tiberius, 1994) and the fast ambiguity search filter (FASF) proposed by Chen (Chen, 1993, 1994). The main

purpose of the ambiguity transformation is to reparametrize the integer ambiguities and overcome the difficulties of ambiguity search in an elongated ambiguity search space, which usually comes from a short time span carrier phase only adjustment. In reality, however, the ambiguity search space in kinematic GPS positioning is always derived using combined carrier and code methods and the elongation problem is usually not present, especially with high precision C/A code pseudorange measurements. In addition, some methods for searching ambiguities within the ellipsoid, regardless its shape, have been developed (Abidin, 1993). Therefore, the ambiguity transformation method is not going to be discussed in the following and only the FASF will be briefly described.

An unique feature of FASF is the sequential computation of ambiguity search intervals. The ambiguities which are assumed integer values are held fixed and excluded from the unknown vector. The covariance matrix of the remaining ambiguity parameters is then updated accordingly. By this way, the observation information related to the satellites with assumed integer ambiguities will help and improve the search interval of the remaining ambiguities due to the correlation among the ambiguity parameters. A similar scheme was also given by Blewitt (1989) for static GPS carrier phase ambiguity resolution, where the most likely 'correct' ambiguity was solved first and the solution as well as the covariance matrix was updated with all the previously fixed ambiguities excluded from the unknown vector.

FASF is based on the sequential least squares adjustment where the *a priori* estimates of position components and floating ambiguities obtained up

to the last epoch is combined with the new observations from the current epoch. Suppose that the sequentially adjusted quantities at a certain epoch are denoted as  $(\hat{\mathbf{x}}, C_{\hat{\mathbf{x}}}, \dots)$ , where  $\hat{\mathbf{x}} = (\hat{x}, \hat{y}, \hat{z}, \hat{N}_1, \hat{N}_2 \dots \hat{N}_n)^T$  is the solution of the unknown position vector and floating ambiguities,  $C_{\hat{\mathbf{x}}}$  is the covariance matrix and  $\dots$  is the quadratic form of residuals corresponding to the floating ambiguity solution. According to the covariance matrix  $C_{\hat{\mathbf{x}}}$ , the standard deviation for the floating ambiguity parameter  $N_n$  is  $\sigma_{N_n} = \sqrt{(C_{\hat{\mathbf{x}}})_{n+3, n+3}}$ . The search interval for  $N_n$  can then be defined as

$$\hat{N}_n - k \sigma_{N_n} \leq N_n \leq \hat{N}_n + k \sigma_{N_n}, \quad (4.4)$$

where  $k$  is a constant factor. Landau and Vollath (1994) have suggested to use  $k = 10$ . Usually, 3 to 10 can be assigned depending on the error behavior in the observations. Setting  $N_n$  to a given integer value, say  $\bar{N}_n$  within the search interval (4.4), is equivalent to the constraint

$$\mathbf{h}_n \hat{\mathbf{x}} = \bar{N}_n, \quad \text{with } \mathbf{h}_n = (0, 0, \dots, 0, 1). \quad (4.5)$$

According to the least squares formulas with constraints (Koch, 1988), the updated solution  $(\hat{\mathbf{x}}(n), C_{\hat{\mathbf{x}}}(n), \dots)$  with  $N_n$  set to integer number  $\bar{N}_n$  can be easily obtained as

$$\hat{\mathbf{x}}(n) = \hat{\mathbf{x}} - \mathbf{c}_{n+3} (\hat{N}_n - \bar{N}_n) / (C_{\hat{\mathbf{x}}})_{n+3, n+3}, \quad (4.6)$$

$$C_{\hat{\mathbf{x}}}(n) = C_{\hat{\mathbf{x}}} - \mathbf{c}_{n+3} \mathbf{c}_{n+3}^T / (C_{\hat{\mathbf{x}}})_{n+3, n+3}, \quad (4.7)$$

$$Q(n) = \dots + (\hat{N}_n - \bar{N}_n)^2 / (C_{\hat{\mathbf{x}}})_{n+3, n+3}, \quad (4.8)$$

where  $\mathbf{c}_{n+3} = ((C_{\hat{x}})_{1,n+3}, (C_{\hat{x}})_{2,n+3}, \dots, (C_{\hat{x}})_{n+3,n+3})^T$  is the last column related to  $N_n$  in  $C_{\hat{x}}$  and  $(C_{\hat{x}})_{n+3,n+3}$  is the diagonal element related to  $N_n$  in  $C_{\hat{x}}$ . It is noted that the updating process only uses the sequentially adjusted quantities  $(\hat{x}, C_{\hat{x}}, \mathbf{h}_n)$  and the constraint vector  $\mathbf{h}_n$ . The original observations are not required any more.

It is easy to show by Eqns. (4.6) and (4.7) that the ambiguity parameter  $N_n$  is set to the integer value  $\bar{N}_n$ , and the last column and row in matrix  $C_{\hat{x}}(n)$  are zero, which means the correlation between the variance of  $N_n$  and the updated variances of the remaining ambiguities is zero and all the satellite geometry information related to  $N_n$  is fully incorporated into the determination of the remaining ambiguity parameters. From Eqn. (4.7), one also notes that the diagonal elements (i.e., the variances) in  $C_{\hat{x}}(n)$  are always smaller than those in the original covariance matrix  $C_{\hat{x}}$ , which means the ambiguity search intervals for the remaining ambiguity parameters are reduced by fixing  $N_n$  to an integer number.

From Eqn. (4.8), the residual quadratic form  $(n)$  with  $N_n$  set to the integer number  $\bar{N}_n$  can be easily computed and it is always larger than the floating (or the previous) residual quadratic form. This is the reason that an early exit is possible. With the corresponding degrees of freedom and Chi-square distribution, the residual quadratic form related to each integer ambiguity within the search range (4.4) can be tested. If the test fails, i. e.

$$(n) > \frac{\chi^2_{f,1-\alpha}}{2}, \quad (4.9)$$

for a given integer ambiguity, this integer ambiguity is rejected and the test skips to the next integer within the search interval. If the test for a given integer number,  $\bar{N}_n$ , passes, this integer ambiguity is retained and combined immediately with the integer ambiguities from the second ambiguity parameter, say  $N_{n-1}$ . At this step, the search range for  $N_{n-1}$  is bounded by the second last diagonal element in  $C_{\hat{x}}(n)$ , i. e. its variance after  $N_n$  being fixed. With the substitution of  $(\hat{x}(n), C_{\hat{x}}(n), (n))$  for  $(\hat{x}, C_{\hat{x}}, )$ , the whole updating process from Eqn. (4.6) to (4.8) is then repeated whereby  $N_{n-1}$  is fixed to an integer number within its search range.

This sequential updating and testing process continues until all the ambiguity parameters are searched. If only one integer ambiguity combination related to all the ambiguity parameters is left and passed through the test, the integer ambiguities are considered to be resolved. If more than one integer ambiguity combinations are available, the ratio of the residual quadratic forms defined by Eqn. (4.2) is examined. In case that the integer ambiguities can not be resolved or all the integer combinations were rejected, the sequential least squares adjustment with all the ambiguity parameters as floating unknowns are carried out at the next epoch and the whole ambiguity search process starts again.

Like the least squares ambiguity search method, FASF is also based on statistics with normal error distributions to select the correct ambiguities. Its effectiveness and reliability are therefore affected by the receiver noise, multipath errors, observation biases, the number and geometry of satellites. Under the presence of excessive multipath or non-Gaussian observation biases,

the minimum quadratic form of residuals may not correspond to the correct integer ambiguities or even the true integer ambiguities may not be included in the computed search ranges defined by Eqn. (4.4). In this case, FASF will fail to find the correct integer ambiguities.

The sequentially computed ambiguity search ranges by Eqn. (4.4) should be large enough to cover the unmodelled errors such as multipath. This can be done by properly adjusting the measurement noise level and the constant factor  $k$ . Shown in Figure 4.5 is an example of the search ranges for five double difference ambiguity parameters. The data set was collected on August 25, 1992 with two NovAtel GPSCard™ receivers which were separated by 240 m.

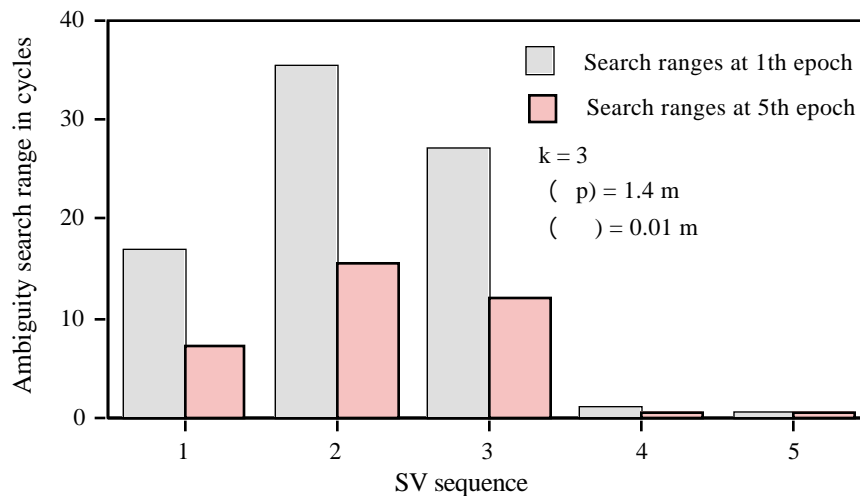


**Figure 4.5 Ambiguity Search Ranges from FASF**

It can be seen from Figure 4.5 that the sequentially computed ambiguity search ranges for the fourth and fifth satellites are substantially smaller than those of the first three satellites. This indeed suggests that only three double difference ambiguities, i.e. four primary satellites, are independent and the

ambiguities related to the rest satellites are fixed once three ambiguities are given. Very little gain is obtained in ambiguity search ranges after fixing the fourth and subsequent satellites, especially after a few epochs of observations. For instance, if only the first three ambiguities are fixed and the fourth is not fixed, the ambiguity search ranges for the fifth satellite is only increased from 0.1 cycles to 0.2 cycles at the first epoch. After five epochs of observations, the computed search range for the fifth satellite is practically the same with respect to fixing or unfixing the fourth satellite ambiguity by FASF. From this observation, it may be concluded that the least squares ambiguity search method would give similar performance if the same FASF computation scheme for ambiguity search ranges is applied to the three primary ambiguities. More studies are recommended in area.

One drawback of FASF when applied to GPS multi-antenna systems is that the baseline constraints can not be directly used to reduce ambiguity search ranges given by Eqn. (4.4) in the sequential adjustment. But they can be used subsequently in isolating the correct ambiguity combination.

It should be mentioned that another ambiguity resolution method developed specifically for use in multi-antenna systems is the motion-based method (Brown and Ward, 1990; Cohen and Parkinson, 1992). The idea behind motion-based integer ambiguity resolution is to take advantage of the constraints imposed on the antenna movements originating from the rigid body antenna mounting. By rotating the antenna platform and collecting the differential carrier phase measurements before and after the rotation, the relative movements of the slave antennas can be determined and, hence, the

initial positions of the baselines. The main advantage of this method is its reliability and robustness since the ambiguities are determined analytically and it is easy to check analytically if there is enough information to resolve the ambiguities. The disadvantage, as the name implies, is to require a relatively large rotation (motion) of the antenna platform. This may require the vehicle to change its course during a mission to initialize the integer ambiguities when cycle slips occur on all or most of the satellites.

#### **4.2 AMBIGUITY RESOLUTION OVER A FIXED BASELINE LENGTH**

The relative antenna positions of a multi-antenna system installed on a rigid body platform can be precisely determined through a proper initialization process. The fixed positions between the antennas impose some geometrical constraints which are to be met by the potential integer ambiguities. The most powerful and widely used geometrical constraint is the fixed baseline lengths among the multiple antennas because some other types of constraints, such as angles, can be derived from the fixed baseline lengths. In this section, an efficient method to construct the potential ambiguity sets on the surface of a sphere with the fixed baseline length is developed. This method is based on Cholesky decomposition and significantly increases the computational speed of the ambiguity searching process.

In the least squares ambiguity search method, only three double difference ambiguities from four primary satellites are searched. The initial ambiguity search space for the slave GPS antenna is usually defined within the

uncertainty space of the corresponding (carrier-smoothed) pseudorange solution (Lachapelle et al., 1993). If the baseline length between the master and the slave antennas is known precisely, as is the case in GPS multi-antenna systems, the potential position solutions for the slave antenna are confined on the surface of a sphere of the radius equal to the fixed baseline length. The three dimensional ambiguity search space is therefore reduced to a two dimensional space. The third integer ambiguity can be directly computed using the known baseline constraint under the condition that the first and the second ambiguities are held to some integer numbers. If the baseline length  $d$  is relatively short, such as  $d \leq 3$  m, the search ranges for the first and second ambiguities can also be properly constrained by the known baseline length. The approach used herein is based on Cholesky decomposition, which is fast in computation and yet simple in derivation.

Suppose that four primary satellites have been chosen and the baseline vector from the master antenna to the remote antenna is  $d = (x, y, z)^T$ . The related three double difference carrier phase observation equations are expressed as

$$a_1 x + a_2 y + a_3 z + N_1 - \lambda \phi_1 = 0, \quad (4.10a)$$

$$b_1 x + b_2 y + b_3 z + N_2 - \lambda \phi_2 = 0, \quad (4.10b)$$

$$c_1 x + c_2 y + c_3 z + N_3 - \lambda \phi_3 = 0, \quad (4.10c)$$

or in matrix form

$$A d + W = 0, \quad (4.11)$$

where  $\lambda$  is the carrier wavelength,  $A$  is a  $3 \times 3$  design matrix and  $W = (w_1, w_2, w_3)^T$  is the  $3 \times 1$  misclosure vector with

$$w_1 = N_1 - \lambda \cdot 1, \quad (4.12a)$$

$$w_2 = N_2 - \lambda \cdot 2, \quad (4.12b)$$

$$w_3 = N_3 - \lambda \cdot 3. \quad (4.12c)$$

From Eqn. (4.11),  $d$  can be solved as

$$d = -A^{-1}W. \quad (4.13)$$

Squaring Eqn. (4.13), we obtain

$$d^2 = d^T d = W^T (AA^T)^{-1} W, \quad (4.14)$$

where  $d^2$  is the square of the known baseline length and  $AA^T$  is a  $3 \times 3$  positive definite matrix which can be Cholesky decomposed into the product of a lower triangle matrix  $L$  times its transpose, i.e.  $AA^T = LL^T$ . With this substitution, Eqn. (4.14) can be rewritten as

$$d^2 = d^T d = (L^{-1}W)^T (L^{-1}W). \quad (4.15)$$

Since  $L$  is a lower triangle matrix, its inverse  $L^{-1}$  is also a lower triangle matrix.

Defining the quantities  $L$ ,  $B$ ,  $C$ , and  $D$  as

$$L^{-1} = \begin{bmatrix} l_{11} & & \\ l_{21} & l_{22} & \\ l_{31} & l_{32} & l_{33} \end{bmatrix}, \quad (4.16)$$

$$B = l_{11}w_1, \quad C = l_{21}w_1 + l_{22}w_2, \quad \text{and} \quad D = l_{31}w_1 + l_{32}w_2 + l_{33}w_3, \quad (4.17)$$

Eqn. (4.15) then becomes

$$d^2 = B^2 + C^2 + D^2 . \quad (4.18)$$

Based on Eqn. (4.18), it can be immediately concluded that the following inequalities have to hold:

$$|B| \leq d \text{ or } -d \leq B \leq d , \quad (4.19)$$

$$|C| \leq \sqrt{d^2 - B^2} \text{ or } -\sqrt{d^2 - B^2} \leq C \leq \sqrt{d^2 - B^2} . \quad (4.20)$$

This is because the baseline length can not be longer than  $d$  and all the solutions are constrained on a sphere of radius  $d$ .

From Eqn. (4.19), the ambiguity search range for the first ambiguity parameter  $N_1$  can be obtained as

$$\frac{(-d/l_{11} + \lambda/2)}{\lambda} \leq N_1 \leq \frac{(d/l_{11} + \lambda/2)}{\lambda} . \quad (4.21)$$

For each integer ambiguity  $N_1$  within the range (4.21),  $w_1$  can be computed and therefore  $B$  is known. Using Eqn. (4.20), the ambiguity search range for the second ambiguity parameter  $N_2$  under  $N_1$  fixed is

$$\frac{((-\sqrt{d^2 - B^2} - l_{21}w_1)/l_{22} + \lambda/2)}{\lambda} \leq N_2 \leq \frac{((\sqrt{d^2 - B^2} - l_{21}w_1)/l_{22} + \lambda/2)}{\lambda} . \quad (4.22)$$

Once  $N_1$  and  $N_2$  are set to integer numbers,  $w_1$  and  $w_2$  can be computed and hence the quantities  $B$  and  $C$  are known. The third ambiguity  $N_3$  can then be solved from Eqn. (4.18) as

$$N_3 = (\pm\sqrt{d^2 - B^2 - C^2} - E) / (l_{33}), \quad (4.23)$$

with  $E = l_{31}w_1 + l_{32}w_2 + l_{33}(-3)$ .

Based on Eqn. (4.23), there are only two trial values for  $N_3$  (rounded to the nearest integers) to be tested for each integer trial set ( $N_1, N_2$ ). Assuming that the ambiguity search ranges for  $N_1$  and  $N_2$  are  $\pm 15$  cycles, then the total potential ambiguity sets to be tested are  $31 \times 31 \times 2 = 1922$ , as opposed to  $31^3 = 29791$  in a brute force check where  $N_3$  is not solved using the known fixed baseline length.

The Cholesky decomposition is only needed to be performed once outside the ambiguity test loop. Only the misclosures  $w_1$  and  $w_2$  and the related constants  $B$ ,  $C$ , and  $E$  are updated with every assignment of the test integer ambiguities ( $N_1, N_2$ ). This greatly speeds up the computation of the ambiguity search process.

The potential ambiguity sets ( $N_1, N_2, N_3$ ) computed from the above Cholesky decomposition method are restricted on the surface of a sphere with a radius equal to the fixed baseline length  $d$ . If the baseline length is not precisely known, the derived formulas can still be used with the minimum and maximum error bounds for the baseline length. In this case, the potential ambiguity sets to be tested are confined in a thin spherical shell with the thickness equal to the error bounds.

It is apparent from Eqns. (4.21) and (4.22) that the number of potential ambiguity sets constructed by the above Cholesky method will increase rapidly for long baselines which are desirable for high accuracy attitude

determination. With GPS pseudorange measurements, however, it is possible to define a search cube within a few metres around the slave GPS antennas. In an experiment with NovAtel GPS receivers, the accuracy of differential pseudorange solutions is at the 1 m level (1 ) (Cannon and Lachapelle, 1992; Lachapelle et al., 1993). Therefore, it is safe to define a  $\pm 3$  search cube at  $\pm 3$  m around the slave antenna regardless of the baseline length. In this case, the ambiguity search ranges for the first and the second primary ambiguity parameters are defined within the bounds of the  $\pm 3$  m search cube and the potential ambiguities for the third ambiguity parameter are then computed with Eqn. (4.23) of the Cholesky decomposition algorithm. By such a cube-Cholesky method, the potential ambiguity sets for the primary satellites are confined on a portion of the surface of a sphere with the radius equal to the fixed baseline length  $d$  and only two trial values for  $N_3$  need to be tested for each integer trial set (  $N_1$ ,  $N_2$ ) within the defined search cube.

In order to show the effectiveness and computational speed of the derived algorithm with respect to different baseline lengths, an experiment was performed using four NovAtel GPS receivers which were placed on a straight metal bar and separated from each other by one metre. The antenna configuration is depicted in Figure 4.6. After collecting seven minutes of GPS data at a 1 second interval simultaneously on all four receivers, Ant 4 was moved to a new position, Ant 4', in Figure 4.6 and another 7 minutes of GPS data was collected. The baseline length from Ant 1 to Ant 4' was 4.5 metres.

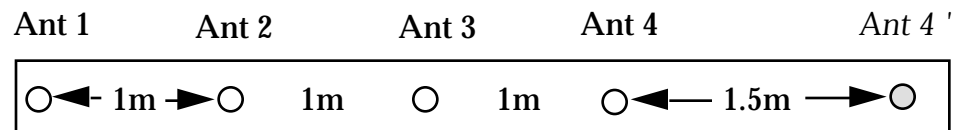


**Figure 4.6 Test with Different Baseline Lengths**

During the test, eight satellites were observed above a  $5^\circ$  elevation angle. The four primary satellites selected were PRN 20, PRN 5, PRN 16 and PRN 6. The RDOP of the primary satellites was about 5.3. A total of 10 trial computations were performed for each baseline, with each trial computation starting 30 seconds forward in time. Shown in Table 4.1 are the averaged results from the ten trial computations for each case.

**Table 4.1 Results of Least Squares Ambiguity Search with Cholesky Decomposition Algorithm**

| Baseline Length | Number of Potential Solutions | Computation Time * (sec.) | Remaining Solutions after First Epoch Test | Epochs Required to Amb. Resolution (1 Hz rate) |
|-----------------|-------------------------------|---------------------------|--|--|
| 1 m             | 85                            | 0.055                     | 12   | 75   |
| 2 m             | 302                           | 0.220                     | 30   | 57   |
| 3 m             | 665                           | 0.494                     | 75   | 59   |
| 4.5 m           | 1265                          | 0.797                     | 154  | 90   |
| $\pm 3$ m cube  | 5618                          | 0.640                     | 85   | 90   |

\*Computation time is for first epoch ambiguity search only and based on a 486/50 computer

For carrier phase ambiguity resolution, the standard deviation of double difference carrier phase observations was assigned to 2 cm and the threshold in the ratio test (4.2) was set to 3. Global Chi-square testing of carrier phase residuals was performed at each epoch, while the ratio test was started only after 50 epochs in order to smooth the multipath effects in the carrier phase.

The fixed baseline length in each case was also used to discriminate the potential correct ambiguity sets with a threshold of 3 cm between the known and the computed baseline lengths to allow for multipath errors and receiver noise.

With the construction of potential ambiguity sets by the Cholesky decomposition method, the number of potential ambiguity sets and the computation time are reduced significantly, as observed in Table 4.1. The computation time is less than 0.06 seconds for one metre baseline and less than 0.8 seconds for a 4.5 m baseline. As compared with the traditional method where the potential ambiguity sets are defined within a three dimensional space inside a sphere (Hatch, 1990; Cannon and Haverland, 1993), the potential ambiguity sets would be 528 for 1 m baseline, 3528 for 2 m baseline, 10962 for 3 m baseline and 39200 for 4.5 m baseline. The computation time for each corresponding case would be 0.11, 0.33, 0.77 and 1.70 seconds. It should be noted, however, the specific values in Table 4.1 may vary with different satellite geometry or different primary satellites selected. However, the trend will be approximately the same.

The results given by the last row in Table 4.1 were obtained based on the data collected over the 4.5 metre baseline, where a  $\pm 3$  m search cube around Ant 4' was used to define the search ranges of the first and the second ambiguity parameters outside the search loop and the third ambiguity was computed by Eqn. (4.23). The search computation is faster than that of the 4.5 m baseline case, even though the later has a smaller number of potential ambiguity sets to be tested. This is because the elimination of computations for

the second ambiguity parameter search range by Eqn. (4.22) in the proposed cube-Cholesky search method.

Since all of the final ambiguities in Table 4.1 were selected by the ratio test which was carried out after 50 epochs of accumulation of carrier phase residuals, the epochs required to final ambiguity resolution ranged from 1 to 1.5 minutes and not significantly different with different baseline lengths. This conclusion is logical because the same statistical parameters, same satellite geometry (slightly different for the 4.5 m baseline and  $\pm 3$ m cube cases) are used for ambiguity resolution. The small differences are due to different error signatures at each antenna.

For full three dimensional attitude determination, two non-collinear baseline vectors,  $d_1$  and  $d_2$ , are needed. One possibility for resolving the ambiguities for the second baseline vector,  $d_2$ , would be to simply repeat the above algorithm to determine three more integer ambiguities. The fixed baseline length between the two slave antennas are used as an additional constraint to test the potential ambiguity sets from the two baselines. This in fact has worked very well for a number of applications, e. g. Lu et al. (1993, 1994). From a geometrical point of view, however, it is possible to constrain the potential ambiguity sets for the second baseline on a circle using the two fixed baseline lengths connecting the second slave antenna, after the first baseline is fixed. This means that the three dimensional ambiguity search space for the second baseline can be reduced to a one dimensional search space because by specifying one of the three primary ambiguities, the other two should be resolvable using the two fixed baseline constraints. However, a

direct formulation would lead to two second order equations that are very difficult to solve. To overcome this problem, a simple approach similar to the one proposed by Quinn (1993) is presented here. Instead of using the so-called artificial phase measurement with known phase ambiguity (Quinn, 1993), the dot product of the two baseline vectors is directly used as one of the measurements.

Since the body frame coordinates for  $d_1$  and  $d_2$  are known *a priori*, their dot product, i.e.  $d_1^T d_2$ , is known and invariant under different coordinate systems. Assuming that we have three double difference carrier phase observation equations defined similarly as Eqns. (4.10a), (4.10b) and (4.10c) for the second baseline vector and the related measurements. One of the equations, say, Eqn. (4.10a), can then be replaced by

$$x_1 x_2 + y_1 y_2 + z_1 z_2 = d_1^T d_2, \quad (4.24)$$

where  $(x_1, y_1, z_1)$  are treated as the equation coefficients which were computed based on a given potential ambiguity set for the first baseline, and  $(x_2, y_2, z_2)$  are the unknowns to be solved. All the equations from (4.11) to (4.23) can be used again with the substitution of  $(x_1, y_1, z_1)$  and  $d_1^T d_2$  for  $(a_1, a_2, a_3)$  and  $w_1$ , respectively. Because  $w_1$  is known, the constant B in Eqn. (4.17) is known. Therefore, there is no need to search the first ambiguity parameter in this case. The search range for the second ambiguity parameter is computed by Eqn. (4.22). For each potential integer ambiguity within the range, the third ambiguity search range is then determined by Eqn. (4.23).

It should be noted that proper variance or weight should be given to Eqn. (4.24) so that it can be combined in a least squares adjustment with the remaining two double difference carrier phase observation equations from the primary satellites. One possibility is to use the square of the 3-D positioning accuracy of the first baseline solution,  $d_1$ , as the variance of Eqn. (4.24).

The above procedure for the second baseline ambiguity search can be always carried out for each potential solution of the first baseline vector,  $d_1$ , no matter if it is right or wrong. Once the solution for the second baseline vector,  $d_2$ , is obtained, all the double difference carrier phase ambiguities related to the second baseline can be calculated and tested by the corresponding residual quadratic form as well as the fixed baseline lengths connected with that slave antenna. In this way, the potential ambiguity sets to be tested for the second baseline are  $m_1 \times m_2 \times 2$ , where  $m_1$  is the number of potential solutions for the first baseline vector and  $m_2$  is the search range of the second ambiguity parameter for the second baseline. It is noted that  $m_1$  should not be too large, say less than 20, in order to get a small number of potential ambiguity sets for the second baseline vector. Otherwise, a direct repeat of the ambiguity search for the second baseline similar for the first baseline would be even more computationally efficient.

### 4.3 AMBIGUITY RESOLUTION WITH THE AIDING OF EXTERNAL LOW COST ATTITUDE SENSORS

In addition to GPS multi-antenna systems, there are several other kinds of attitude sensors widely used on surveying vessels, such as Motion Reference Units (MRUs), TSS units, Hippy units and gyro compasses (Dinn and Loncarevic, 1994). The price of these instruments ranges from a few thousand dollars to some thirty thousand dollars and the typical static accuracy for attitude measurements ranges from  $0.5^\circ$  to  $0.05^\circ$  (Mathisen and Orpen, 1994; Loncarevic, 1993). These sensors are usually composed of angular rate gyros, fluxgate compasses and accelerometers to measure the attitude information of a platform. They are affected by the platform dynamics such as accelerations and turning and are subject to some long term drift. Therefore, an integration of these attitude sensors with a GPS multi-antenna system will benefit in two aspects. The first will be the calibration and correction of the long term or transient drifts of MRUs and gyro compasses using drift-free GPS attitude information, while allowing the advantage of the high output rate from MRUs and gyro compasses. The second will be the aiding of carrier phase ambiguity resolution of a GPS multi-antenna system by using the *a priori* attitude values from MRUs and gyro compasses. This second aspect is the main focus of the following investigations. The discussions will be concentrated on the available *a priori* attitude information and its accuracy, rather than on which sensors the information is supplied.

Assuming that at a certain epoch the platform attitude parameters, e. g. yaw, pitch and roll, and their accuracy are provided by some external

onboard attitude sensors. With the *a priori* attitude parameters ( $y, p, r$ ) and the known antenna body frame coordinates in a multi-antenna system, the antenna's coordinates in the local level system can be computed by

$$\begin{matrix} x \\ y \\ z \end{matrix} = \mathbf{R}^T(y, p, r) \begin{matrix} x^b \\ y^b \\ z^b \end{matrix}, \quad (4.25)$$

where  $(x, y, z)^T$  are the antenna's local level coordinates,  $(x^b, y^b, z^b)^T$  are the corresponding known body frame coordinates and  $\mathbf{R}^T(y, p, r)$  is the transpose of the rotation matrix evaluated at the *a priori* values ( $y, p, r$ ). Applying the error propagation law to Eqn. (4.25), the covariance matrix for  $(x, y, z)$  is

$$\begin{matrix} \sigma_{xx}^2 & \sigma_{xy} & \sigma_{xz} \\ \sigma_{yx} & \sigma_{yy}^2 & \sigma_{yz} \\ \sigma_{zx} & \sigma_{zy} & \sigma_{zz}^2 \end{matrix} = \mathbf{A} \begin{matrix} \sigma_{yaw}^2 \\ \sigma_{pitch}^2 \\ \sigma_{roll}^2 \end{matrix} \mathbf{A}^T, \quad (4.26)$$

with  $\mathbf{A} = \begin{matrix} \frac{\mathbf{R}^T}{y} \mathbf{b} & \frac{\mathbf{R}^T}{p} \mathbf{b} & \frac{\mathbf{R}^T}{r} \mathbf{b} \end{matrix}$ , where  $\mathbf{b} = (x^b, y^b, z^b)^T$ .

Once the local level coordinates  $(x, y, z)$  and their corresponding standard deviations  $(\sigma_{xx}, \sigma_{yy}, \sigma_{zz})$  are computed for a given slave GPS antenna, a search cube, say  $(\pm 3\sigma_{xx}, \pm 3\sigma_{yy}, \pm 3\sigma_{zz})$ , can be built around the derived local level coordinates  $(x, y, z)$ . The search ranges for the three primary double difference ambiguities can then be defined within the search cube. If the baseline length related to that slave antenna is known precisely, the cube-Cholesky algorithm derived in Section 4.2.1 can also be applied in this case to determine the potential integer numbers of the third ambiguity parameter.

In order to show the performance of ambiguity resolution by using the *a priori* attitude information, two data sets were analyzed. The first one was the static data collected on a 3 m baseline and the second one was the ship-borne data collected off the coast of British Columbia.

### **Static Baseline Test Results**

The seven minutes of static GPS data collected on the 3 m baseline described in Figure 4.2 was used in the following analysis. The *a priori* azimuth and elevation (pitch) values for the baseline were determined by averaging the instantaneous results over the whole seven minutes of GPS data. According to the error estimation formulas given by Eqns. (3.24) and (3.27), the accuracy of the averaged azimuth and elevation should be better than  $0.5^\circ$ . In the test computations, different accuracies were assigned to the *a priori* values in order to assess the effectiveness of ambiguity resolution with respect to different search cube sizes. Over the seven minutes of data, the least squares ambiguity search process was performed at each observation epoch independently and the averaged results were given in Table 4.2.

It can be seen from Table 4.2 that the instantaneous ambiguity resolution with one epoch observation can be achieved 98% of the time within a 30 cm search cube and 90% of the time within a 1 m search cube for this particular data set. With the further increase of the search cube, the success rate decreases rapidly. These results agreed well with those reported by Cannon et al. (1993) for a 2 m bar test. The search computation time for all the cases is less than 0.06 seconds which is the computer clock tick resolution.

**Table 4.2 Ambiguity Resolution Within the *a priori* Search Cube  
(Static Baseline Test, 3 m Bar, 458 Sample Epochs)**

| Accuracy<br>for Known<br>Heading and<br>Elevation<br>(1 ) | Search<br>Cube Size<br>(3 ) | Ambiguity Resolution Success Rate |                               | Computer<br>Time for<br>Search<br>(seconds) |
|---|-----------------------------|-----------------------------------|-------------------------------|---|
|   |                             | With One Epoch<br>Observation     | With 10 Epoch<br>Observations |   |
| 0.5°  | ±0.08 m                     | 100%                              | 100%                          | < 0.06                                      |
| 1.0°  | ±0.16                       | 98.0                              | 100                           | < 0.06                                      |
| 2.0°  | ±0.32                       | 90.0                              | 97.8                          | < 0.06                                      |
| 3.0°  | ±0.47                       | 90.0                              | 97.8                          | < 0.06                                      |
| 4.0°  | ±0.63                       | 59.8                              | 76.1                          | < 0.06                                      |
| 5.0°  | ±0.79                       | 46.3                              | 67.4                          | < 0.06                                      |

If the ambiguity search process starts independently every 10 epochs, which means that the next 9 epochs of observations could be used to further test the remaining potential ambiguity sets if the ambiguities were not resolved at the first epoch, the success rate increases moderately, especially for the cases where the search cubes are larger than 1 m. This is because 10 seconds of observations are generally not enough to smooth out the multipath effects in the carrier phase observations, as pointed out by Cannon et al. (1993).

### **Ship-borne Kinematic Results**

A GPS multi-antenna system consisting of four NovAtel GPSCard™ receivers was tested off the coast of British Columbia on May 31 and June 1, 1994. The system was installed on a 72 m long vessel and the baseline lengths among the multiple antennas ranged from 5 to 15 metres. During the test, the

ship azimuth from a gyro compass, Sperry Mark 23 Model C, was simultaneously collected and time synchronized with the GPS data from the multi-antenna system. A detailed description of the test and results can be found in Lu et al. (1994).

From the previous analysis, it is known that the ship gyro compass azimuth was accurate to about  $0.16^\circ$  during the straight section and  $0.35^\circ$  during turns. Because of the low centrifuge of the ship, its pitch and roll were within  $\pm 0.25^\circ$  and  $\pm 2^\circ$ , respectively, even when the ship was in rapid turns. Therefore, it can be safely assumed that the yaw, pitch and roll of the ship were known *a priori* within the accuracies of  $0.4^\circ$ ,  $0.25^\circ$  and  $2^\circ$ , respectively. Based on these *a priori* attitude information, a search cube for each slave GPS antenna in the system can be determined by Eqns. (4.25) and (4.26). The carrier phase ambiguity search can then be performed subsequently within the defined cubes. The results obtained with one hour data from May 31 were given in Table 4.3, where the ambiguity resolution process was carried out independently at each observation epoch. Six to eight satellites were in view above  $5^\circ$  elevation angle and the GDOP was between 2 to 3.

It is shown that the instantaneous ambiguity resolution for the four-receiver multi-antenna system can be achieved 98.7% of the time with the aiding of the *a priori* ship attitude parameters accurate to about  $0.4^\circ$  for yaw,  $0.25^\circ$  for pitch and  $2^\circ$  for roll. If the above *a priori* accuracies were dropped to  $0.5^\circ$  for yaw and  $2^\circ$  for pitch and roll, the performance of ambiguity resolution only slightly decreases to 95.8% of the time. For each case, the computation time for ambiguity searching is less than 0.06 seconds. No degradation was

observed either for ambiguity resolution or for attitude estimation during sharp turns of the ship.

**Table 4.3 Ambiguity Resolution with External Ship Attitude Information  
(Ship-borne Data, May 31, 1993, 4067 Sample Epochs)**

| <i>A priori</i><br>Accuracy                   | Search Cube Size<br>(m)   | Baseline Length<br>to the Origin<br>(Ant 1) | One Epoch<br>Resolution Rate<br>for the System |
|---|---|---|--|
| a p r   | $[\pm 3, \pm 3, \pm 3 \text{ h}]$   | Ant 2 Ant 3 Ant 4                           |  |
| 0.4° 0.25° 2.0°                               | Ant 2: $[\pm 0.11, \pm 0.29, \pm 0.19]$<br>Ant 3: $[\pm 0.11, \pm 0.19, \pm 0.48]$<br>Ant 4: $[\pm 0.17, \pm 0.05, \pm 0.48]$ | 14.9 m 5.3 m 4.8 m                          | 98.7%  |
| 0.5° 2.0° 2.0°                                | Ant 2: $[\pm 0.37, \pm 0.38, \pm 1.51]$<br>Ant 3: $[\pm 0.15, \pm 0.20, \pm 0.53]$<br>Ant 4: $[\pm 0.20, \pm 0.06, \pm 0.49]$ | 14.9 m 5.3 m 4.3 m                          | 95.8%  |
| No <i>a priori</i><br>attitude<br>information | Ant 2: $\pm 3$ m cube<br>Ant 3: $\pm 3$ m cube<br>Ant 4: $\pm 3$ m cube   | 14.9 m 5.3 m 4.8 m                          | 28.1%  |

As a comparison, the success rate of one epoch (instantaneous) ambiguity resolution without the aiding of any *a priori* attitude information is only 28% of the time, where a  $\pm 3$  m search cube around each slave antenna is used.

The performance of instantaneous ambiguity resolution shown in Table 4.3 clearly demonstrates the advantages of the integration of a multi-antenna GPS system with other low cost attitude sensors. In this case, the attitude sensors play two important roles, namely 1) to provide approximate platform attitudes for ambiguity resolution and 2) to output the attitude information during outages of GPS signals. Since the ambiguities can be resolved using one epoch of observation with a fast computational speed and high reliability, cycle slips will no longer pose a problem in the integrated system because the phase ambiguities can be resolved and tested from epoch to epoch.

It should be pointed out that for most marine applications, the data rate required for attitude output is at 10 to 50 Hz (Loncarevic, 1993), which most of the current GPS receivers can not meet. In this regard, the integration of GPS multi-antenna system with other high data rate attitude sensors, such as MRUs or a TSS, would be required. The accurate, drift-free attitudes from the multi-antenna system can then be used to calibrate the attitude sensors with inherent drift problems so that an accurate and high data rate integrated system can be realized.

#### **4.4 AMBIGUITY RESOLUTION WITH SPECIAL ANTENNA CONFIGURATIONS**

The antennas in a GPS multi-antenna system may be arranged into a special configuration in order to provide extra geometrical constraints and speed up the ambiguity resolution. For instance, if three antennas are placed

collinearly on a straight line, a collinear constraint will result among the potential solutions of the three antennas. The price paid for that constraint is that one of the antennas is solely dedicated to ambiguity resolution and does not contribute to attitude determination. Therefore, more than three antennas are needed in this case for full three dimensional attitude estimation, which usually means to pay more for the hardware component of the system. In this section, a well-known antenna configuration proposed by Adroit Systems, Inc. (Jurgens et al, 1991, 1992) is discussed with the emphasis on its advantages, limitations and some modifications.

The basic idea for Adroit's antenna configuration is to place three GPS antennas collinearly on a straight line, with two of them within one carrier wavelength distance, say 12 cm, as shown in Figure 4.7.

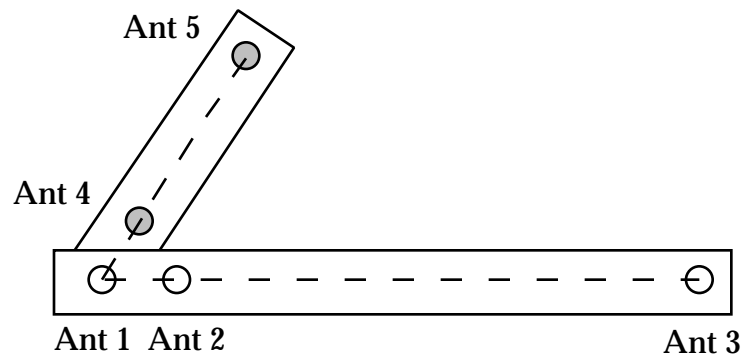


**Figure 4.7 Adroit's Antenna Configuration**

For azimuth determination, one baseline with at least three antennas is needed, while for three dimensional attitude estimation, two non-collinear baselines with at least 5 antennas are necessary with this configuration. As known from the previous analysis, reducing the separation between the two antennas will limit the number of potential ambiguities to consider, however, what may be

gained in efficiency in the ambiguity resolution for short baselines is lost in the achievable attitude accuracy which is inversely proportional to the baseline lengths. The Adroit configuration is one of the solutions that tries to overcome these two contradicting problems.

As shown by the results in the first two rows of Table 4.2, the ambiguities over the short baseline (Ant 1 - Ant 2) can be instantaneously resolved almost all the time due to its very small ambiguity search space. Thus, the approximate azimuth and elevation can be derived from the short baseline and used to extrapolate a limited potential ambiguity search space for the long baseline. Once the ambiguities for the long baseline are resolved, more accurate attitude parameters can then be computed using the long baseline configuration.

The extrapolation formulas for the position of the long baseline are

$$\lambda_3 = \lambda_1 + L_{1-3} \cos(\alpha) \cos(\beta) / R, \quad (4.27a)$$

$$\lambda_3 = \lambda_1 + L_{1-3} \sin(\alpha) \cos(\beta) / (R \cos(\alpha_1)), \quad (4.27b)$$

$$h_3 = h_1 + L_{1-3} \sin(\beta), \quad (4.27c)$$

where  $\alpha$  and  $\beta$  are the approximate azimuth and elevation derived from the short baseline,  $L_{1-3}$  is the baseline length from Ant 1 to Ant 3 and  $R$  is the radius of the earth. In order to define a search cube for the long baseline, the extrapolated position error for Ant 3 of the long baseline is needed, which can be derived as

$$\sigma_3 = L_{1-3} (\sin^2(\alpha) \cos^2(\beta) \sigma_\alpha^2 + \cos^2(\alpha) \sin^2(\beta) \sigma_\beta^2)^{1/2} / R, \quad (4.28a)$$

$$\sigma_{\theta} = L_{1-3} (\cos^2(\theta) \cos^2(\alpha)^2 + \sin^2(\theta) \sin^2(\alpha)^2)^{1/2} / (R \cos \alpha), \quad (4.28b)$$

$$h_3 = L_{1-3} \cos(\alpha), \quad (4.28c)$$

where  $\sigma_{\theta}$  and  $\sigma_{\alpha}$  are the standard deviations of the approximate azimuth and elevation. Usually, the search cube for the long baseline is defined at the 2 to 3 level.

Shown in Table 4.4 are the results from a test performed on the roof of The University of Calgary Engineering Building. Three antennas were placed collinearly on a metal plate 4.5 m long. The short baseline between Ant 1 and Ant 2 was 11.5 cm and the long baseline between Ant 1 and Ant 3 was 1 m. In order to test the performance with different baseline lengths, a fourth antenna was also placed collinearly at 4.5 m apart from Ant 1. Ten minutes data was collected at a 1 Hz rate and eight satellites were observed. Ambiguity resolution was performed independently at each observation epoch.

**Table 4.4 Ambiguity Resolution with a Special Antenna Configuration  
(1 m and 4.5 m baselines, 598 epochs)**

| Short baseline | Long baseline | Search cube size<br>[ $\pm 2 \sigma_{\theta}$ , $\pm 2 \sigma_{\alpha}$ , $\pm 2 h$ ] | One epoch ambiguity<br>resolution rate |
|----------------|---------------|---|--|
| 0.115 m        | 1 m           | [ $\pm 0.35$ , $\pm 0.03$ , $\pm 0.35$ ]  | 99.3%                                  |
| 0.115 m        | 4.5 m         | [ $\pm 1.56$ , $\pm 0.04$ , $\pm 1.56$ ]  | 87.6%                                  |

The instantaneous ambiguity resolution rate was 99.3% of the time for a 1 m baseline and the ambiguity search interval was about  $\pm 2$  cycles (L1 carrier). For a 4.5 m baseline, however, the resolution rate drops to 87.6% of the time.

This is due to the increase of the search cube which is about  $\pm 8$  cycles in this case.

From Eqn. (4.28), it is obvious that the position errors for the long baseline are proportional to its length. Since the short baseline is usually less than 19 cm, the standard deviation of the estimated azimuth and elevation is about  $3^\circ \sim 4^\circ$  if a 1 cm accuracy is assumed for differential carrier phase positioning. Thus, the extrapolated search cube (1 ) is about  $\pm 0.2$  m for a 3 m baseline and  $\pm 0.7$  m for a 10 m baseline. Using high performance GPSCard™ receivers, the accuracy of carrier phase smoothed pseudorange solutions for the remote antenna is also about  $\pm 0.7$  m (Lachapelle, et al, 1993). Therefore, such an antenna configuration is only advantageous and applicable to the system with relatively short antenna separation, say less than 3 m. If a longer baseline is needed for more accurate attitude determination and cost is not a problem, a fourth antenna can be added at a further distance collinearly with Ant 1, Ant 2 and Ant 3. Another possibility still using three collinear antennas for a very long baseline is to place Ant 2 at a proper distance larger than 19 cm with respect to Ant 1, as shown in Figure 4.8 for a 50 m baseline.

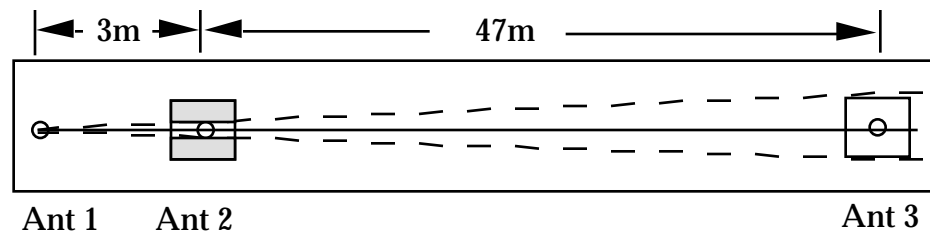


**Figure 4.8 Modified Adroit Configuration For Long Baseline**

Suppose that a 1 m positioning accuracy from pseudorange measurements is available to define a  $\pm 3\text{m}$  (3 ) search cube around Ant 3. For

a 50 m baseline, this translates into an accuracy of  $3.5^\circ$  for baseline azimuth and elevation. Therefore, the search cube around Ant 2 of the short baseline, which is 3 m long in the above example, is limited to  $\pm 0.18$  m. The shadowed areas of the search cube around Ant 2 are excluded by the approximate azimuth and elevation from the long baseline. For an  $\pm 0.18$  m search cube, the ambiguities over the short baseline can be instantaneously resolved most of the time, which provides a better baseline azimuth and elevation at an accuracy level about 12 arc minutes. With the more accurate attitude information from the 3 m short baseline, a much smaller search cube for the long baseline can be obtained, which is about  $\pm 0.17$  m (1 ) in the above example. Hence, the ambiguity search over the long baseline can be greatly accelerated. It should be noted that for different baseline lengths, the position of Ant 2 may vary in the same principal in order to achieve the best performance. Apparently, a better solution for long baseline situation would be an integrated system of two GPS antennas with low cost attitude sensors that have an accuracy level ranging from  $0.5^\circ \sim 1^\circ$ , as shown by the results in Table 4.3.

Another problem restricting the Adroit configuration to be used for long baselines is the antenna mounting. For short baseline cases, it is relatively easy to place three or four antennas in a straight line. For long baselines (>15 m) in a complex environment such as a ship, it would be very difficult to do so. However, as a self-contained GPS multi-antenna system capable of instantaneous ambiguity resolution, the Adroit-type configuration has its own merits for short antenna separations.

## CHAPTER 5

### SOFTWARE DEVELOPMENT AND SOME RELATED TOPICS

Software design is an integral part of development of GPS multi-antenna systems. In this chapter, some special criteria adopted for developing GPS attitude determination software are discussed. The antenna installation requirements are outlined and the process for initialization of antenna body frame coordinates is described. Since GPS carrier phase observations are susceptible to cycle slips, quality control methods used in the developed program are also presented.

#### 5.1 SOFTWARE DEVELOPMENT

Based on the presented theories and algorithms for on-the-fly least squares ambiguity resolution and attitude estimation using vector observables, a software package, MULTINAV (MULTI-antenna NAVigation), has been developed in C-language on a 486 personal computer. The program package consists of two parts, the pre-processor and the main program. The pre-processor decodes the raw GPS measurements collected by a multi-antenna system and creates standard input observation and ephemeris files for the

main program which in turn computes the platform attitude at each observation epoch after carrier phase ambiguities are resolved. The pre-processor is receiver-dependent because different kinds of GPS receivers may have different raw data structures defined by the manufacturers. The main program, on the other hand, can process the data collected by different kinds of receivers as long as the pre-processor provides the observation and ephemeris in the required standard formats. Double difference observables are used in the data processing scheme so that the developed program is suitable for either a multiple receiver system comprised of three or four independent GPS receivers or a dedicated single oscillator multi-antenna system.

In order to adapt to a wide range of application scenarios, a number of special criteria were employed during the program development. They include

- (1) use with either three or four GPS antenna systems,
- (2) no restriction on antenna configurations and baseline lengths except for a non-collinear antenna array requirement,
- (3) fast and reliable on-the-fly ambiguity resolution capability,
- (4) ability to use *a priori* attitude information from other onboard sensors to speed up the ambiguity resolution,
- (5) easy modification and implementation for real-time system,
- (6) initialization capability for antenna body frame coordinates and,
- (7) quality control methods for cycle slips and incorrect ambiguity detection.

The flowchart of the MULTINAV program system is shown in Figure 5.1.

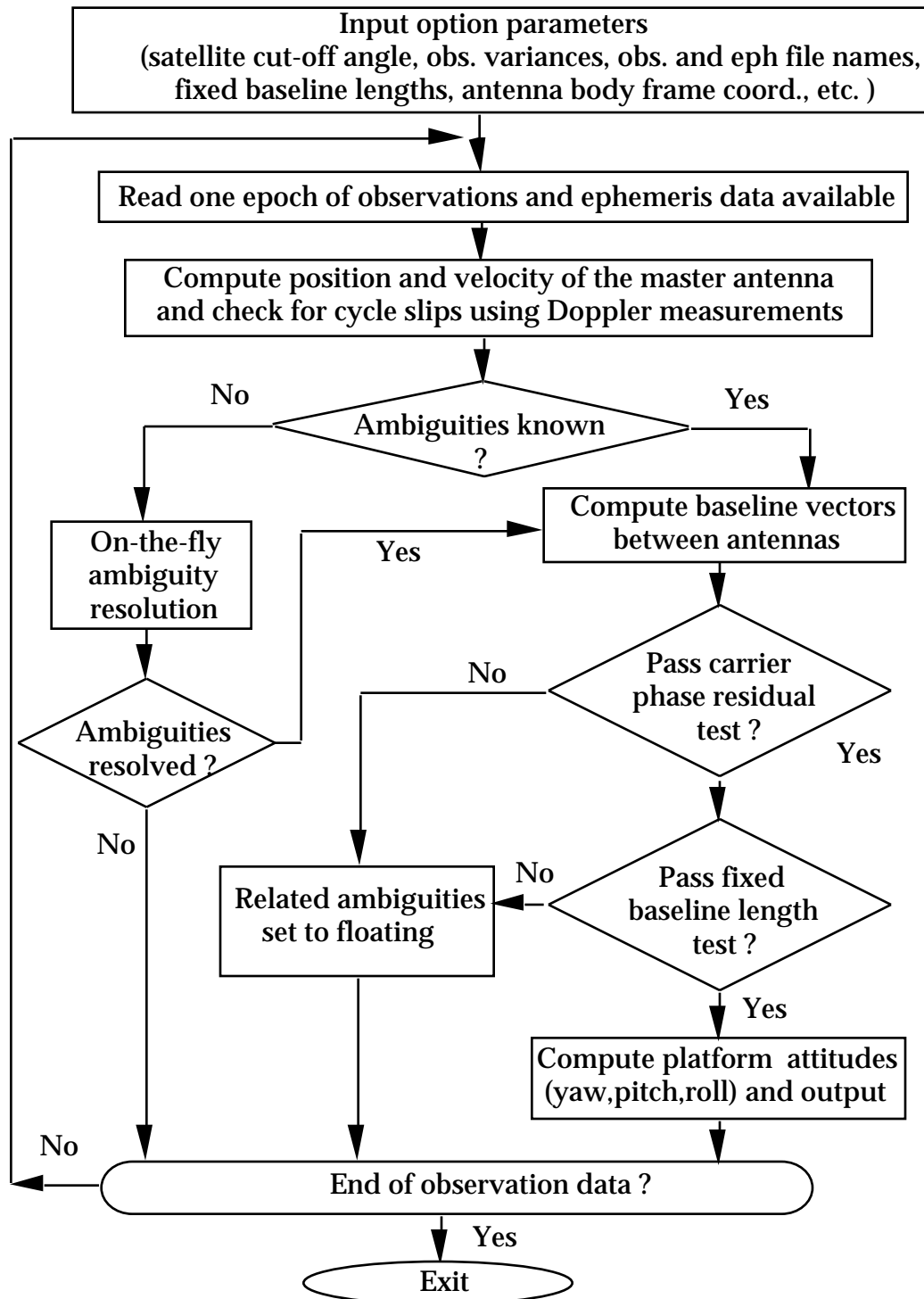


Figure 5.1 Flowchart of MULTINAV Program System

After reading one epoch of observations, the program computes the single point position and velocity using the measurements from the master antenna. This position is used to define the origin of the local level coordinate system at that epoch. The data processing modules in the program can be classified into two groups, one for carrier phase ambiguity resolution and the other for attitude estimation with fixed carrier phase ambiguities. A least squares ambiguity search method is implemented presently for on-the-fly ambiguity resolution. In addition to the Chi-square and ratio tests performed on the quadratic forms of residuals, all the available external information such as fixed baseline lengths between antennas and *a priori* platform attitude values from other sensors is also utilized to improve the speed and reliability of selecting the correct ambiguities. Once the ambiguities are resolved, the data flow in the program is directed to the attitude estimation procedure using the implicit least squares model. Before the final attitude values are output from the program, two quality control methods are employed to ensure the correctness of the results. One is the carrier phase residual test and the other is the known fixed baseline check. It should be noted that the fixed baseline check can be replaced by some other equivalents such as baseline-angle combinations or the inner product of two vectors. A further description of the quality check methods will be given in the last section of this chapter.

Currently, MULTINAV estimates the platform attitude in post-mission. However, it should be relatively easy to adapt this program to a real-time system since all the algorithms and procedures are written with this aim. Depending on the GPS receivers and hardware available for developing a real-time system, the major modification is the replacement of the observation

input subroutine with a real-time data logger which simultaneously collects and properly buffers the measurements from multiple GPS receivers, converts the measurements into the required data structure and then calls the main program MULTINAV. As an example, a real-time heading (two antenna) system has been successfully implemented in a helipod navigation system based on a modified version of MULTINAV (Cannon and Haverland, 1993).

## 5.2 ANTENNA INSTALLATION

There are several factors that should be considered when installing a GPS multi-antenna system. They are the GPS antenna locations, baseline lengths between antennas and stability of the antenna mounts. Each antenna location should be in an open sky area and away from any obstructing objects. This is to prevent GPS signal interruption and multipath effects. The baseline lengths between the antennas affect the accuracy of the estimated platform attitude parameters. The longer the baseline, the better the accuracy. The stability of GPS antenna mounts is also crucial for the accuracy of the estimated attitude parameters. Since the platform is considered to be a rigid body, any movement of the antennas will be transformed into the variations of attitude parameters through the estimation process unless a deformation model is included. For airborne applications where antennas are mounted on the wings, an aircraft wing flexure model has been successfully developed and combined with the aircraft attitude estimation using four antenna GPS attitude systems (Cohen et al., 1993; Cannon et al., 1994). Even though the antenna installation is conceptually simple, it can be a difficult task, as shown by past experience,

especially when mounting antennas on a complex platform surface such as a ship or an airplane. Sometimes, compromises have to be made to select an appropriate location for an antenna with regard to the above-mentioned factors.

When installing the system, Antenna 1 (master antenna) should be in the best position with the least multipath effects. The direction from Antenna 1 to Antenna 2 defines the yaw of the platform (within an offset angle). Therefore, the direction from Antenna 1 to Antenna 2 should be close to the ship's or airplane's physical yaw direction. The antenna platform is formed by the plane defined by Antenna 1, Antenna 2 and Antenna 3. If possible, Antenna 3 or the antenna that defines the considered plane with Antenna 1 and Antenna 2 should be as far away as possible from the baseline formed by Antenna 1 and Antenna 2. This will improve the roll estimation accuracy of the platform.

### **5.3 INITIALIZATION**

The initialization process includes three types of tasks: misalignment angle determination, precise baseline length determination and antenna body frame coordinate determination.

#### **5.3.1 Misalignment Angle Determination**

If the antenna body frame coordinate system is not identical or parallel to the vehicle's platform coordinate system, the misalignment angles (e.g. the

yaw, pitch and roll misalignments) between the two coordinate systems should be determined. One way to determine the misalignment angles is to precisely survey the antenna coordinates in the vehicle's platform coordinate system and then calculate the misalignment angles using the formulae given in Section 3.2.2 based on the surveyed antenna coordinates.

In MULTINAV, if the input misalignment angles are set to zero, the program will output the attitude information of the antenna body frame coordinate system. Therefore, if the attitude results from a GPS multi-antenna system are to be compared with the output of another system, the misalignment angles between the two systems should be determined. One analytical way to determine the misalignment angles will be given in Chapter 6 when the attitude results from different systems are compared.

### **5.3.2 Precise Baseline Determination**

The baselines between all the GPS antennas should be determined separately with an accuracy better than 1 cm. These baseline lengths are input to MULTINAV to help resolve the double difference carrier phase ambiguities faster, to check for cycle slips in the carrier phase measurements and to adjust the GPS-derived antenna coordinates.

The baseline lengths can be measured with either a steel tape, an EDM instrument or through a GPS survey. MULTINAV provides an option to compute all the baseline lengths between the antennas based on static or kinematic GPS data collected by the multi-antenna system. In this case,

however, the user still needs to know the approximate baseline lengths with an accuracy of approximately 10 cm. In order to reduce multipath effects on GPS computed baseline lengths, the final baseline lengths are obtained by averaging the epoch by epoch results from a long observation session used for initialization.

### **5.3.3 Antenna Coordinates Determination**

Precise GPS antenna coordinates in the antenna body frame coordinate system are needed for the least-squares estimation of the platform attitude parameters. If all the baseline lengths are known precisely, the antenna coordinates in the antenna body frame coordinate system can be calculated based on the baseline configuration. MULTINAV also provides an option to compute the antenna coordinates in the antenna body frame coordinate system based on the static or kinematic data collected. This is done through the direct attitude computation method described in Section 3.2.2. Once the attitude parameters are computed at an epoch, the antenna coordinates in the local level frame are rotated into the corresponding antenna body frame coordinates. In order to reduce multipath effects, optimal values for the antenna body frame coordinates are then obtained by averaging the results over a sufficiently long period, typically more than one hour.

#### 5.4 QUALITY CONTROL FOR ESTIMATED ATTITUDE PARAMETERS

Precise attitude estimation using GPS depends on carrier phase observations with correctly resolved ambiguities. In an operational environment, however, it is possible that cycle slips may happen due to the obstruction of GPS signals or electronic interference inside a GPS receiver or from other onboard instruments. Since ambiguities change when cycle slips occur, new ambiguities related to the slipped satellites have to be resolved, otherwise the estimated attitude parameters may be severely distorted. In some extreme situations with strong multipath effects, wrong ambiguities may even be chosen from the beginning by on-the-fly ambiguity resolution methods. Therefore, it is necessary that quality control methods are implemented in the data processing scheme to validate the correctness of the results.

In the developed program, cycle slips are first checked by a Doppler prediction method (Cannon, 1991). Because the Doppler measures the phase rate at an instantaneous epoch, a predicted carrier phase measurement at the current epoch can be obtained by adding the phase change (Doppler  $\times$  epoch interval) to the phase measurement at the previous epoch. The predicted and the measured phases are then compared. If the difference is larger than a preset tolerance, a cycle slip is found on that particular satellite. Depending on the accuracy of the Doppler measurement and the platform dynamics, the tolerance can be a few cycles to tens of cycles. Therefore, this method is only suitable for a coarse check of cycle slips in carrier phase measurements.

Another method to check cycle slips is statistical testing of the adjusted carrier phase residuals. As shown in Chapter 4, the quadratic form of the carrier phase residuals is assumed to have a Chi-square distribution under the correctly fixed ambiguities. With a chosen significance level and the corresponding degrees of freedom, this quadratic form of residuals can be tested at each epoch. If the test fails, possible cycle slips may occur and an identification scheme, called data-snooping, can be applied to each individual carrier phase residual. The purpose of identification is to locate which satellite has cycle slips (Lu and Lachapelle, 1991). The statistic for data-snooping is usually defined as (Vanicek and Krakiwsky, 1986)

$$t_i = \frac{\hat{v}_i}{\hat{\sigma}_i} \sim N(0,1) \quad , (5.1)$$

where  $\hat{v}_i$  is the adjusted ( ) carrier phase residual related to satellite  $i$ ,

$\hat{\sigma}_i$  is the standard deviation of  $\hat{v}_i$  , and

$N(0,1)$  is the standard normal distribution.

In the above derivation, the correlation between the double difference carrier phase observations was disregarded and the observation variance was assumed to be known. With a properly chosen significance level, the residuals from each satellite can be tested using Eqn. (5.1). Previous investigations have shown that the Chi-square test on the quadratic form of residuals is generally good at detecting the occurrence of cycle slips in carrier phase data and Eqn. (5.1) is effective for identification of cycles slips occurring only on one satellite (Gao et al., 1992; Lu and Lachapelle, 1991). For multiple cycle slips on many satellites, the identification process is not reliable, and thus a re-initialization of all ambiguities has to be performed. If cycle slips are detected and correctly

identified and at least four non-slipped satellites are available, the new ambiguities of the slipped satellites can be computed using the position determined by the non-slipped satellites (Cannon, 1991).

In a GPS multi-antenna system, the baseline lengths among antennas are usually determined to the millimetre level from the initialization process. On a rigid body platform, these fixed baseline lengths can then be used as external constraints to check for the initially resolved carrier phase ambiguities or cycle slips. As shown by Cannon (1991), wrong ambiguities, which may result from incorrect initial ambiguity resolution or cycle slips, will cause a drift in the estimated positions of the remote antenna due to the changing satellite geometry. Translating this phenomenon to a multi-antenna system on a moving platform, a drift will be seen in the differences between the GPS computed baseline length and the known fixed baseline length. Shown in Figure 5.2 are the results of two tests with simulated wrong integer ambiguities. The data set used was collected on the ship Matthew on June 29, 1993. A detailed description of this test will be given in Chapter 6. The simulated wrong ambiguities in the tests are as follows:

- Test 1: Ambiguity of PRN 29 from antenna 2 (yaw direction)  
changed by -1 cycle from its true integer value;
- Test 2: Ambiguities of PRN 29 and PRN 28 from antenna 2  
changed by -1 cycle from their true values.

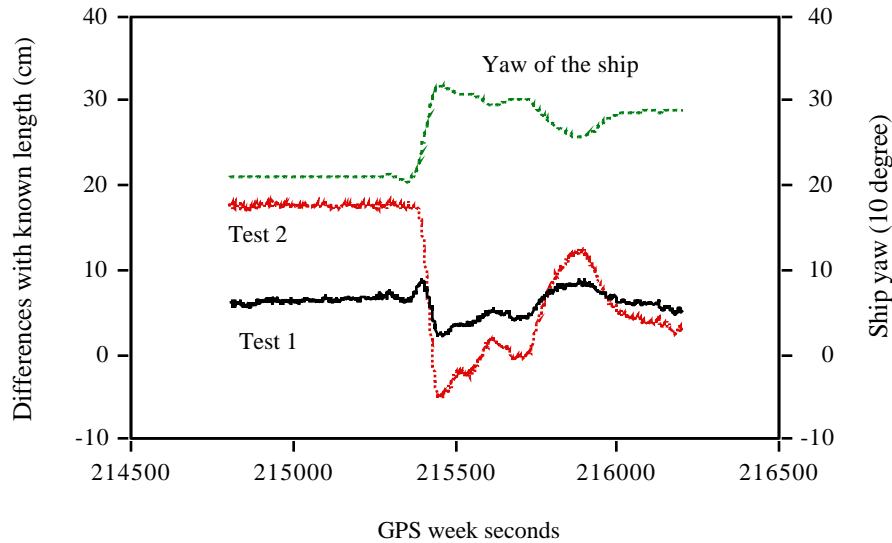


**Figure 5.2 Differences between the Known and the Computed Lengths with Wrong Ambiguities for Baseline 1-2**

It can be seen from Figure 5.2 that baseline errors induced from incorrect carrier phase ambiguities can reach about 6 cm for a single cycle slip on one satellite (Test 1) and 17 cm for one cycle slip on two satellites (Test 2). These kinds of error magnitudes are larger than the baseline errors caused by carrier phase multipath effects which are usually less than 2 cm, as will be seen in Chapter 6. Therefore, the test criterion for cycle slips or wrong ambiguities based on the fixed baseline length is formulated as

$$|\hat{d} - d_{\text{fix}}| < (m) , \quad (5.2)$$

where  $\hat{d}$  is the computed baseline length using ( ) carrier phase, and  $d_{\text{fix}}$  is the known fixed baseline length.

If the above equation is not satisfied at a preset number of consecutive epochs, the ambiguities related to this baseline are set to invalid and are re-initialized

by the ambiguity search process. The tolerance in eqn. (5.2) is a function of accuracy of the known baseline length, carrier phase multipath effects, measurement noise and any possible structural deformations in the baseline length direction. Generally speaking, it should not be less than 2 cm in order to absorb the multipath effects on the GPS computed baseline lengths, even if the fixed baselines are measured to the millimetre level.

It is also shown in Figure 5.2 that baseline errors resulting from incorrect ambiguities are highly correlated with the relative geometry between the baseline vector and GPS satellites. When the ship was stationary or in a straight course, the baseline errors drifted slowly due to the slow change of satellite constellation with respect to the baseline vector on the ship. When the ship turned at 215316s, which brought a change of the relative geometry between the baseline vector and satellites, the baseline errors in Test 2 decreased rapidly from 17 cm to -5 cm and then reached about 12 cm. During the period from 215554s to 215742s (3 minutes), the baseline errors were within  $\pm 2$  cm, which could not be detected by eqn. (5.2) if only the baseline errors from baseline 1-2 were checked. Fortunately, the baseline errors from the fixed baselines 2-3 and 2-4, which were connected to Antenna 2, showed 6 ~ 8 cm error magnitudes to enable detection in this case. Therefore, all the fixed baselines in a multi-antenna system should be used for quality checks on the estimated results. Because the GPS computed baseline drift is highly correlated with the relative geometry change, it would be very helpful to detect the wrong ambiguities if the platform makes 360° turns, which induces a rapid relative geometry change between the baseline vector and satellites.

Shown in Figure 5.3 are the differences between the estimated attitude parameters when using correct and incorrect ambiguities. Only the yaw and pitch components from Test 1 are plotted.

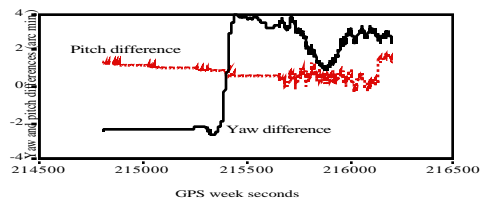


**Figure 5.3 Yaw and Pitch Differences for Test 1 with Correct and Incorrect Ambiguities**

The attitude errors induced from incorrect ambiguities are not constant and also vary with the change of relative geometry between the baseline vector and satellites. Due to the wide antenna spacing in this shipborne experiment, i. e. 42 m long in the yaw direction and 12 m in the roll direction, the magnitude of attitude errors caused by position errors from incorrect ambiguities is relatively small. For short baseline cases, the same position errors would produce more severe distortions in the estimated attitude parameters.

In a GPS multi-antenna system, most of the cycle slips can be detected instantaneously using the fixed baseline length test and the Chi-square test on residual quadratic forms. If cycle slips or wrong ambiguities can not be detected at the current epoch due to the effect of a special relative geometry between the baseline vectors and satellites, the baseline errors and the carrier phase residuals will eventually become large enough to be detectable with the continuous changing of satellite geometry and antenna platform movements. In this case, the time delay for detection may be a few seconds to a few minutes

depending on the relative geometry. A more detailed investigation of this aspect is recommended.

## CHAPTER 6

### TESTS AND RESULTS

In order to assess the performance of GPS multi-antenna systems consisting of three or four independent GPS cards or engines and evaluate the methods and software developed in this research, extensive shipborne tests were carried out in recent years jointly between The University of Calgary and the Canadian Hydrographic Service (CHS), and also between the university and the Defence Research Establishments Pacific and Ottawa, National Defence of Canada. In this chapter, two of these tests were selected and analyzed. The first one is the comparison of the results between a dedicated GPS multi-antenna unit and a non-dedicated GPS attitude system composed of three GPSCard™ receivers. The second one is the evaluation of a non-dedicated four-receiver attitude system against a high quality INS which is used as an attitude reference.

Although the main focus of this research is placed on the attitude determination for marine applications, the developed algorithms and software package MULTINAV can also be used for airborne cases, as shown by the results given in Cannon et al. (1994) for a flight test based on four GPSCard™

receivers, where a modification in the software to include an airplane wing flexing parameter was made.

## **6.1 SHIPBORNE TEST WITH DEDICATED AND NON-DEDICATED GPS ATTITUDE SYSTEMS**

The purpose of this test was to compare ship attitude results from dedicated and non-dedicated GPS attitude systems under the same operational environment and thereby establish the agreement level achievable by these two receiver configurations. Attitude estimation theory and on-the-fly ambiguity resolution methods described in the previous chapters were also tested.

### **6.1.1 Test Description**

A marine survey launch test was conducted by the Canadian Hydrographic Service and The University of Calgary on September 3, 1992 off the coast of Sidney, British Columbia. A dedicated 4-antenna 3DF attitude system manufactured by Ashtech, Inc. and a non-dedicated 3-GPSCard™ system were set up on a 12 m survey launch. All the antennas were mounted on two wooden beams placed across the width of the bow and stern of the boat. Baseline lengths between the antennas were measured with a tape with an accuracy of 1 to 2 cm. The antenna configurations are shown in Figure 6.1.

The Ashtech 4-antenna 3DF system has 24 tracking channels operating from a single oscillator. Each antenna can track up to six satellites and only L1 C/A code and carrier measurements are collected. Since the 3DF is a standard C/A code receiver, the pseudorange measurement noise is at the 1 m level, while the carrier phase measurement noise is 0.2 mm (Ashtech, 1991). The NovAtel GPSCard™ is a high performance 10-channel C/A code receiver which has two unique characteristics, namely a 10-cm code noise and narrow correlator spacing to reduce code multipath effects (Fenton et al., 1991; Van Dierendonck et al., 1992). The carrier phase measurement noise from the GPSCard™ is 0.75 mm.

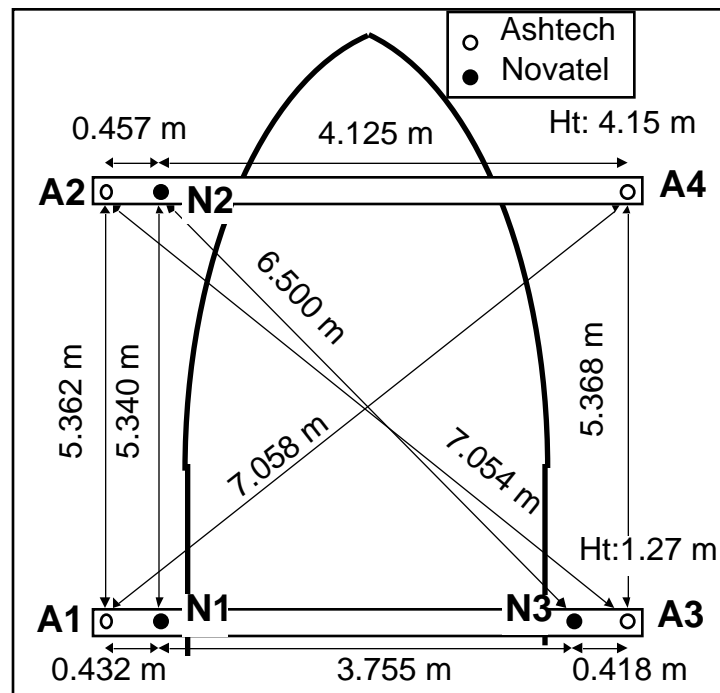


**Figure 6.1 Survey Launch GPS Antenna Configuration**

During the test, the boat was cruising at speeds of 10 to 15 knots and the weather was calm. GPS measurements were collected simultaneously from

both attitude systems over a period of 50 minutes at a 1 Hz rate. Six satellites were observed and the PDOP varied between 1.9 and 2.6. The 3DF raw data was logged internally while the data from the three GPSCard™s were logged by two Grid laptop computers (two receivers were housed in one Grid). GPSCard™ Antennas 1 and 3 had choking ground planes while Antenna 2 had none. No choking ground planes were available for the 3DF antennas. The survey launch trajectory during the test period is shown in Figure 6.2.

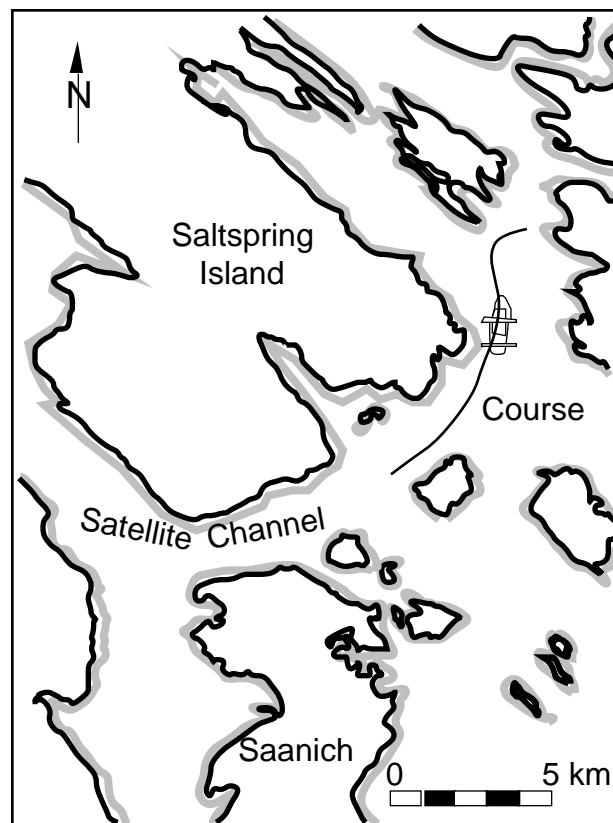


**Figure 6.2 Survey Launch Trajectory**

For attitude determination, it is assumed herein that the platform plane is defined by Antennas 1, 2, and 3 from each system. The direction from Antenna 1 to Antenna 2 defines the ship's yaw, i.e.  $y^b$ -axis in the antenna's

body frame coordinate system. The  $x^b$ -axis is orthogonal to the  $y^b$ -axis and lies in the platform plane. The  $z^b$ -axis then forms a right-handed system with  $x^b$  and  $y^b$  axes. It can be seen from Figure 6.1 that the body frame coordinate system defined by the 3DF antennas is not parallel to that defined by the GPSCard™ antennas. The misalignment angles between these two systems have to be determined before the attitude results from the two systems can be compared. One analytical method to determine the misalignment angles will be given in Section 6.1.3. As shown in Figure 6.1, the two wooden beams for antenna mounting were not placed in the same horizontal plane, which resulted in a pitch angle of about 32.487 degrees of the antenna platform.

### 6.1.2 Data Processing

The data from the Ashtech 3DF system and the 3-receiver NovAtel GPSCard™ system were processed using the MULTINAV program previously described in Chapter 5. The precise antenna body frame coordinates and baseline lengths between the antennas were computed by the program using the initialization option. Shown in Tables 6.1 and 6.2 are the final antenna body frame coordinates as well as the baseline lengths obtained by averaging the epoch-by-epoch results over the entire 50 minutes of kinematic GPS data collected. The purpose of averaging results over a long period is to smooth out the carrier multipath and noise effects so that the computed body frame coordinates can be determined to the cm-level accuracy. The averaged antenna body frame coordinates given in Table 6.1 are held fixed and used in the least

squares attitude estimation procedure to determine the optimal attitude parameters.

**Table 6.1 Antenna Body Frame Coordinates  
( Origin: Ant 1 [0, 0, 0] )**

| System      | Ant 2<br>[x, y, z] m | Ant 3<br>[x, y, z] m | Ant 4<br>[x, y, z] m  |
|-------------|----------------------|----------------------|-----------------------|
| Ashtech 3DF | [0.0, 5.367, 0.0]    | [4.602, 0.012, 0.0]  | [4.574, 5.379, 0.009] |
| GPSCard™    | [0.0, 5.370, 0.0]    | [3.761, 0.088, 0.0]  | N/A                   |

**Table 6.2 Baseline Lengths between GPS Antennas**

| Lines | Ashtech 3DF System |                  |            | GPSCard™ System |                  |            |
|-------|--------------------|------------------|------------|-----------------|------------------|------------|
|       | GPS<br>Computed    | Tape<br>Measured | Difference | GPS<br>Computed | Tape<br>Measured | Difference |
| 1-2   | 5.367 m            | 5.362 m          | 0.005 m    | 5.370 m         | 5.340 m          | 0.030 m    |
| 1-3   | 4.602              | 4.604            | -0.002     | 3.762           | 3.755            | 0.007      |
| 2-3   | 7.061              | 7.054            | 0.007      | 6.484           | 6.500            | -0.016     |
| 1-4   | 7.060              | 7.058            | 0.002      |                 |                  |            |
| 2-4   | 4.574              | 4.582            | -0.008     |                 | N/A              |            |
| 3-4   | 5.367              | 5.368            | -0.001     |                 |                  |            |

It can be seen from Table 6.2 that the differences between the GPS-computed and the tape-measured baseline lengths are generally within 1 cm. This indeed confirms that the GPS-derived average baseline lengths, and thus the body frame coordinates, are at the sub-cm level if the accuracy (1~2 cm) of tape-measured baseline lengths are taken into account.

In order to compare the attitude results from the non-dedicated and dedicated attitude systems under similar conditions, only three antennas from the 4-antenna Ashtech 3DF system, namely A1, A2 and A3, which are close to the three GPSCard™ antennas as indicated in Figure 6.1, are used to compute the Ashtech antenna platform attitude. The data from the two multi-antenna systems were processed separately with their own corresponding antenna body frame coordinates. No misalignment angles were applied to either systems. Listed in Table 6.3 are some of the user-selectable input parameters for multi-antenna GPS data processing with MULTINAV.

**Table 6.3 Input Parameters for Multi-Antenna GPS Data Processing**

| Parameter                             | Ashtech 3DF System               | GPSCard™ System                  |
|---------------------------------------|----------------------------------|----------------------------------|
| Standard deviation of Carrier Phase   | 1.0 cm                           | 1.5 cm                           |
| Baseline check (constraint) tolerance | 0.03 m                           | 0.03 m                           |
| Antenna platform                      | Three antennas used (A1, A2, A3) | Three antennas used (N1, N2, N3) |
| Satellite Cut-off Angle               | 10°                              | 10°                              |

The slightly poorer accuracy assigned to GPSCard™ carrier phase observations in Table 6.3 was due to the fact that stronger multipath effects were observed on GPSCard™ antennas without choking ground planes, as shown later in Figure 6.9.

In this experiment, the ambiguity search space for an antenna pair of the 3DF system was defined on a sphere with a radius equal to the fixed baseline length between the antennas. This leads to a maximum sphere radius at about

5.4 m which is smaller than the uncertainty cube of 3~9 m (1 ) level derived by kinematic differential pseudorange positioning with a standard C/A code receiver in a marine environment (Lachapelle et al., 1991). Since the GPSCard™ is a high performance C/A code receiver with 10-cm code noise, the ambiguity search interval was set at  $\pm 15$  cycles around the carrier phase ambiguities derived from the code solution, i.e.  $\pm 15$  cycles is approximately  $\pm 2.8$  m (3 ). The ambiguities for the 3DF system using only three antennas were resolved in 7 kinematic epochs at the beginning of the session, while the ambiguities for GPSCard™ system were resolved using 8 epochs of kinematic observations. Once the ambiguities are resolved, the platform attitudes are computed by a least squares procedures at each observation epoch. For comparison purposes, the attitude results by the direct computation method are also output. Given in Figures 6.3, 6.4 and 6.5 are the yaw, pitch and roll of the survey launch derived from GPSCard™ system and 3DF system using three antennas.

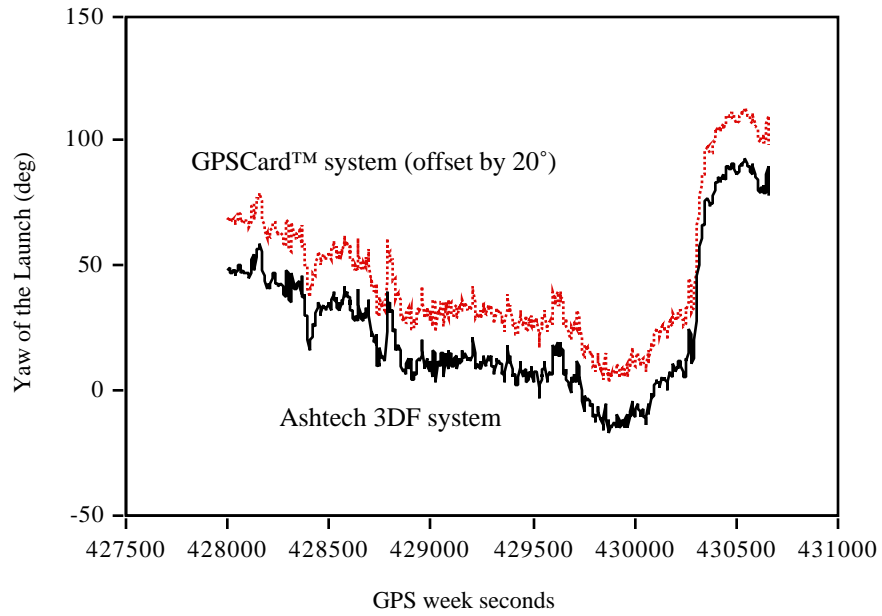


**Figure 6.3 Yaw of the Launch Estimated by the LS method**

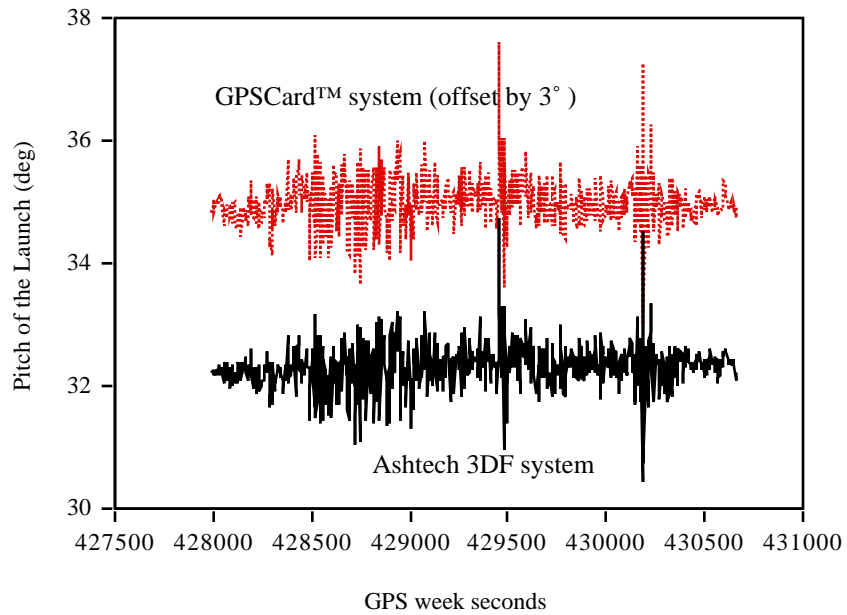


**Figure 6.4 Pitch of the Launch Estimated by the LS method**

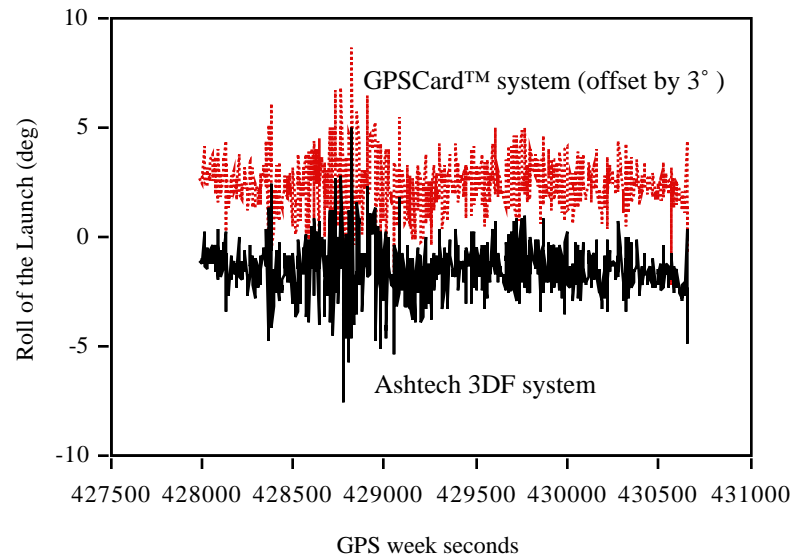


**Figure 6.5 Roll of the Launch Estimated by the LS method**

### 6.1.3 Misalignment Angle Determination

In order to compare the attitude results of the 3DF system with the GPSCard™ system, the ideal situation would be that both platforms were perfectly parallel in space so the two systems could be compared directly. However, the antennas from each system were not placed exactly on one line on the wooden beams, nor was the heading baseline of the 3DF system parallel to that of the GPSCard™ system. Therefore, orientation differences existing in yaw, pitch and roll between the two platforms had to be determined before the results could be compared.

If the two platforms considered are rigid body platforms, the misalignment angles will be constant no matter how the vehicle or ship is turning or rolling. One way to determine the misalignment angles is to

precisely survey the antenna body frame coordinates of one system with respect to the other antenna body frame and then calculate the misalignment angles using the direct computation formulae given in Chapter 5 based on the surveyed antenna coordinates. The problem with this method is that surveying antenna coordinates is hard to do sometimes in an operational environment. In the following, an analytical method to determine the misalignment angles is given, which only uses the platform attitude results output from the two systems considered.

Suppose that two attitude systems are collecting data simultaneously at synchronized epochs. Based on the attitude values output at each epoch from the two systems, two attitude (rotation) matrices can be formed by  $R_{I/L}(y_I^i, p_I^i, r_I^i)$  and  $R_{G/L}(y_G^i, p_G^i, r_G^i)$ , where  $R_{I/L}$  is the rotation matrix from local level to the body frame I of the first attitude system computed using the yaw, pitch and roll values  $(y_I^i, p_I^i, r_I^i)$  at epoch  $i$  and  $R_{G/L}$  is the rotation matrix from local level to the body frame G of the second attitude system computed using the corresponding attitude values  $(y_G^i, p_G^i, r_G^i)$ . From the *cascade* property of rotation matrices, the rotation matrix from body frame G to body frame I can be easily obtained as

$$R_{I/G}(y^i, p^i, r^i) = R_{I/L}(y_I^i, p_I^i, r_I^i) R_{G/L}^T(y_G^i, p_G^i, r_G^i). \quad (6.1)$$

Once the rotation matrix  $R_{I/G}$  is computed using the attitude values output from the two systems by Eqn. (6.1), the misalignment angles from the body frame G to body frame I, i.e.  $(y^i, p^i, r^i)$ , can then be determined by Eqn. (3.3) given in Chapter 3. Due to noise and multipath effects in the estimated attitude values from the two GPS multi-antenna systems, the computed

misalignment angles will be slightly different from epoch to epoch even though they should be constant for rigid body platforms. More accurate misalignment angles are therefore obtained by averaging the epoch-by-epoch misalignment angles over a long time span, say one hour or the whole observation session. The averaged misalignment angles are calculated as

$$\bar{y} = \frac{1}{n} \sum_{i=1}^n y^i, \quad (6.2a)$$

$$\bar{p} = \frac{1}{n} \sum_{i=1}^n p^i, \quad (6.2b)$$

$$\bar{r} = \frac{1}{n} \sum_{i=1}^n r^i. \quad (6.2c)$$

Obviously, the mean misalignment angles given by Eqn. (6.2) include the physical misalignment between the two body frames as well as the error effects that have not been smoothed out by averaging. Once the misalignment angles are determined, the attitude parameters from one body frame can then be rotated into the other body frame and compared with the attitude parameters output from the other attitude system.

#### **6.1.4 Comparison of the Attitude Results from Dedicated and Non-Dedicated Multi-Antenna Systems**

As the true misalignment angles between the Ashtech 3DF system and the GPSCard™ system are not known, the mean misalignment angles were computed by averaging the epoch-by-epoch misalignment angles through the whole observation session using Eqn. (6.2). The attitude parameters of the 3DF

platform were then rotated by the amounts of the computed mean misalignment angles and compared with the attitude of the GPSCard™ platform. The yaw, pitch and roll differences between the two systems are plotted in Figures 6.6, 6.7 and 6.8. The mean of the differences is zero because the mean misalignment angles were used to correct the attitudes from one body frame to the other in this case. The presence of carrier phase multipath effects is clearly shown in Figures 6.6, 6.7 and 6.8 by the cyclic pattern of the attitude differences, especially in yaw and pitch components where the GPSCard™ antenna 2 had no chokering ground plane.

Summarized in Table 6.4 are the mean misalignment angles and the standard deviations of the attitude differences.

**Table 6.4 Attitude Differences Between the 3DF and the CPSCard™ Systems**

| Attitude Component | LS Attitude Estimation           |                             | Direct Attitude Estimation       |                             |
|--------------------|----------------------------------|-----------------------------|----------------------------------|-----------------------------|
|                    | Mean Misalignment Angle (arcmin) | Standard Deviation (arcmin) | Mean Misalignment Angle (arcmin) | Standard Deviation (arcmin) |
| Yaw                | -20.82                           | 5.64                        | -21.06                           | 7.74                        |
| Pitch              | -20.10                           | 8.76                        | -21.12                           | 9.78                        |
| Roll               | 38.22                            | 13.20                       | 37.74                            | 13.20                       |

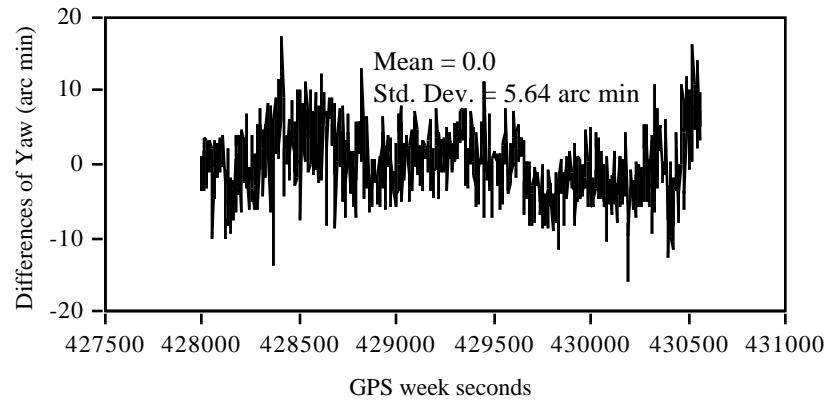


**Figure 6.6 Yaw Differences of the Launch from the Two Systems**

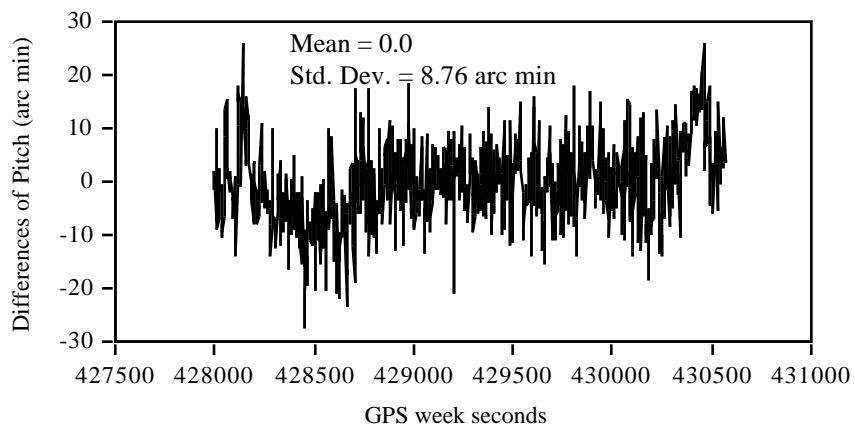


**Figure 6.7 Pitch Differences of the Launch from the Two Systems**

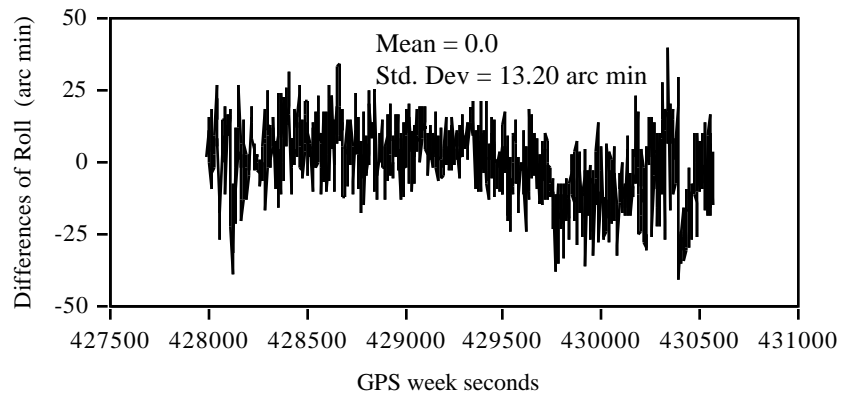


**Figure 6.8 Roll Differences of the Launch from the Two Systems**

The agreement between the estimated attitude parameters from the two systems are at the range of 5 arc minutes to some 14 arc minutes (standard deviation). The poorer accuracy in the roll component is due to the shorter antenna baseline in the roll direction. This level of agreement approaches the limit of the achievable accuracy of differential GPS positioning. For example, suppose that a 5 mm relative positioning accuracy is available from both the 3DF and GPSCard™ systems. The accuracy for yaw determination would be 3.4 arc minutes for either system based on a 5 metre antenna separation and the yaw difference from the two systems would be  $4.8 (\sqrt{2} \times 3.4)$  arc minutes which is very close to 5 arc minutes. In the marine environment, multipath is the dominant error which can easily induce position errors exceeding 5 mm level and reaching more than 1 cm level during some periods, as will be shown later in the comparison between the GPS computed and the fixed baseline lengths for both the dedicated and non-dedicated multi-antenna systems. Therefore, the attitude determination accuracy from the non-dedicated GPSCard™ system is comparable to the dedicated 3DF system since multipath, which is significantly larger than receiver carrier phase noise, is the major error source for both systems. A similar study performed independently by the Defence Research Establishment Ottawa using the Ashtech 3DF, the Trimble TANS Vector and the above proposed four-receiver GPSCard™ system with chokering ground planes has also confirmed that the same accuracy level was obtained with these three kinds of attitude systems in a marine experiment where the reference attitudes were provided by an INS (McMillan et al., 1994). Another observation that can be made based on Table 6.4 is that the agreement of the least squares estimates of the attitude parameters for the two systems

are slightly better than those from the direct computation method. This is because all the antenna position information is used in the LS estimation.

To further show multipath effects for attitude estimation in kinematic marine environment, the differences between the GPS computed and the known baseline lengths are plotted in Figures 6.9 and 6.10 for the two systems. Since the baseline lengths between antennas are considered fixed, the differences actually reflect the errors caused by multipath and receiver noise.

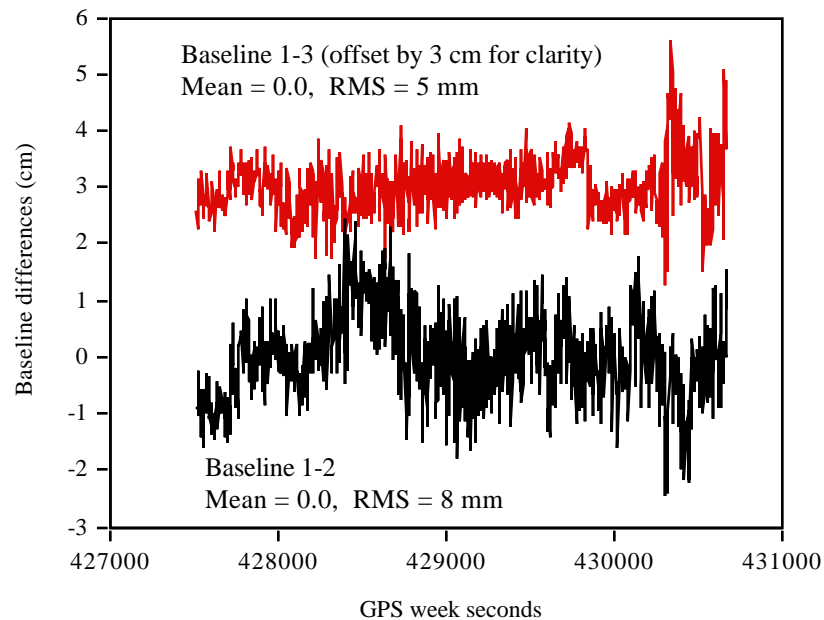


**Figure 6.9 Differences between GPS Computed and Fixed Baseline Lengths for the GPSCard™ System**

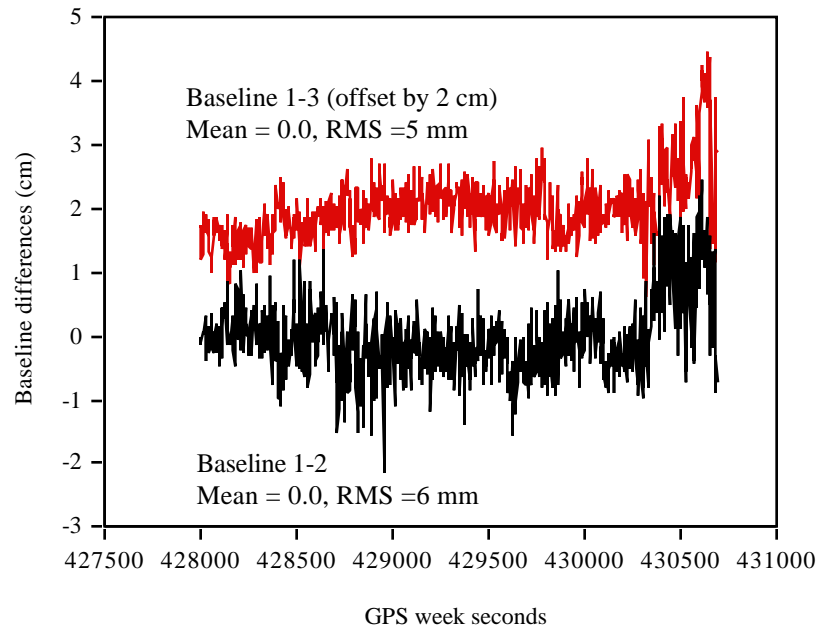


**Figure 6.10 Differences between GPS Computed and Fixed Baseline Lengths for the Ashtech 3DF System**

As shown by the cyclical trend in the baseline differences, multipath effects on the GPS computed baseline lengths are evident in both the 3DF and GPSCard™ multi-antenna systems. The periods with the discrepancy larger than 1 cm level range from a few seconds to some 5 minutes in the worst case. For the GPSCard™ system, the multipath effects on the baseline 1-3 with both chokering ground planes are significantly reduced as compared with those on the baseline 1-2 which has only one chokering ground plane. It is also observed that the magnitude of multipath influence on the Ashtech 3DF system is almost at the same level of GPSCard™ receivers equipped with chokerings. Without chokering ground planes, GPSCard™ receivers are more affected by multipath than the 3DF system. The different multipath signatures from the two systems without chokerings likely arises from the use of different types of antennas.

Shown in Table 6.5 are the RMS (root mean square) values of double difference carrier phase residuals with fixed ambiguities for both the Ashtech and GPSCard™ systems. The base satellite for double differencing was SV 23. For the GPSCard™ antennas, only Antenna 2 had no choking ground plane. As a result, slightly larger RMS values are obtained for the carrier phase residuals related to baseline 1-2. With choking ground planes on both antennas (baseline 1-3), the RMS values for carrier phase residuals from the GPSCard™ system are even smaller than those from the Ashtech 3DF system with which no choking ground planes were used.

**Table 6.5 RMS of Double Difference Carrier Phase Residuals for the Ashtech and GPSCard™ Systems**

| SV | Elevation | Ashtech 3DF                            |                       | GPSCard™ System       |                       |
|----|-----------|--|-----------------------|-----------------------|-----------------------|
|    |           | Line 1-2<br>(RMS: cm)                  | Line 1-3<br>(RMS: cm) | Line 1-2<br>(RMS: cm) | Line 1-3<br>(RMS: cm) |
| 17 | 71° - 55° | 0.387                                  | 0.388                 | 0.429                 | 0.378                 |
| 3  | 40° - 22° | 0.298                                  | 0.319                 | 0.457                 | 0.244                 |
| 28 | 34° - 48° | 0.284                                  | 0.321                 | 0.374                 | 0.263                 |
| 26 | 35° - 28° | 0.318                                  | 0.351                 | 0.398                 | 0.279                 |
| 21 | 31° - 48° | 0.292                                  | 0.327                 | 0.426                 | 0.277                 |
| 23 | 71° - 86° | Base satellite for double differencing |                       |                       |                       |

Shown in Figures 6.11 and 6.12 are examples of double difference carrier phase residuals (SVs 21-23) with fixed integer ambiguities for the 3DF and GPSCard™ systems. Note that the residuals for Antennas 1-3 have been offset by -1 cm for clarity.

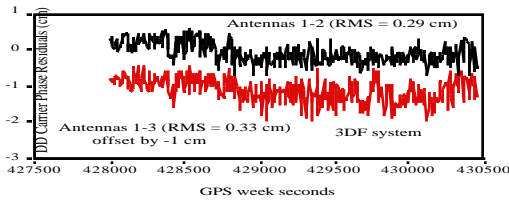


**Figure 6.11 Double Difference Carrier Phase Residuals for 3DF System (SVs 21-23)**

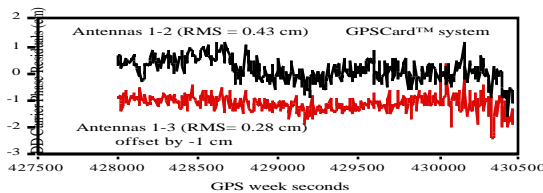


**Figure 6.12 Double Difference Carrier Phase Residuals for GPSCard™ System (SVs 21-23)**

It is evident from Figure 6.12 that the slightly larger RMS values for the carrier phase residuals related to baseline 1-2 of the GPSCard™ system are caused by the multipath. With choking ground planes, the multipath effects on carrier phase observations are significantly reduced in this case. To achieve the ultimate attitude determination accuracy, multipath influences on carrier phase observations should be reduced as much as possible.

To summarize the results in this section, it has been shown that the accuracy level of attitude parameters estimated from the non-dedicated attitude system is comparable with that from the dedicated attitude system since multipath is the dominant error source for both systems and is much larger than the carrier phase receiver noise. The advantage of using the non-dedicated attitude system is the flexibility in the selection of GPS receivers and the cost-effectiveness of the system with the emergence of low-cost GPS receivers. The results also show that depending on the receivers and antennas

used, choking ground planes can be effective in reducing carrier phase multipath effects and should be used whenever possible.

## **6.2 SHIPBORNE TEST OF A NON-DEDICATED MULTI-ANTENNA GPS SYSTEM WITH AN INS**

The purpose of this test was to assess the performance and the achievable accuracy of a non-dedicated multi-antenna GPS system for hydrographic surveys. The reference attitude for evaluation was provided by a high accuracy ring laser gyro (RLG) INS installed on the ship. This test provides an independent check on the performance of the non-dedicated GPS attitude system whereas the previous test has shown the consistency between different GPS-based attitude systems.

When multi-beam echo sounders are used for seafloor mapping and bottom imagery, yaw, pitch and roll information of the ship are needed to correct the echoed acoustic beams so that accurate vertical depths can be derived. The suggested accuracy for yaw, pitch and roll determination for this experiment was  $0.1^\circ$  (Lachapelle, et al., 1994). Typically, the accuracy standards set by the International Hydrographic Organization for charting depths greater than 30 m is 1% of the depth (Dinn and Loncarevic, 1994). In this shipborne test, a wide antenna spacing of up to 42 metres was used in order to obtain accurate attitude information from the multi-antenna GPS system.

### 6.2.1 Test Description and Antenna Setup

In the summer of 1993, the Canadian Hydrographic Service and The University of Calgary jointly conducted a sea trial on the continental shelf near Halifax, Nova Scotia. A GPS multi-antenna system consisting of four independent NovAtel GPSCard™ sensors and a Honeywell HG1050 strap-down ring laser gyro (RLG) INS were installed on the 52 m CHS ship Matthew. As is known, three non-collinear antennas provide the minimal configuration required to determine the three attitude parameters. The selection of the four independent receiver configuration was used to provide redundancy. As well, the GPSCard™ sensors have shown to be effective with minimal cycle slips in previous shipborne tests (Lu et al., 1993; Lachapelle et al., 1993). In order to simulate various sea states, the ship was put through a number of manoeuvres including acceleration, deceleration, 90° and 360° turns which induce 12° ship roll.

In order to obtain high accuracy estimates of attitude parameters, the separation between the GPS antennas should be as far as possible since the error of the estimated attitude parameters is inversely proportional to the baseline length. In addition, each antenna should be placed in an open area away from the ship mast, radar and other ship-borne radio equipment that may obstruct and interfere with GPS signals. The four GPS antennas with their chokering ground planes were deployed on the ship Matthew, as shown in Figure 6.13. The antennas were mounted on 3 to 6 metre vertical steel pipelines that provided a solid support under the various ship manoeuvres.

The antenna platform was defined using Ant 1 (Aft), Ant 2 (Forward) and Ant 3 (starboard). The origin is at Ant 1 and the y-axis runs from Ant 1 to Ant 2, and defines the yaw of the ship obtained by the multi-antenna system. The x-axis points to the starboard and lies on the plane defined by Ant 1, Ant 2 and Ant 3. Finally, the z-axis forms a right-handed system with the x and y axes. This antenna platform has a pitch of about  $3.4^\circ$  and a roll of about  $-12.5^\circ$  with respect to the horizontal plane.

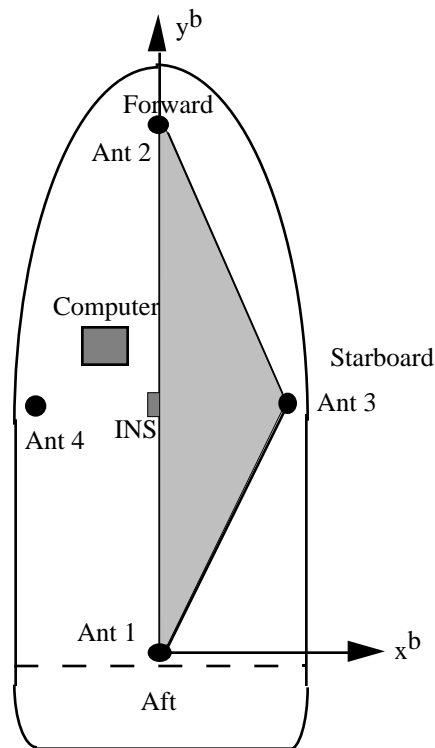


**Figure 6.13 Antenna Layout on Ship Matthew**

The antenna locations in the antenna platform coordinate system were determined using the measurements made on June 24, 1993 when the ship was tied to the wharf. Since the ship was submitted to slight motion due to the wind and tides, the final antenna coordinates were computed by averaging the

instantaneous coordinates at each epoch obtained by on-the-fly carrier phase ambiguity resolution solutions using 1.5 hours of data. The resulting antenna coordinates in the antenna platform coordinate system are given in Table 6.6. Shown in Table 6.7 are the distances between the antennas determined by GPS measurements. These pre-determined antenna coordinates and baseline lengths are held fixed in the least squares estimation of the attitude parameters and also during carrier phase integer ambiguity searching and cycle slip checking.

**Table 6.6 GPS Computed Antenna Coordinates in Antenna Platform Coordinate System**

| Antenna | x(m)   | y(m)   | z(m)  |
|---------|--------|--------|-------|
| 1       | 0.000  | 0.000  | 0.000 |
| 2       | 0.000  | 42.735 | 0.000 |
| 3       | 6.096  | 25.837 | 0.000 |
| 4       | -5.586 | 25.997 | 2.579 |

**Table 6.7 Distances between GPS Antennas**

| Lines         | 1-2    | 1-3    | 1-4    | 2-3    | 2-4    | 3-4    |
|---------------|--------|--------|--------|--------|--------|--------|
| Distances (m) | 42.735 | 26.546 | 26.715 | 17.963 | 17.832 | 11.963 |

Based on the multiple GPS antenna configuration on the ship and assuming a 1-cm accuracy for the GPS-derived relative coordinate components x, y and z, the accuracy of the estimated attitude parameters using the direct

computation method using Ant 1, Ant 2 and Ant 3 would only be approximately 0.8' for yaw and pitch and 5.6' for the roll in this experiment.

### **6.2.2 INS Installation and Data Collection**

In order to provide an accurate reference attitude for comparison with the GPS estimated ship attitude, a Honeywell HG1050 strap-down ring laser gyro INS was setup in the Sonar Transducer compartment at the lower level of the ship. The INS data rate was recorded at 50 Hz. A 1 pulse-per-second (PPS) timing signal and its corresponding GPS time from a Magnavox 4200D GPS receiver were sent to the INS data logging computer to synchronize the INS and GPS data. Accurate time tagging between INS and GPS was the basic requirement for comparison between the GPS and INS derived attitudes. The estimated timing error was about  $\pm 10$  ms (Loncarevic, 1993). Due to the relatively low ship dynamics, the effect of this timing uncertainty on comparison of the ship roll, pitch and heading can be neglected. The time from different GPS receivers can be reasonably assumed to be within the 1 ms level since the receiver clocks are always reset to the GPS system time within a 1 ms difference. Thus, this error can also be neglected.

The INS data collection and data processing were performed by Applied Analytics Corporation (AAC), Markham, Ontario. A Kalman filter was used to post-process INS raw measurements and integrate the INS solutions with differential GPS C/A code positioning solutions. The solution output rate from the Kalman filter was also 50 Hz. The attitude accuracy from the integrated

INS and GPS solution is 2' for the yaw (heading) and 0.25' for the pitch and roll (Lachapelle et al., 1994). The INS yaw component achieved an accuracy of 6 arc minutes after approximately 20 minutes following initialization of the Kalman filter and continued to improve afterwards. The final accuracy for INS yaw at the steady state is about 2 arc minutes. It should be noted that INS yaw is referred to the geographic north and GPS multi-antenna yaw is referred to the geodetic north. However, the yaw differences caused by these two different reference systems are seldom larger than 15 arc seconds for most of the regions on the earth (Schwarz and Krynski, 1992), and thus can be ignored in the yaw comparison.

### **6.2.3 Data Processing and Analysis**

Kinematic multi-antenna GPS data were collected on two different days. On June 29, 1993 (Day 180), the ship carried out her first multi-antenna GPS test in the Bedford Basin and approximately 1.5 hours data from the four GPSCard™ receivers were collected. The GPS data rate was at 10 Hz. The INS measurements were also simultaneously collected at a 50 Hz rate. On July 14, 1993 (Day 195), a second test was performed in open sea near Halifax. Two hours data were collected in this case. The data rate was at 1 Hz for the first hour (Session A) and 5 Hz for the second hour (Session B). During the tests, the weather was generally calm. Therefore, the ship was put through a number of manoeuvres to produce rapid heading and roll changes.

With a full constellation of 24 GPS satellites, observation windows were generally good at all times during the tests. The GDOP was between 2 and 3. At least five satellites were tracked above a 10° elevation throughout the trials and only a few cycle slips were detected on low elevation satellites. All the data sets from the two days were successfully processed from beginning to end. The RMS of the double difference ( ) carrier phase residuals is of the order of 2 to 5 mm, which is within the anticipated range for this type of receiver and antennas equipped with chokering ground planes in the marine environment. The distance error (1 ) between the GPS computed and fixed baseline lengths among the antennas is within 5 mm. The performance of the GPS multi-antenna system was fully satisfactory.

The input option parameters for on-the-fly ambiguity resolution were 1 cm (1 ) for double difference carrier phase observations and 3 cm tolerance between the computed and the fixed baseline lengths. The ambiguities were resolved in 2 seconds at the beginning for Day 180 test, 11 seconds for Session A, Day 195 test and 3 seconds for Session B, Day 195 test. On-the-fly ambiguity resolution was only performed once at the beginning of each observation session since more than five satellites were tracked during all the tests.

Listed in Table 6.8 are the statistics of comparisons between the INS and GPS estimated attitude for the tests on two different days. The mean misalignment angles between INS and GPS platforms were computed for each observation session using the INS and GPS derived attitudes by the method described in Section 6.1.3. The GPS derived attitudes were then rotated to the INS reference platform based on the computed mean misalignment angles and

compared with the INS attitude values interpolated at the corresponding GPS time. Since the INS was initialized en route each day and its heading direction had a very small variation with time, the mean misalignment angles were computed for each observation session instead of using constant values throughout the whole experiment. The attitude parameters from the GPS multi-antenna system were estimated at each epoch using the four-antenna configuration shown in Figure 6.13.

**Table 6.8 Statistics of Comparisons between INS and GPS Estimated Attitude**

| Session | Num. of samples | Data rate (Hz) | Mean misalignment angle (degrees) |        |        | RMS between INS and GPS (arc minutes) |       |      |
|---------|-----------------|----------------|-----------------------------------|--------|--------|---------------------------------------|-------|------|
|         |                 |                | yaw                               | pitch  | roll   | yaw                                   | pitch | roll |
| 180L    | 41722           | 10             | -0.129                            | -3.524 | 12.453 | 3.12                                  | 0.78  | 2.65 |
| 180S    | 26725           | 10             | -0.097                            | -3.516 | 12.454 | 0.87                                  | 0.86  | 2.70 |
| 195a    | 3446            | 1              | -0.038                            | -3.497 | 12.462 | 0.85                                  | 0.57  | 2.81 |
| 195b    | 9922            | 5              | -0.017                            | -3.492 | 12.452 | 1.96                                  | 0.63  | 3.30 |

The results in Table 6.8 show an excellent agreement between the GPS and INS derived ship attitudes. The RMS values of the differences are less than 0.8' for pitch, 3.3' for roll and 3.2' for yaw. For the Day 180 results, two comparisons were made. The first one is denoted as 180L and started at time  $t=43500s$  (UTC seconds of the day) where the INS had been only running for 10 minutes and was still in the initialization process. The yaw accuracy from the INS was about 9.5' at the start of comparison and gradually improved to 4.5' after 25 minutes later at the time  $t=45000$  seconds. The yaw agreement for

this data set was 3.12 arc minutes. To reduce the INS yaw errors in the results, a second comparison was then started at  $t=45000$  seconds and denoted as 180S. The yaw agreement for this sub-set was 0.87 arc minutes. The INS yaw accuracy improvement during the initialization process is clearly shown in Figure 6.14. From the mean misalignment angles it can be seen that the INS yaw was slowly drifting with time while the INS pitch and roll outputs were very stable.

Based on the above analysis and the stated INS roll and pitch accuracy of 15", it can be concluded that the accuracy for the GPS estimated roll and pitch components in these experiments are better than 3.3' for roll and 0.9' for pitch. The poorer accuracy for roll determination from the GPS multi-antenna system is due the short baseline length in the roll direction. From the least squares attitude estimation procedure, the *a posteriori* standard deviations for GPS derived attitude parameters were approximately 0.6' for the yaw and pitch and 4.0' for the roll, which are close to the RMS values given in Table 6.7. The yaw agreement between the multi-antenna GPS system and INS is better than 2', which is the stated INS yaw accuracy in the steady mode. The poorer RMS values for yaw component may be due to the low yaw accuracy from INS. It has been found that the INS yaw may have a small bias or drift from its true value (Liu, 1992). In the above comparisons, the constant bias or the mean of the drift in the INS yaw was removed by the attitude rotation using mean misalignment angles between the two systems. Therefore, the agreement in yaw may reach about 0.9' for some sessions, which is well below the INS yaw accuracy of 2'. This is indeed a strong indication that high accuracy yaw estimation from the GPS multi-antenna system has been achieved. Since yaw

and pitch from the multi-antenna system have approximately the same accuracy level based on the least squares estimation procedure or direct computation method, and the pitch accuracy is proven to be better than 0.9' based on the accurate INS reference, it may reasonably be concluded that yaw estimation from the GPS multi-antenna system in this experiment is also at the 0.9' level.

No accuracy degradation of the attitude parameters from the GPS multi-antenna system was observed with respect to different data rates and rapid ship manoeuvres. Traditionally, when the low-cost gyro and accelerometer-based attitude sensors such as TSS and HIPPY are used for ship attitude determination, it is necessary for the ship to make turns outside the survey area and to allow sufficient "run-in" time for the sensors to settle down before data collection begins (Dinn and Loncarevic, 1994). With GPS multi-antenna systems, such operational restrictions for surveying vessels can be removed and thus the productivity can be improved.

Shown in Figures 6.14, 6.15 and 6.16 are the yaw, pitch and roll differences between the multi-antenna GPS attitude system and INS for the Day 180 test in the Bedford Basin.

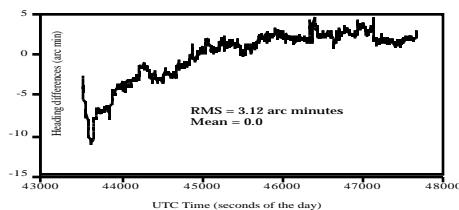


**Figure 6.14 Yaw Differences (GPS-INS) for Day 180, 1993**

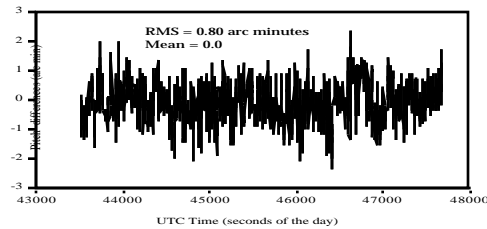


**Figure 6.15 Pitch Differences (GPS-INS) for Day 180, 1993**

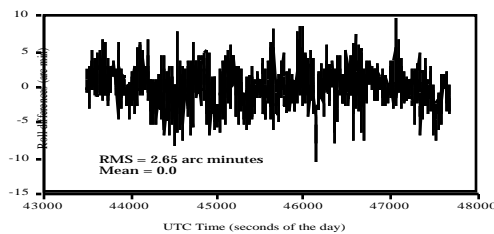


**Figure 6.16 Roll Differences (GPS-INS) for Day 180, 1993**

The ship ground trajectory on the Day 180 (June 29, 1993) is shown in Figure 6.17. To simulate various sea states, the ship underwent a series of manoeuvres including acceleration, deceleration and full speed  $90^\circ$ ,  $180^\circ$  and  $360^\circ$  turns. The maximum cruising speed reached about 12 knots during manoeuvres. GPS-derived yaw, pitch and roll values are shown in Figures 6.18, 6.19 and 6.20. A positive pitch angle corresponds to a tilting of the ship towards the stern while a positive roll angle corresponds to a tilting of the ship towards starboard. The roll reached  $\pm 12.5^\circ$  during rapid turns. The ship yaw change rate and roll change rate were plotted in Figures 6.21 and 6.22. The change rate reached about  $2.5^\circ$  per second during the turns.

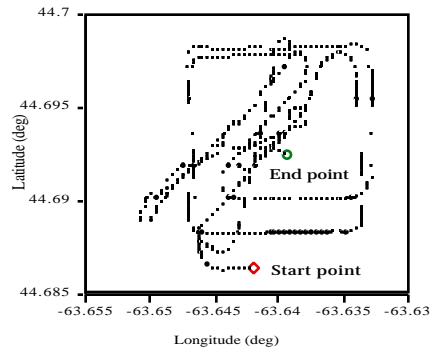


**Figure 6.17 Ship Trajectory for June 29 (Day 180) Test**

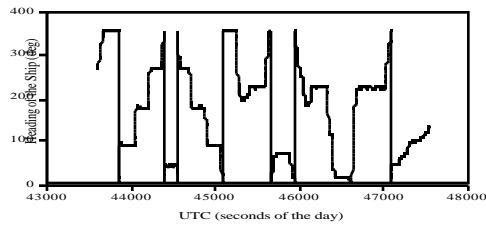


**Figure 6.18 Ship Yaw Derived from GPS Attitude System (Day 180)**

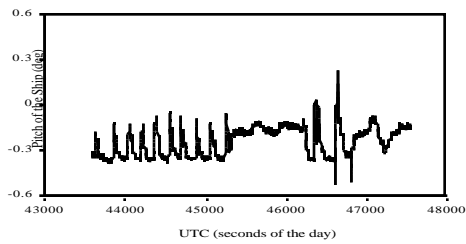


**Figure 6.19 Ship Pitch Derived from GPS Attitude System (Day 180)**

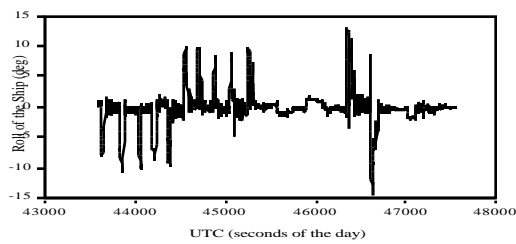


**Figure 6.20 Ship Roll Derived from GPS Attitude System (Day 180)**

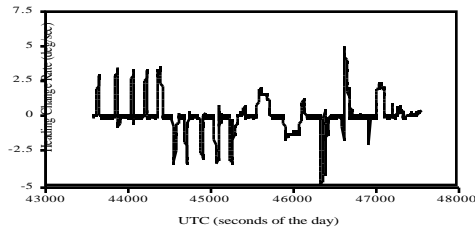


**Figure 6.21 Yaw Change Rate for Day 180**

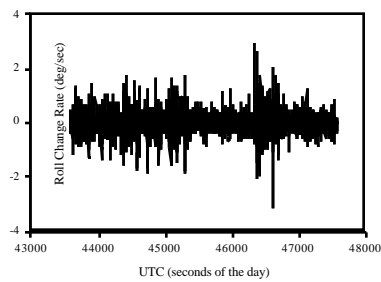


**Figure 6.22 Roll Change Rate for Day 180**

To examine multipath effects and carrier phase accuracy in this sea experiment, differences between the GPS-computed and the known baseline lengths as well as the double difference carrier phase residuals with fixed ambiguities are analyzed. Shown in Figure 6.23 are the baseline differences for the Day 180 test. The RMS of the baseline differences is less than 5 mm.

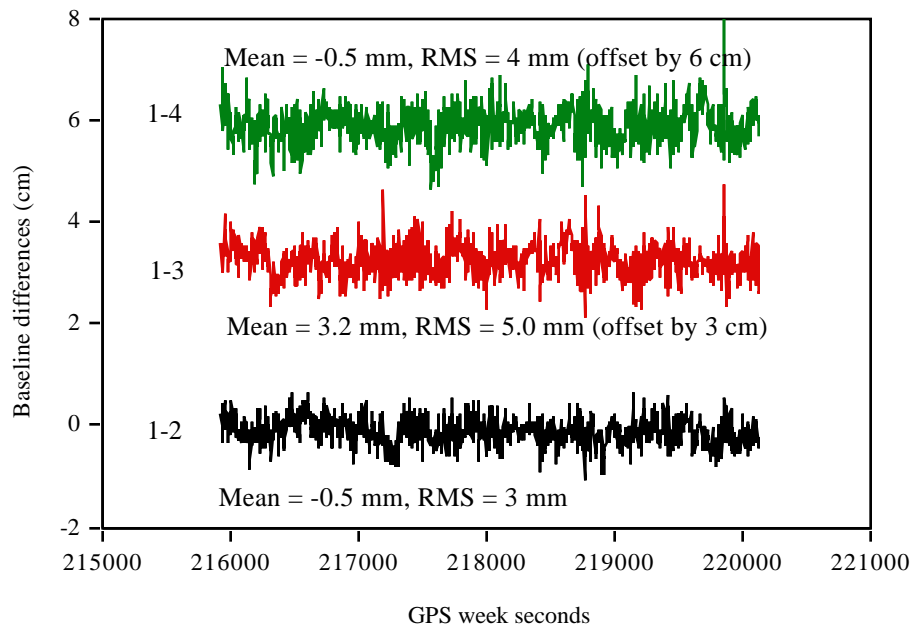


**Figure 6.23 Differences between GPS computed and Known Baseline Lengths for Day 180 Test**

It can be seen from Figure 6.23 that carrier phase multipath effects on the baseline determination are visible since the baseline differences change with time in a quasi-cyclical pattern. However, the magnitudes are generally within 1 cm level due to the use of chokering ground planes. At the peaks of multipath influence, the baseline differences can exceed 1 cm level for a period of a few seconds in this case. It is also noted that stronger multipath effects are observed at Antennas 3 and 4 which are located in the middle of the ship and close to the ship mast, radio equipment antennas and ship-borne radar.

Shown in Figures 6.24 and 6.25 are two examples of double difference carrier phase residuals with fixed ambiguities. The base satellite for double differencing is SV 22 with elevation angles from  $78^\circ$  to  $41^\circ$ . SV 18 is considered as a relatively high elevation satellite with elevation angles from  $26^\circ$  to  $41^\circ$ ,

while SV 3 is a relatively low elevation satellite with elevation angles from 33° to 10° in this test.

The analyses have indicated that the RMS values of adjusted double difference carrier phase residuals are all less than 5 mm in these marine tests. Even though multipath effects are greatly reduced by using chokering ground planes, they are still one significant error source for carrier phase observations, especially for antennas with poorer locations. This is clearly reflected in Figures 6.24 and 6.25 for carrier phase residuals related to Antennas 3 and 4, which are close to the mast and ship radar. As expected and also shown by the figures, the RMS values from the low elevation satellites are slightly worse than those from the high elevation satellites.

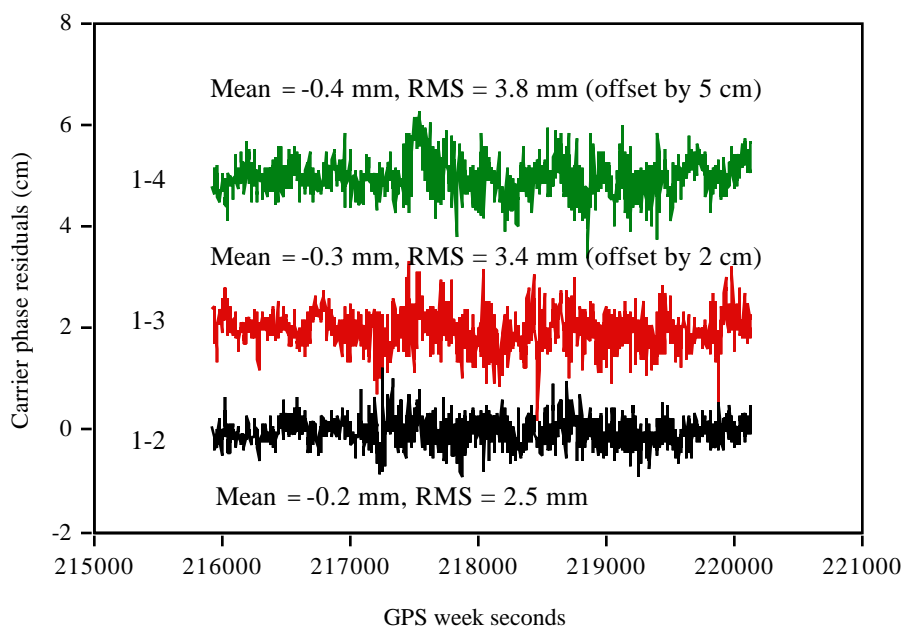


**Figure 6.24 Double Difference Carrier Phase Residuals for Day 180 Test (SVs 28-22)**

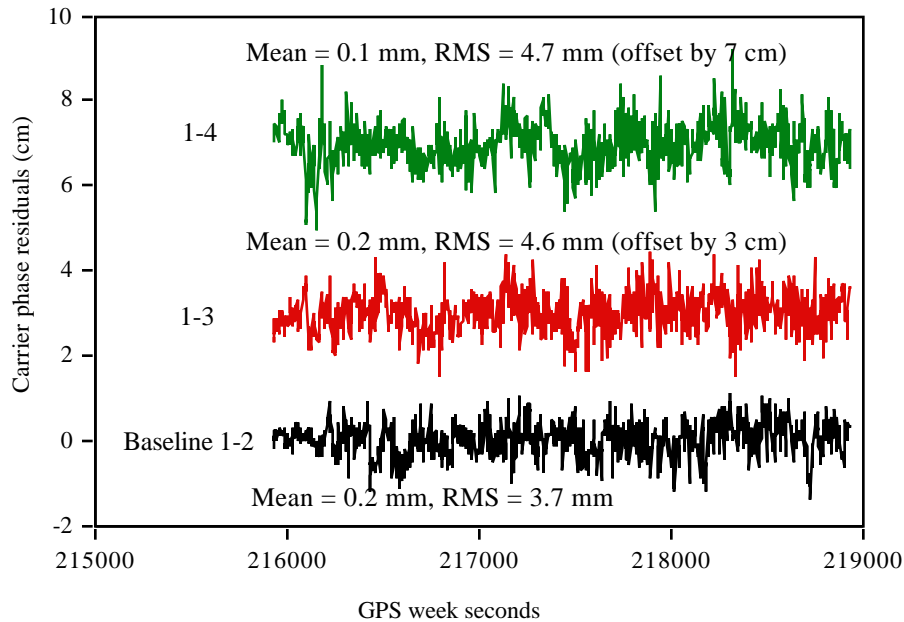


**Figure 6.25 Double Difference Carrier Phase Residuals for Day 180 Test (SVs 3 -22)**

To summarize the results in this section, it has been shown that the non-dedicated four-antenna GPS attitude system and the developed software and algorithms have delivered a satisfactory level of performance during the sea trials. The phase tracking loops of the GPS sensors selected were very stable during all the ship manoeuvres. The attitude parameters estimated from the GPS multi-antenna system are drift-free as compared with gyro-based attitude sensors. The comparisons between the GPS and INS derived attitude parameters suggest that the attitude accuracy from the multi-antenna system tested is better than 2 arc minutes for yaw, 0.9 arc minutes for pitch and 3.3 arc minutes for roll. To reduce carrier phase multipath effects, chokering ground planes should be used with the GPS antennas whenever possible in a marine environment.

## CHAPTER 7

### CONCLUSIONS AND RECOMMENDATIONS

In this research, a GPS multi-antenna system consisting of multiple off-the-shelf GPS sensors has been successfully developed and extensively tested in operational marine environments. The advantages of such a system are the flexibility in the installation and usage of the GPS sensors, the cost-effectiveness with the emerging low-cost GPS receivers which output high quality carrier phase observations and the increased productivity of equipment which can be assembled into a multi-antenna system or disassembled for other positioning purposes. The strategy to integrate multiple GPS sensors into a multi-antenna system is mainly software-oriented, which poses little or no hardware change requirements on each independent GPS receiver. The use of non-dedicated GPS multi-antenna systems with wide antenna spacing for hydrographic applications has not been studied in the past.

Theoretical investigations in this research include platform attitude estimation using vector observables and on-the-fly carrier phase ambiguity resolution techniques for a multi-antenna system. A direct computation method for attitude parameters and the related error propagation formulas are presented in detail. A least squares attitude estimation procedure based on an

implicit adjustment model is developed, which is able to use the covariance matrices from both the *a priori* body frame coordinates and the GPS computed local level coordinates. For on-the-fly ambiguity resolution in multi-antenna systems, the emphasis has been placed on the utilization of baseline constraints and external attitude information, which are particular for multi-antenna GPS systems. A special formula based on Cholesky decomposition for constructing potential ambiguity sets on a fixed baseline is derived. Some numerical results concerning the speed of computation and the reliability of ambiguity resolution under different scenarios are also presented.

The software is the instrument, which is especially true for GPS technologies. As an integral part of the research, a software package capable of processing raw GPS measurements from non-dedicated as well as dedicated GPS multi-antenna systems was developed and tested. The software and the related algorithms are designed to optimally use all the positional and *a priori* information among the antennas and provide as much flexibility as possible for GPS antenna configurations and mounting in order to accommodate a wide range of applications. The non-dedicated GPS multi-antenna system used for experiments was formed by three or four NovAtel GPSCard™ receivers and the performance of the system and software in various marine environments was satisfactory. Currently, the software works in the post-processing mode. However, it should be relatively easy to modify it for real-time implementations with a GPS multi-antenna system since all the algorithms and the program structure are designed with the aim for real-time applications.

In addition to the above concluding remarks, the following specific conclusions can also be drawn from the findings of this research:

- (1) Direct computation formulas for attitude estimation are fast and robust, but are sub-optimal in a sense that only the antenna positions that define the platform are used. On the other hand, a least squares attitude estimation procedure based on the implicit adjustment model gives optimal attitude solution by using all the antenna position and covariance information. Using the initial attitude values provided by the direct computation formulas for linearization, least squares attitude estimation is also fast and robust since less than two iterations are needed in almost all cases. Another advantage of least squares attitude estimation is the output of the *a posteriori* accuracy quantities from the estimation process. However, these *a posteriori* accuracy quantities for attitude parameters should be used with caution because they may be too optimistic in case that inadequate (optimistic) variance factors were assigned to GPS measurements.
- (2) As a general rule, the accuracy of the estimated attitude parameters from a GPS multi-antenna system is inversely proportional to the baseline lengths between the antennas. Using long baseline lengths in the roll and pitch directions is the easiest and most efficient way to obtain high accuracy attitude parameters. If the baseline length varies from 3 m to 50 m, the expected attitude accuracy will change approximately from  $0.2^\circ$  to  $0.01^\circ$  under a good satellite geometry (GDOP 3) and moderate multipath effects. Optimization of the antenna

configuration on a relatively large scale on a ship or an airplane is very difficult due to the complexity of the platform surface and the limited space for antenna mounting.

- (3) On-the-fly carrier phase ambiguity resolution is the key to accurate and reliable attitude determination with a multi-antenna GPS system. Numerical results have shown that within an initial search cube of  $\pm 3$  m or equivalent and by using the fixed baseline constraints on potential ambiguity sets, on-the-fly ambiguity resolution can be achieved in a few seconds of observations to some 60 seconds of observations depending on the magnitude of carrier phase multipath influences. In a strong multipath situation, incorrect ambiguities may even be selected.
- (4) The construction of potential ambiguity sets on the sphere using the fixed baseline length and Cholesky decomposition method speeds up the computation time of ambiguity searching by 30% ~ 50%, as compared with the traditional search within the entire cube or sphere.
- (5) The reliability and computation speed of ambiguity resolution will be significantly improved for an integrated system of a multi-antenna GPS system with other low-cost attitude sensors. Test results show that the ambiguities can be correctly resolved 98% of the time if the external attitude sensors can provide the ambiguity search cubes of the size of  $\pm 0.5$  m, which translates to approximately  $2^\circ$  accuracy from the external attitude sensors for a 15 m long baseline.

- (6) The Adroit type antenna configurations requiring extra GPS sensors are mainly applicable to the short baseline situation where high attitude accuracy, e. g.  $< 0.1^\circ$ , is not required.
- (7) The fixed baseline check and carrier phase residual test are needed to ensure the correctness of the attitude results and detect carrier phase cycle slips and incorrect ambiguities. All the fixed baseline lengths in a multi-antenna system should be used for quality checks. If the ambiguities are wrong, the GPS computed baseline length will drift from its known fixed length and the carrier phase residuals will become larger due the change of the relative geometry between the baseline vector and satellites. The quicker the relative geometry change with time, the faster the baseline drift rate. Depending on the relative geometry as well as its rate of change, wrong ambiguities or cycle slips can be detected instantaneously or after a time delay normally within one minute.
- (8) Carrier phase multipath has been observed as one of the major error sources for attitude determination using either dedicated or non-dedicated GPS multi-antenna systems in a marine environment. The magnitude of carrier phase multipath can easily reach above the 1 cm level. For NovAtel GPSCard™ sensors, the use of choking ground planes has resulted a 20% reduction of carrier phase multipath effects. Choking ground planes should be used whenever possible.
- (9) Marine tests have shown that the dedicated and the non-dedicated multi-antenna systems deliver the same level of accuracy for attitude

determination since multipath is the major error source for GPS carrier phase observations. For a platform with a 5.3 m baseline in the yaw and pitch directions and a 4 m baseline in the roll direction, the attitude agreement from the 3DF system and the three antenna GPSCard™ system was 5 arc minutes, 7 arc minutes and 14 arc minutes for yaw, pitch and roll, respectively.

- (10) By using a non-dedicated four-GPSCard™ attitude system with wide antenna spacing on the CHS ship Matthew, accurate and reliable ship attitude parameters were obtained. Compared with the attitude reference from a high accuracy HG1050 INS onboard the ship, the accuracy from the GPS attitude system was better than 2 arc minutes for yaw, 0.9 arc minute for pitch and 3.3 arc minutes for roll. The GPS derived attitude parameters are drift free and the accuracy is not affected by ship manoeuvres and data collection rate. This is a clear advantage of GPS multi-antenna systems over the traditional accelerometer-based attitude sensors, e. g. TSS, HIPPY, which require a settling time up to 3 minutes after a sharp 90° turn. The performance of the proposed non-dedicated GPS multi-antenna system and the developed processing software was satisfactory during all simulated ship manoeuvres.

Based on the results and conclusions from this research, the following recommendations regarding the use and further investigations of GPS multi-antenna systems can be made:

- (1) In view of the excellent performance of GPS multi-antenna systems in the performed experiments, it is strongly recommended that they be used in future hydrographic surveys to provide ship attitude information. For this purpose, the relatively low cost and high performance GPS sensors with a stable carrier phase tracking capability are desirable.
- (2) The integration of a GPS multi-antenna system with other low cost onboard attitude sensors such as gyrocompass, inclinometer and accelerometer-based MRUs is also recommended. The integrated system will significantly increase the reliability and speed of carrier phase ambiguity resolution, enhance the quality assurance of the attitude results, bridge outages of the GPS signal and greatly reduce the drift problems in the gyro attitude sensors. The long term high accuracy of GPS estimated attitude parameters is optimally combined with the short term accuracy and fast update rate of the conventional attitude sensors.
- (3) The implementation of a real-time attitude determination system with three or four GPS sensors should be carried out in the near future. The algorithms and structure of the post-processing program MULTINAV are designed with the aim for a real-time system. The major modification would be the replacement of the observation input subroutine with a real-time data logger which simultaneously collects and properly buffers the measurements from multiple GPS receivers,

converts the measurements into the required data structure and then calls the main program MULTINAV.

- (4) In addition to the non-dedicated GPS multi-antenna system consisting of NovAtel GPSCard™ receivers, tests of other brand of GPS sensors for attitude determination would be beneficial from a user's point of view in selecting a variety of GPS boards available on the market.
- (5) Even though the main focus of this research is on marine applications, more tests of a non-dedicated GPS multi-antenna system in land and airborne environments are recommended in order to assess the performance of the system in various application scenarios. For the airborne case, some special problems that need to be investigated along with attitude determination include aircraft wing flexing, structure variation with the change of temperature and banking effects on satellite signals.

It is no doubt that with the increasing performance and the decreasing price of GPS sensors, non-dedicated or dedicated GPS multi-antenna systems will be widely used on the platforms whose attitude parameters are needed. The integration of GPS multi-antenna systems with other low cost attitude sensors and the improvement of multipath reduction techniques and carrier phase ambiguity resolution methods will further enhance the reliability and the achievable accuracy from the GPS multi-antenna technology.

**REFERENCES**

- Abidin, H. Z. (1993): Computational and Geometrical Aspects of On-The-Fly Ambiguity Resolution, Technical Report No. 164 (Ph. D Dissertation), Department of Surveying Engineering, The University of New Brunswick, Fredericton, N. B. Canada, 1993.
- Axelrad, P., C. J. Comp, P. F. MacDoran (1994): Use of Signal-to-Noise Ratio for Multipath Error Correction in GPS Differential Phase Measurements: Methodology and Experimental Results, Proceedings of the seventh International Technical Meeting of the Satellite Division of the ION, GPS-94, Salt Lake City, Utah, 20-23 September 1994.
- Axelrad, P. and L. M. Ward (1994): On-Orbit GPS Based Attitude and Antenna Baseline Estimation, Proceedings of the National Technical Meeting of The Institute of Navigation, San Diego, CA, January 24-26, 1994.
- Ashjaee, J., R. Lorenz, R. Sutherland, J. Dutilloy, J. B. Minazio, R. Abtahi, J. Eichner, J. Kosmalka and R. Helkey (1989): New GPS Developments and Ashtech M-XII, Proceedings of the Second International Technical Meeting of the Satellite Division of the ION, GPS-89, Colorado Springs, CO, September 26-29, 1989.
- Ashjaee, J. and R. Lorenz (1992): Precision GPS Surveying after Y-Code, Proceedings of the Fifth International Technical Meeting of the Satellite Division of the ION, GPS-92, Albuquerque, N. M. 16-18 September 1992.
- Ashtech, Inc. (1991): 3DF 24-Channel GPS Measurement System, Published by Ashtech, Inc., Sunnyvale, CA, May 1991.

- Bingham, P. M. and M. Fryer (1993): Highly Integrated Chipset for GPS Receivers Using RISC, Proceedings of the sixth International Technical Meeting of the Satellite Division of the ION, GPS-93, Salt Lake City, Utah, 22-24 September 1993.
- Bishop, G. J., Klobuchar and P. H. Doherty (1985): Multipath Effects on the Determination of Absolute Ionospheric Time Delay from GPS Signals, Radio Science, Vol. 20, No. 3, 1985, pp. 388-396.
- Blewitt, G. (1989): Carrier Phase Ambiguity Resolution for the Global Positioning System Applied to Geodetic Baseline up to 2000 km, Journal of Geophysical Research, Vol. 94, No. B8 August 10, 1989, pp. 10,187-10,203.
- Braasch, M. S. and F. Van Graas (1991): Guidance Accuracy Considerations for Realtime GPS Interferometry, Proceedings of the Fourth International Technical Meeting of the Satellite Division of the ION, GPS-91, Albuquerque, N. M. 11-13 September 1991.
- Brown, A. K., W. M. Bowles and T. P. Thorvaldsen (1982): Interferometric Attitude Determination Using the Global Positioning System, Proceedings of the Third Geodetic Symposium on Satellite Doppler Positioning, February, Las Cruces, N. M.
- Brown, R. (1992): Instantaneous GPS Attitude Determination, Proceedings of IEEE Position, Location and Navigation Symposium (PLANS'92), Monterey, CA. March, 1992.
- Cannon, M. E., H. Sun, T. E. Owen and M. A. Meimdl (1994): Assessment of a Non-dedicated GPS Receiver System for Precise Airborne Attitude Determination, Proceedings of the seventh International Technical Meeting of the Satellite Division of the ION, GPS-94, Salt Lake City, Utah, 20-23 September 1994.
- Cannon, M. E., E. Berry and M. King (1993a): Testing a lightweight GPS/GIS Terminal for Sub-Meter DGPS Positioning, Proceedings of

the sixth International Technical Meeting of the Satellite Division of the ION, GPS-93, Salt Lake City, Utah, 22-24 September 1993.

Cannon, M. E. and M. Haverland (1993b): Experiences of GPS Attitude Determination within a Helicopter Pod, Proceedings of the sixth International Technical Meeting of the Satellite Division of the ION, GPS-93, Salt Lake City, Utah, 22-24 September 1993.

Cannon, M. E., J. B. Schleppe, J. F. McLellan and T. E. Ollevier (1992): Real-Time Heading Determination Using an Integrated GPS-Dead Reckoning System, Proceedings of the Fifth International Technical Meeting of the Satellite Division of the ION, GPS-92, Albuquerque, N. M. 16-18 September 1992.

Cannon, M. E. and G. Lachapelle (1992): Analysis of a High-Performance C/A Code GPS Receiver in Kinematic Mode, *Navigation*, Vol. 39, No. 3, 1992

Cannon, M. E. (1992): Critical GPS Errors, Internal Report for Canagrav, April, 1992

Chen, D. S. (1993): Fast Ambiguity Search Filter (FASF): A Novel Concept for GPS Ambiguity Resolution, Proceedings of the sixth International Technical Meeting of the Satellite Division of the ION, GPS-93, Salt Lake City, Utah, 22-24 September 1993.

Chen, D. S. (1994): Fast Ambiguity Resolution Approach for Precise Rapid Static and Kinematic Positioning, Proceedings of the Third International Symposium on Differential Satellite Navigation Systems DSNS94, London, England, April 18-22, 1994.

Chen, D. S. and G. Lachapelle (1994): A Comparison of the FASF and Least Squares Search Algorithms for Ambiguity Resolution On The Fly, Proceedings of the International Symposium on Kinematic Systems in Geodesy, Geomatics and Navigation, Banff, Canada, August 30-September 2, 1994.

- Cohen, C. E., B. D. McNally, and B. W. Parkinson (1993): Flight Tests of Attitude Determination Using GPS Compared Against an Inertial Navigation Unit, Proceedings of the National Technical Meeting of The Institute of Navigation, San Francisco, CA, January 20-22, 1993.
- Cohen, C. E., E. G. Lightsey, W. A. Feess and B. W. Parkinson (1993): Space Flight Tests of Attitude Determination Using GPS, Proceedings of the sixth International Technical Meeting of the Satellite Division of the ION, GPS-93, Salt Lake City, Utah, 22-24 September 1993.
- Cohen, C. E., H. S. Cobb and B. W. Parkinson (1992): Two Studies of High Performance Attitude Determination Using GPS: Generalizing Wahba's Problem for High Output Rates and Evaluation of Static Accuracy Using A Theodolite, Proceedings of the Fifth International Technical Meeting of the Satellite Division of the ION, GPS-92, Albuquerque, N. M. 16-18 September 1992.
- Cohen, C. E. and B. W. Parkinson (1992): Aircraft Applications of GPS-Based Attitude Determination, Proceedings of the Fifth International Technical Meeting of the Satellite Division of the ION, GPS-92, Albuquerque, N. M. 16-18 September 1992.
- Cohen, C. E. and B. W. Parkinson (1991): Mitigating Multipath in GPS-Based Attitude Determination, AAS Guidance and Control Conference, Keystone, CO, 1991.
- Comp, C. (1993): Optimal Antenna Configuration for GPS Based Attitude Determination, Proceedings of the sixth International Technical Meeting of the Satellite Division of the ION, GPS-93, Salt Lake City, Utah, 22-24 September 1993.
- Dinn, D. and B. Bosko (1994): An Evaluation of Ship Motion Sensors (MMST-93), Proceedings of the International Symposium on Kinematic Systems in Geodesy, Geomatics and Navigation, Banff, Canada, August 30-September 2, 1994.

- Ellis, J. F. and G. A. Greswell (1979): Interferometric Attitude Determination with the Global Positioning System, *Journal of Guidance and Control*, (November-December), pp. 523-527.
- Evans, A. G. (1986): Roll, Pitch and Yaw Determination Using a Global Positioning System Receiver and an Antenna Periodically Moving in a Plane, *Marine Geodesy*, Vol. 10, No. 1, 1986.
- Fenton, P. C., B. Falkenberg, T. Ford, K. Ng and A. J. VanDierendonck (1991): NoVatel's GPS Receiver - The High Performance OEM Sensor of the Future, *Proceedings of the Fourth International Technical Meeting of the Satellite Division of the ION, GPS-91*, Albuquerque, N. M. 11-13 September 1991.
- Gao, Y., E. J. Krakiwsky and J. Czompo (1992): A Robust Testing Procedure for Multiple Blunder Detection and Identification, *The Journal of Surveying Engineering*, Vol. ???, No. ???, 1992, pp. ??? - ???.
- Geiger, A. (1988): Modeling of Phase Center Variation and Its Influence on GPS Positioning, In *Lecture Notes in Earth Sciences, Vol. 19, GPS Techniques Applied to Geodesy and Surveying*, Springer-Verlag, Berlin.
- Georgiadou, Y. and A. Kleusberg (1988): On Carrier Phase Multipath Effects in Relative GPS Positioning, *manuscripta geodaetica*, Vol. 13, 1988, pp. 172-179.
- Hatch, R. (1991): Instantaneous Ambiguity Resolution, *Proceedings of IAG Symposium No. 107 on Kinematic Systems in Geodesy, Surveying and Remote Sensing*, Springer Verlag, New York.
- Hatch, R. (1989): Ambiguity Resolution in the Fast Lane, *Proceedings of the Second International Technical Meeting of the Satellite Division of the ION, GPS-89*, Colorado Springs, CO, September 26-29, 1989.

- Hermann, B. R. (1985): A Simulation of the Navigation and Orientation Potential of the TI-AGR, *Marine Geodesy*, Vol. 9, No. 2, 1985, pp. 133-143.
- Jurgens, R. D., C. E. Rodgers and L. C. Fan (1991): GPS Azimuth Determining System (ADS), Cycle Resolution, System Design, and Army Test Results, Proceedings of the National Technical Meeting of The Institute of Navigation, San Francisco, January 22-24, 1991.
- Knight, J. and Hatch, R. (1991): Attitude Determination via GPS. Proceedings of IAG Symposium No. 107 on Kinematic Systems in Geodesy, Surveying and Remote Sensing, Springer Verlag, New York.
- Koch, K. R. (1988): *Parameter Estimation and Hypothesis Testing in Linear Models*, Springer-Verlag, Berlin Heidelberg 1988.
- Krakiwsky, E. J. (1992): *The Method of Least Squares: A Synthesis of Advances*, Lecture Notes, Department of Geomatics Engineering, The University of Calgary, Calgary, Canada.
- Krakiwsky, E. J. (Ed.) (1987): *Papers For The CISM Adjustment and Analysis Seminars*, Second Edition, The Canadian Institute of Surveying and Mapping, Box 5378, Station F, Ottawa, Ont. Canada.
- Kruczynski, L. R., P. C. Li, A. G. Evans and B. R. Hermann (1989): Using GPS to Determine Vehicle Attitude: USS YORKTOWN Test Results, Proceedings of the Second International Technical Meeting of the Satellite Division of the ION, GPS-89, Colorado Springs, CO, September 26-29, 1989.
- Kruczynski, L. R., P. C. Li, A. G. Evans and B. R. Hermann (1988): Using GPS to Determine Vehicle Attitude, Proceedings of the First International Technical Meeting of the Satellite Division of the ION, GPS-88, Colorado Springs, CO, September 19-23, 1988.

- Lachapelle, G., B. Falkenberg, D. Neufeldt and P. Kielland (1989): Marine DGPS Using Code and Carrier in a Multipath Environment, Proceedings of the Second International Technical Meeting of the Satellite Division of the ION, GPS-89, Colorado Springs, CO, September 26-29, 1989.
- Lachapelle, G., M. E. Cannon and G. Lu (1992): High-Precision GPS Navigation with Emphasis on Carrier-Phase Ambiguity Resolution, *Marine Geodesy*, Vol. 15, No. 4, 1992, pp. 253-269.
- Lachapelle, G., M.E. Cannon and G. Lu (1992): High-Precision GPS Navigation with Emphasis on Carrier-Phase Ambiguity Resolution, *Marine Geodesy*, Vol. 15, pp. 253-269.
- Lachapelle, G., C. Liu, G. Lu, B. Townsend, M. E. Cannon, and R. Hare (1993): Precise Marine DGPS Positioning Using P Code and High Performance C/A Code Technologies, *Geomatica*, Canadian Institute of Geomatics, Ottawa, Vol 47, No. 2, pp. 117-128.
- Lachapelle, G. (1993): NAVSTAR GPS: Theory and Applications, ENGO 625 Lecture Notes, Department of Geomatics Engineering, The University of Calgary, Calgary, Canada.
- Landau, H. and H. J. Euler (1992): On-the-Fly Ambiguity Resolution for Precise Differential Positioning, Proceedings of the Fifth International Technical Meeting of the Satellite Division of the ION, GPS-92, Albuquerque, N. M. 16-18 September 1992.
- Landau, H. and U. Vollath (1994): Differential GPS - New Developments on High Precision Positioning with On-the-Fly Ambiguity Resolution, Proceedings of the Third International Symposium on Differential Satellite Navigation Systems DSNS94, London, England, April 18-22, 1994.
- Langley, R. B., G. Beutler, D. Delikaraoglou, B. Nickerson, R. Santerre, P. Vanicek and D. E. Well (1984): Studies in the Application of the GPS

- to Differential Positioning, Technical Report No. 108, University of New Brunswick, Canada.
- Liu, Z. (1992): Comparison of Statistical Methods for the Alignment of Strapdown Inertial Systems, UCGO Report No. 20047, Department of Geomatics Engineering, The University of Calgary, Calgary, 1992.
- Loncarevic, B. (1993): Cruise Report: Matthew Motion Sensor Trials, Geological Survey of Canada, Open File Report No. 93-2730.
- Lu, G., G. Lachapelle, M. E. Cannon, and B. Vogel (1994): Performance Analysis of a Shipborne Gyrocompass with a Multi-Antenna GPS System, Proceedings of IEEE PLANS'94, Las Vegas, 11-15 April, pp. 337-343.
- Lu, G., M. E. Cannon, G. Lachapelle, and P. Kielland (1993): Attitude Determination in a Survey Launch Using Multi-Antenna GPS Technologies, Proceedings of National Technical Meeting of The Institute of Navigation, San Francisco, January 22-24, 1991, pp. 251-260.
- Lu, G. and G. Lachapelle (1992): Statistical Quality Control for Kinematic GPS Positioning, *manuscripta geodaetica*, Vol. 17, 1992, pp. 270-281.
- Mader, G. L. (1990): Ambiguity Function Techniques for GPS Phase Initialization and Kinematic Solutions, Proceedings of the Second International Symposium on Precise Positioning with the Global Positioning System, Ottawa, Canada, 3-7 September, pp. 1233-1247.
- Markley, F. L. (1988): Attitude Determination Using Vector Observations and the Singular Value Decomposition, *The Journal of the Astronautical Sciences*, Vol. 36, No. 3, July-September 1988, pp. 245-258.
- Mathisen, T. and O. Orpen (1994): Use of GPS Determined Attitude in Combination with Conventional Attitude Sensors, Proceedings of

the Third International Symposium on Differential Satellite Navigation Systems DSNS94, London, England, April 18-22, 1994.

McMillan, J., D. A. G. Arden, G. Lachapelle and G. Lu (1994): Dynamic GPS Attitude Performance Using INS/GPS Reference, Proceedings of the seventh International Technical Meeting of the Satellite Division of the ION, GPS-94, Salt Lake City, Utah, 20-23 September 1994.

Meehan, T. K. and L. E. Young (1992): On-Receiver Signal Processing for GPS Multipath Reduction, Proceedings of the Sixth International Geodetic Symposium on Satellite Positioning, The Ohio State University, Columbus, Ohio, 17-20 March 1992.

Meehan, T. K., J. M. Srinivasan, D. J. Spitzmesser, C. E. Dunn, J. Y. Ten, J. B. Thomas, T. N. Munson and C. B. Duncan (1992): The Turbo Rogue GPS Receiver, Proceedings of the Sixth International Geodetic Symposium on Satellite Positioning, The Ohio State University, Columbus, Ohio, 17-20 March 1992.

Nolan, J. S. Gourevitch and J. Ladd (1992): Characterizing Receiver Performance, Proceedings of the Fifth International Technical Meeting of the Satellite Division of the ION, GPS-92, Albuquerque, N. M. 16-18 September 1992.

Phillips Business Information, Inc. (1993): Who's Who in GPS Equipment - A Technical Reference, 1201 Seven Locks Road, Potomac, MD.

Quinn, P. (1993): Instantaneous GPS Attitude Determination, Proceedings of the sixth International Technical Meeting of the Satellite Division of the ION, GPS-93, Salt Lake City, Utah, 22-24 September 1993.

Remondi, B. W. (1984): Using the Global Positioning System (GPS) Phase Observable for Relative Geodesy: Modeling, Processing, and Results. Ph. D Dissertation, Centre for Space Research, University of Texas at Austin, Texas.

- Schwarz, K. P. and G. Zhang (1994): Testing of A Low Cost Integrated GPS/INS, Proceedings of the seventh International Technical Meeting of the Satellite Division of the ION, GPS-94, Salt Lake City, Utah, 20-23 September 1994.
- Schwarz, K. P., A. El\_Mowafy and M. Wei (1992): Testing a GPS Attitude System in Kinematic Mode, Proceedings of the Fifth International Technical Meeting of the Satellite Division of the ION, GPS-91, Albuquerque, N. M. 16-18 September 1992.
- Schwarz, K. P. and J. Krynski (1992): Fundamentals of Geodesy, UCGO Report No. 10014, Department of Geomatics Engineering, The University of Calgary, Calgary, Canada.
- Shuster, M. D. and S. D. Oh (1981): Three-Axis Attitude Determination from Vector Observations, *Journal of Guidance and Control*, Vol. 4, No. 1, 1981, pp. 70-77.
- Spinney, V. W. (1976): Applications of Global Positioning System as an Attitude Reference for Near Earth Users, ION National Aerospace Meeting, Naval Air Development Center, Warminster, PA, April, 1976.
- Teunissen, P. J. G. (1994): A New Method for Fast Carrier Phase Ambiguity Estimation, Proceedings of IEEE PLANS'94, Las Vegas, 11-15 April, pp. 562-573.
- Torge, W. (1980): *Geodesy*, Walter de Gruyter, Berlin New York, 1980.
- Van Dierendonck, A. J., P. C. Fenton and T. Ford (1992): Theory and Performance of Narrow Correlator Spacing in A GPS Receiver, Proceedings of the National Technical Meeting of The Institute of Navigation, San Diego, CA, 27 January 1992.

- Van Graas and M. Braasch (1991): GPS Interferometric Attitude and Heading Determination: Initial Flight Test Results, *Navigation*, Vol. 38, No. 4, Winter 1991-1992.
- Van Nee, R. (1992) : The Multipath Estimating Delay Lock Loop, Proceedings of The IEEE Second International Symposium on Spread Spectrum Techniques and Applications, Yokohama, Japan, November 29- December 2, 1992.
- Van Nee, R., J. Sierveld, P. C. Fenton and B. R. Townsend (1994): The Multipath Estimating Delay Lock Loop - Approaching Theoretical Accuracy Limits, Proceedings of IEEE PLANS'94, Las Vegas, 11-15 April, pp. 246-251.
- Wahba, G. (1965): A Least Squares Estimate of Spacecraft Attitude, *SIAM Review* Vol. 7, No. 3, July 1965, p. 409.
- Wei, Z. (1986): Positioning with NAVSTAR, the Global Positioning System, Report No. 370, Department of Geodetic Science and Surveying, The Ohio State University, Columbus, Ohio, 1986.
- Wells, D. E., N. Beck, D. Delikaraoglou, A. Kleusberg, E. J. Krakiwsky, G. Lachapelle, R. B. Langley, M. Nakiboglou, K. P. Schwarz, J. M. Tranquilla and P. Vanicek (1987): Guide to GPS Positioning, University of New Brunswick Graphic Services, Fredricton, N. B. Canada.
- Wilson, G. J. and J. D. Tonnemacher (1992): Trimble Navigation GPS Attitude Determination System, Proceedings of the Fifth International Technical Meeting of the Satellite Division of the ION, GPS-92, Albuquerque, N. M. 16-18 September 1992.
- Wertz, J.R. (Ed.) (1978): *Spacecraft Attitude Determination and Control*, Kluwer Academic Publishers, The Netherlands.

**Wubben, G. (1989): The GPS Adjustment Software Package GEONAP: Concepts and Models, Proceedings of the 5th International Geodetic Symposium on Satellite Positioning, Physical Science Laboratory, New Mexico State University.**

**Zhang, J. Q. (1993): Inertial Platform Stabilization Using GPS Velocity Feedback, Proceedings of the sixth International Technical Meeting of the Satellite Division of the ION, GPS-93, Salt Lake City, Utah, 22-24 September 1993.**

## APPENDIX

### 1) Local Level Coordinates and their Covariance Matrix

According to Torge (1980), the transformation between the local level system and the CT-system defined in Figure 3.1 is

$$\begin{pmatrix} y \\ x \\ z \end{pmatrix} = T \begin{pmatrix} X \\ Y \\ Z \end{pmatrix}, \quad (\text{a1})$$

where

$$T = \begin{pmatrix} -\sin \cos & -\sin \sin & \cos \\ -\sin & \cos & 0 \\ \cos \cos & \cos \sin & \sin \end{pmatrix}, \quad (\text{a2})$$

$x, y, z$  are the local level coordinates with origin at  $P$ ,

$X, Y, Z$  are the coordinate increments for a baseline vector in the CT system from the origin  $P$  to a point  $P_1$ , i. e.,  $X = X_1 - X_p$ ,

$$Y = Y_1 - Y_p, \quad Z = Z_1 - Z_p, \text{ and}$$

$(\quad, \quad)$  are the latitude and longitude of the local level origin at  $P$ .

In differential GPS positioning, the origin  $P$  (monitor station) is held fixed and the remote station  $P_1$  is solved through double difference observations. Differentiating eqn. (a1) with respect to  $X, Y$  and  $Z$ , the error of the local level coordinates is

$$\begin{pmatrix} dy \\ dx \\ dz \end{pmatrix} = T \begin{pmatrix} dX_1 \\ dY_1 \\ dZ_1 \end{pmatrix}. \quad (\text{a3})$$

By error propagation laws, the covariance matrix of the transformed local level coordinates is obtained as



are explicitly or implicitly used for platform attitude computations. The error relationships between the local level coordinates and the horizontal position  $(x, y)$  of the origin can be obtained by differentiating eqn. (a1) as

$$dy = -(\cos \alpha \cos \beta X + \cos \alpha \sin \beta Y + \sin \alpha Z)d\alpha + (\sin \alpha \sin \beta X - \sin \alpha \cos \beta Y)d\beta, \quad (\text{a6})$$

$$dx = -(\cos \alpha X + \sin \alpha Y)d\alpha, \quad (\text{a7})$$

$$dz = -(\sin \alpha \cos \beta X + \sin \alpha \sin \beta Y - \cos \alpha Z)d\alpha - (\cos \alpha \sin \beta X - \cos \alpha \cos \beta Y)d\beta. \quad (\text{a8})$$

Under SA, the single point positioning accuracy with C/A code pseudorange measurements is about 100 m (2DRMS) horizontally (Lachapelle, 1992). The worse value for  $x$  or  $y$  would be 50 m. Suppose that  $X = Y = Z = 30$  m (i.e. 52 m long baseline) and  $d\alpha = d\beta = 50$  m. The errors for  $dx$ ,  $dy$  and  $dz$  would be about 0.5 mm, -0.1 mm and 0.5 mm, respectively, for  $\alpha = 51^\circ$  E and  $\beta = 114^\circ$  W, the location of Calgary. These errors are negligible compared to carrier phase multipath effects.